

Innovative Science and Technology after the Emergence of COVID-19

January
6th-7th,
2022

The 25th SANKEN International Symposium

The 20th SANKEN Nanotechnology International Symposium

The 9th Kansai Nanoscience and Nanotechnology International Symposium

The 17th Handai Nanoscience and Nanotechnology International Symposium

The 3rd AIRC-SANKEN International Symposium

ONLINE
SYMPOSIUM

SANKEN



SCOPE

The emergence of COVID-19 as a global pandemic has created an international crisis, and its impact has forced people to accept lifestyles different from the conventional way of life. It goes without saying that finding effective medical approaches to cope with COVID-19 has been an urgent issue. Nonetheless, the pandemic has accelerated a remarkable development of scientific and technological ideas that had only been nascent previously. This international symposium, featuring leading scientists and young researchers working on innovative science and technology during the pandemic, provides an excellent opportunity for the outlining of upcoming developments in these fields.

The 25th SANKEN International Symposium

Organizing Committee

Prof. Yasushi YAGI

Prof. Tomonao HOSOKAI

Prof. Mamoru FUJITSUKA (Chair)

Prof. Yoichi YOSHIDA

SANKEN (The Institute for Scientific and Industrial Research),

Osaka University

Program at a Glance

January 6, 2022		January 7, 2022					
10:00		10:00					
11:00		11:00	Poster				
12:00		12:00	Lunch				
13:00		13:00	(Y1-1) T. Fujita	(Y2-1) T. Yokoi	(Y3-1) K. Lu	(Y4-1) H.-B. Li	(Y5-1) H. Yamaguchi
	Opening, Tohru Sekino (Osaka University, Japan)		(Y1-2) T. Araki	(Y2-2) Y. Kondo	(Y3-2) M. Somiya	(Y4-2) H. Momida	(Y5-2) T. Matsui
	(IL01) Kikuo Kishimoto (NEDO, Japan)		(Y1-3) T. Morita	(Y2-3) T. Goto	(Y3-3) Y. Osakada	(Y4-3) N. Kamiuchi	(Y5-3) H. Miki
14:00	(IL02) Fujio Toriumi (The University of Tokyo, Japan)	14:00	(Y1-4) S. Wu			(Y4-4) Y. Komoto	(Y5-4) Y. Okada
	Break						(Y5-5) D. Suemasa
15:00	(IL03) Akinori Kuzuya (Kansai University, Japan)	15:00	(PL04) Jai Pal Mittal (National Academy of Sciences, India)				
	(IL04) Yuji Sano (Institute for Molecular Science, Japan)	16:00					
16:00	Break	16:00	(IL05) Kiyohiko Kawai (Osaka University, Japan)				
	(PL01) Sven Groppe (University of Lübeck, Germany)	17:00	(IL06) Hidekazu Tanaka (Osaka University, Japan)				
17:00		17:00	Closing and Group Photo				
18:00	(PL02) Jens Sobek (University of Zurich, Switzerland)	18:00					
19:00	(PL03) Domenico Furfari (AIRBUS Operations GmbH, Germany)	19:00					
20:00	Group Photo	20:00					

The 25th SANKEN International Symposium

Thursday, January 6, 2022

13:30	13:40	Opening Remark by Prof. Tohru Sekino, Director of SANKEN, Osaka University
Chair: Yasushi Yagi		
13:40	14:10	(IL01) Kikuo Kishimoto (New Energy and Industrial Technology, Japan) Promising innovations in the post-COVID world
14:10	14:40	(IL02) Fujio Toriumi (The University of Tokyo, Japan) All you need is not only the facts- Analysis of the infordemic during the COVID-19 pandemic -
Break		
Chair: Tomonao Hosokai		
15:10	15:40	(IL03) Akinori Kuzuya (Kansai University, Japan) DNA nanodevices for single-molecule optical detection of various biomolecules
15:40	16:10	(IL04) Yuji Sano (Institute for Molecular Science, Japan) Fundamentals of laser peening and its industrialization through quantum beam technology
Break		
Chair: Masayuki Numao		
16:40	17:40	(PL01) Sven Groppe (University of Lübeck, Germany) Leveraging artificial intelligence and machine learning in pandemics using COVID-19 as a case study
Break		
Chair: Kiyohiko Kawai		
17:50	18:50	(PL02) Jens Sobek (University of Zurich, Switzerland) The oxidation of guanine in oligonucleotides monitored at single molecules using a modified DNA sequencer
Break		
Chair: Yuji Sano		
19:00	20:00	(PL03) Domenico Furfari (AIRBUS Operations GmbH, Germany) Towards innovation for in-service technologies and future aircraft programs
Group Photo		

Friday, January 7, 2022		
10:30	12:00	Poster Session (see poster program)
Break		
Creation of new science and technology by integrating information sciences, and development to society		
Discussion Leader: Tomoya Nakamura		
13:00	13:20	(Y1-1) Takafumi Fujita (Osaka University, Japan) Introducing machine learning to semiconductor single-spin quantum computation
13:20	13:40	(Y1-2) Teppei Araki (Osaka University, Japan) Flexible sensor sheet for healthcare monitoring
13:40	14:00	(Y1-3) Takashi Morita (Osaka University, Japan) Toward end-to-end unsupervised classification of animal vocalization
14:00	14:20	(Y1-4) Shuqiong Wu (Osaka University, Japan) Facilitating computed-tomography-based diagnosis using deep learning techniques
Discussion Leader: Zhan Jin		
13:00	13:20	(Y2-1) Taishi Yokoi (Tokyo Medical and Dental University, Japan) Development of octacalcium phosphate-based functional biomaterials
13:20	13:40	(Y2-2) Yasuyuki Kondo (Osaka University, Japan) Charge-discharge reactions of aqueous energy-storage devices
13:40	14:00	(Y2-3) Tomoyo Goto (Osaka University, Japan) Development of seaweed-like sodium titanate as a sorbent material for environmental purification
Discussion Leader: Yasuko Osakada		
13:00	13:20	(Y3-1) Kai Lu (Osaka University, Japan) Going fast and nano: Rediscoveries of the fluorescent protein toolbox for thermometry and nanoscopy in biological cells
13:20	13:40	(Y3-2) Masaharu Somiya (Osaka University, Japan) Analysis of intracellular trafficking of extracellular vesicles for cytoplasmic biomacromolecule delivery
13:40	14:00	(Y3-3) Yasuko Osakada (Osaka University, Japan) Development of photo-functional nanomaterials with new properties and their application to bioscience
Basic researches of nanotechnology		
Discussion Leaders: Seihou Jinnai, Masao Gohdo		
13:00	13:20	(Y4-1) Hao-Bo Li (Osaka University, Japan) Synthesis of highly reduced strongly correlated oxide SrCoO ₂
13:20	13:40	(Y4-2) Hiroyoshi Momida (Osaka University, Japan) Piezoelectricity of wurtzite materials: A first-principles study

13:40	14:00	(Y4-3) Naoto Kamiuchi (Osaka University, Japan) Nanostructure of Rh/SnO ₂ catalyst under CO oxidation reaction
14:00	14:20	(Y4-4) Yuki Komoto (Osaka University, Japan) DNA detection and discrimination using of nanogap single-molecule measurement
Advanced applications based on nanotechnology Discussion Leader: Masaaki Geshi, Yoshikata Nakajima		
13:00	13:20	(Y5-1) Hiroki Yamaguchi (Daikin Industries, Ltd., Japan) Improvement of water repellency of fluoroalkyl (meth) acrylate-based polymer with chemical and physical approaches
13:20	13:40	(Y5-2) Taisuke Matsui (Panasonic Corporation, Japan) Development of perovskite solar cells
13:40	14:00	(Y5-3) Hiroko Miki (Toshiba Corporation, Japan) Wafer-scalable graphene sensors for biological detection in ionic liquids
14:00	14:20	(Y5-4) Yasuaki Okada (Murata Manufacturing Co., Ltd., Japan) Atomic scale simulations for pseudocapacitive MXene electrode
14:20	14:40	(Y5-5) Daichi Suemasa (JSR Corporation, Japan) Laboratory automation for high-level expression of recombinant protein-A in escherichia coli
Break		
Chair: Yoichi Yoshida		
15:00	16:00	(PL04) Jai Pal Mittal (National Academy of Sciences, India) Scientific and technological advances in India during COVID-19
Break		
Chair: Yoichi Yoshida		
16:10	16:40	(IL05) Kiyohiko Kawai (Osaka University, Japan) Single molecule analysis and diagnosis by measuring chemical reaction rates
16:40	17:10	(IL06) Hidekazu Tanaka (Osaka University, Japan) Nanotechnology platform at SANKEN- Current and future beyond COVID-19 -
Closing and Group Photo		

The 25th SANKEN International Symposium, Poster Presentations

Creation of new science and technology by integrating information sciences, and development to society	
P1-1	Kenta Saito (Osaka University, Japan) High-sensitive strain sensing using tunnel magnetoresistance effect
P1-2	Toshiaki Morita (Osaka University, Japan) Temperature dependence of spin-orbit torque in ferromagnet/antiferromagnet-insulator/heavy-metal tri-layer structure
P1-3	Rei Kawabata (Osaka University, Japan) Noise characterization of organic transistor circuit for light sensor array
P1-4	Xiang Li (Osaka University, Japan) End-to-end model-based gait recognition using synchronized multi-view pose constraint
P1-5	Chi Xu (Osaka University, Japan) Real-time gait-based age estimation and gender classification from a single image
P1-6	Hayato Futase (Osaka University, Japan) Towards open-domain chatbot talking from explainable behaviors
Challenges and opportunities for new materials and beam sciences toward post-COVID society	
P2-1	Yintong Huang (Osaka University, Japan) Skin-adhesive, -breathable and -compatible cellulose nanopaper for comfortable on-skin biosignal measurement
P2-2	Kazuki Omote (Osaka University, Japan) Tuning of the electrical properties of carbonized cellulose nanopaper
P2-3	Chenyang Li (Osaka University, Japan) Redispersion and aggregation behavior of surface-modified TEMPO-oxidized cellulose nanofibers as anticorrosion layers on electrodes
P2-4	Xiang Li (Osaka University, Japan) Chitin nanofiber-derived elastic carbon aerogel for frequency-tunable microwave absorption
P2-5	Thanakorn Yeamsuksawat (Osaka University, Japan) Carbonized chitin nanopaper and its photothermal heating performance
P2-6	Kosuke Takahashi (Osaka University, Japan) Anisotropic thermally conductive papers with uniaxially aligned carbon fibers embedded in cellulose nanofiber matrix

P2-7	Manabu Mizukami (Osaka University, Japan) Structure analyses of cellulose nanofibers prepared by TEMPO-mediated oxidation and potassium permanganate oxidation
P2-8	Yurika Teraoka (Osaka University, Japan) Acetylation of cellulose nanopapers prepared by TEMPO-mediated oxidation
P2-9	Jun Shirahama (Osaka University, Japan) Iodine-treated cellulose for photothermal heating
P2-10	Do Hyung Han (Osaka University, Japan) Large scale chemical bottom-up synthesis of nanostructured peroxy titanates
P2-11	Sunghun Cho (Osaka University, Japan) Synthesis of one-dimensional nanostructures in low temperature
P2-12	Shin-ichiro Tanaka (Osaka University, Japan) Momentum-resolved resonance photoelectron spectroscopic study on TiSe ₂
P2-13	Yoshio Mizuta (Osaka University, Japan) Improvement of residual stress and fatigue properties of metal materials using a compact low-energy laser peening device
P2-14	Naveen Pathak (Osaka University, Japan) Electron beam chirp dexterity in staging laser wakefield acceleration
P2-15	Zhan Jin (Osaka University, Japan) Development of laser-wakefield acceleration platform
P2-16	Kai Huang (KPSI, Nat. Inst. for Quantum Sci.&Tech (QST), Japan) Investigation on the emission timings of electron bunches from laser wakefield acceleration via EO spatial decoding
P2-17	Kaoru Kobayashi (Utsunomiya University, Japan) THz source driven by femtosecond laser created plasma with applied transverse electric field in air
P2-18	Taketoshi Matsumoto (Osaka University, Japan) Upcycling silicon swarf to advanced electrode materials
P2-19	Itsuki Nishibata (Osaka University, Japan) Pulse duration dependence of dry laser peening effects in the femtosecond-to-picosecond regime
New chemical and biological approaches for society after the COVID-19 crisis	
P3-1	Jie Xu (Osaka University, Japan) Utilizing triplet-triplet energy transfer kinetics to explore the dynamics of nucleic acids at the single-molecule level

P3-2	Zuoyue Liu (Osaka University, Japan) Optical luminescence from protein-directed Au ₂₀ clusters upon hard X-ray irradiation
P3-3	Xinxi Li (Osaka University, Japan) Synthesis and photocatalytic improvement of metal-porphyrin containing nanodisks from covalent organic frameworks
P3-4	Shinobu Takizawa (Osaka University, Japan) Machine-learning-assisted multi-parameter screening for flow and electrochemical reactions
P3-5	Bimolendu Das (Osaka University, Japan) Sensing RNA internal loops and their binding molecules by a small-molecule fluorescence probe ANP77
P3-6	Jiranan Chotitumnavee (Osaka University, Japan) Design, synthesis, and biological evaluation of HDAC8-targeting PROTACs
P3-7	Sohei Nakano (Osaka University, Japan) The expression of MacAB is controlled by Rof through Rho dependent transcription termination system
P3-8	Ryohei Noma (Osaka University, Japan) A photoswitchable fluorescent protein for hours-time-lapse and sub-second-resolved super-resolution imaging
New nanoscience and nanotechnology	
P4-1	Kyungmin Kim (Osaka University, Japan) Manipulation of metal-insulator transition in VO ₂ thin films by using step-terrace orientations of TiO ₂ (110) substrates
P4-2	Jinfeng Yang (Osaka University, Japan) Relativistic femtosecond-pulsed electron microscopy
P4-3	Sakura Utsunomiya (Osaka University, Japan) Synthesis and physical properties of B-N fused nir-absorbing dyes with naphthobisthiadiazole unit toward organic semiconductor
P4-4	Jiho Ryu (Osaka University, Japan) Single-molecule classification based on intermolecular hydrogen bond by modified nano-gap and single-molecule time series analysis
P4-5	Takahito Ohshiro (Osaka University, Japan) Single-molecule electrical RNA detection towards COVID-19 detection
P4-6	Akira Kitajima (Osaka University, Japan) Summary about Nanotechnology Open Facilities, Osaka University

P4-7	Liliany Novyanty Pamasi (Nara Institute of Science and Technology, Japan) Modulated three-dimensional ferromagnetic anisotropy of pyramidal shape Fe nanofilms
P4-8	Ayu Enomoto (The University of Shiga Prefecture, Japan) Additive effects of Cu and K to perovskite solar cells
P4-9	Riku Okumura (The University of Shiga Prefecture, Japan) Effects of alkali metal and organic cation addition to Cu-based perovskite solar cells
P4-10	Iori Ono (The University of Shiga Prefecture, Japan) Perovskite solar cell with guanidinium added to the photoactive layer
P4-11	Atsushi Suzuki (The University of Shiga Prefecture, Japan) Material design based on first-principles calculation and characterization of lanthanide compound incorporated perovskite solar cells

Leveraging Artificial Intelligence and Machine Learning in Pandemics using COVID-19 as a Case Study

Sven Groppe ^{a,*}

*a: Institute of Information Systems (IFIS), University of Lübeck,
Ratzeburger Allee 160, D-23562 Lübeck, Germany*

Email: groppe@ifis.uni-luebeck.de (email address of corresponding author)

The COVID-19 pandemic slows down or even often stopped the world's activities in economy, education, society and other areas of our daily life, but was a huge trigger for research. Smart and hardworking scientists all over the world are still extending the knowledge about the COVID-19 virus and are contributing to various technologies to fight against the COVID-19 pandemic. Continuously newly occurring mutations of the original virus demand for still working on and improving the developed technologies against the pandemic.

This talk covers a short introduction into the effects of the COVID-19 pandemic by naming its winner and losers. Losers of the COVID-19 pandemic include infected humans (suffering more than necessary from overburdened health systems), economy (caused by lockdowns), students (having to catch up with missed topics due to closed schools) and society (suffering from cancelled events). There are also some winners of the COVID-19 pandemic like vaccine developers (with increasing stock price performance), sellers of medical products (increasing their sales) and technologies used to overcome pandemics (the development of which is enormously triggered by funded research).

This talk tries to provide an overview to answer where computers can help in our fight against the pandemic. Many areas and technologies have been identified for this purpose. According to my opinion, the most important technology for a short-time reaction to the COVID-19 virus in medical research is sequencing a genome and analyzing it via supercomputers. One of the most prominent examples for other developed approaches are the predictions of incidence rates and other COVID-19 data (like hospitalization rates) considering COVID-19 confinements and other contexts by computer simulations and machine learning approaches. There is also a need for the management of physical contacts, e.g., at events and restaurants, and apps for personal contact tracking to warn a group of or single persons in the case they have been in contact with an infected person. In order to overcome security risks different approaches for contact tracking have been discussed and developed like mobile operator, location-based and proximity-based contact tracing. Software within health systems has been improved or introduced, e.g. patient registration and status in hospitals, automatically recognizing COVID-19 patients from e.g. their computer tomography scans, and publicly available databases of confirmed COVID-19 cases and other COVID-19 related data, which are the basis for deeper analysis of the COVID-19 pandemics. On the basis of the achieved knowledge about the COVID-19 virus and the effects of the COVID-19 pandemic, a set of COVID-19 knowledge graphs have been released, which provide automatic means for answering related questions and help to structure the information flood of COVID-19 related data. Because of the enormous list of developed and used technologies related to COVID-19, this talk could not dive into all of them. For further reading, the contributions (1) and (2) provide overviews of current state-of-the-art in research of the discussed topics.

References:

- (1) Le Gruenwald, Sarika Jain, Sven Groppe (Ed.): Leveraging Artificial Intelligence in Global Epidemics, Elsevier, 2021. <https://doi.org/10.1016/C2020-0-03043-4>
- (2) Gurdeep Singh Hura, Sven Groppe, Sarika Jain, Le Gruenwald: Artificial Intelligence in Global Epidemics, Part 1. New Generation Computing **39** (3-4), 2021. <https://doi.org/10.1007/s00354-021-00138-y>

The oxidation of guanine in oligonucleotides monitored at single molecules using a modified DNA sequencer

Jens Sobek,* Ralph Schlapbach

Functional Genomics Center Zurich, Switzerland

Email: jens.sobek@fgcz.ethz.ch

We investigated chemical reactions that occur during hybridisation of dye labeled short oligonucleotides to an immobilised probe. Experiments were conducted in a zero-mode waveguide (ZMW) nanostructured chip using a modified single-molecule DNA sequencer (RSII+, Pacific Biosciences). In single-molecule fluorescence traces (Figure), hybridisation results in a sequence of pulses from which kinetic rate constants can precisely be determined. Unexpectedly, we found that nucleotides in double stranded DNA are oxidized by photoinduced electron transfer to the labeling dye.¹ Chemical reactions at nucleotides, that affect the stability of the hybrid, typically cause characteristic changes of the original pulse pattern. Moreover, since many dyes including CY3 have an affinity to base pairs and typically interact by stacking, the fluorescence intensity changes when the base (pair) is converted.² This can be used to identify the nature of the reaction product(s).³ For example, a characteristic decrease of pulse intensity was observed for the oxidation of guanine (G), in a base pair with cytosin, to 8-oxo-7,8-dihydroguanine (OG). This was confirmed by measurements of static fluorescence and the kinetics of hybridisation by SPR and single-molecule measurements, using OG modified oligonucleotides.

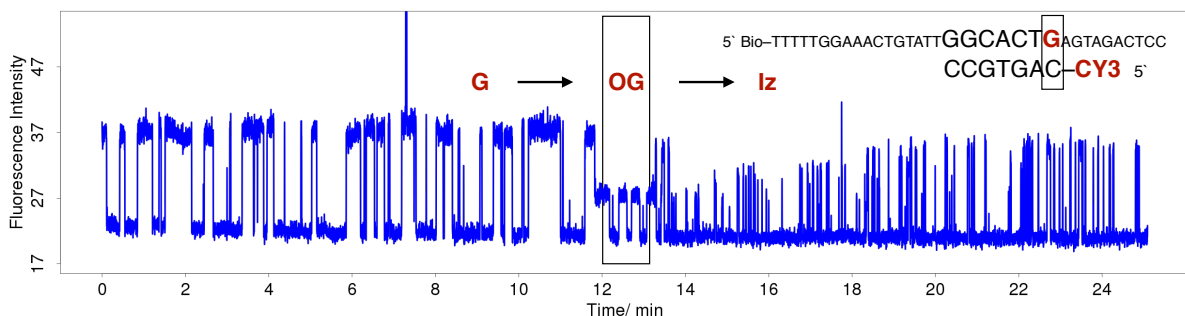


Figure: Single-molecule fluorescence trace of hybridisation demonstrating the formation of OG and a secondary product (Iz)

Since OG is easier to oxidise than G, its pulse pattern changes within seconds to minutes leading to a product of low hybrid stability that we assign to 2,5-diamino-4H-imidazol-4-one (Iz).⁴ Fluorescence traces can be recorded over a long period with a time resolution of approximately one second. This enables the investigation of sequences of chemical reactions by product analysis, using oligonucleotides carrying the corresponding modifications. In a typical measurement in a ZMW chip, hybridisation of 10000-30000 single molecules can be studied in parallel, giving rise to an excellent statistics and the possibility to study reaction pathways and yields, short-lived intermediates, and rare events.

In this talk I will give an introduction into a promising new method for the investigation of chemical reactions at the single-molecule level.

References:

- (1) Sobek, J. et al. *Methods Appl. Fluoresc.* **8** 035010 (2020).
- (2) Sobek, J., Schlapbach, R. *Molecules* **25**, 5369 (2020).
- (3) Fleming, A. M., Burrows C. J. *Free Radic Biol Med* **117** 35 (2017).
- (4) Kino, K., Sugiyama, H. *Chem. Biol.* **8**, 369 (2001).

Towards Innovation for in-service Technologies and Future Aircraft Programs

Domenico Furfari

Airbus Operations GmbH, Germany
Email: domenico.furfari@airbus.com



Aviation is an irreplaceable force that keeps our world united and accessible especially in post-COVID19 pandemic scenario. 4.5 billion passengers in 2019 (the equivalent almost 2/3 of the Human population) were linked in more than 3700 airports with scheduled services routes of more than 48000 served globally all around the world.

The future of the aviation industry has shown in the past decades to be a growth industry with passenger demand that will continue to grow. To keep or even increase trust in air travel post COVID19 pandemic it is important to focus on innovations as overall ambitions in the aeronautic industry. Innovation is in the Airbus DNA and has been one of the major drivers for over 4 decades. Short and long terms objectives are equally important and part of the Research & Technologies Airbus Domain. Maximising customer satisfaction with Airbus Services is part of a short term development plan focusing on innovative material and process which provides a continuous increase of performance aiming to assist our customers to operate the Airbus fleet safely and profitably. While keeping Customers in the center of Airbus attention, simultaneously freezing, and then reducing our carbon footprint represent the long term Company objective. Airbus is investing in key technologies to preserve the future of the aviation industry with the final goal of Decarbonisation of aviation. Today, Airbus already offers the most eco-efficient aircraft family: from the A220 to the A350 XWB, it provides a 25% reduction in CO2 emissions vs. the previous aircraft generation but Airbus is exploring game-changing concept aircraft—ZEROe for the near future of aviation. This new Airbus concept aircraft aims at putting hydrogen at the heart of future aircraft for entry-into-service in 2035 which implies the implementation of new materials, technologies and design as core R&T activities for existing and future products.

A novel design incorporating a through the thickness metallic local reinforcement in CFRP structural joint (named Redundant High Efficiency Assembly) will be presented including coupon test program to demonstrate the enhancement of the mechanical performance for potential use in future aircraft program¹. In the frame of continuous support Airbus Customers to repair metallic airframes of already in-service aircraft to reduce maintenance cost cold spray surface technology is presented. Cold Spray is solid-state material deposition technique where metallic powder particles bond to a substrate as a result of high-velocity impact (supersonic speed) and the associated plastic deformation resulting in high density and compaction of sprayed material being able to restore the shape of damaged aircraft components². An overview of repair capability using this technology will be provided

and the minimum industrial requirements for portable equipment will be presented. The lecture will be completed presenting residual stress engineering as a field of engineering aiming to improve the economic and ecological impact of future aircraft structures by controlling the residual stresses induced by Laser Shock Peening (LSP) technology³. The aeronautical industry requirements for future developments of the laser shock process will also be included for applications ranging from the repair environment to design and manufacturing of aircraft structures.

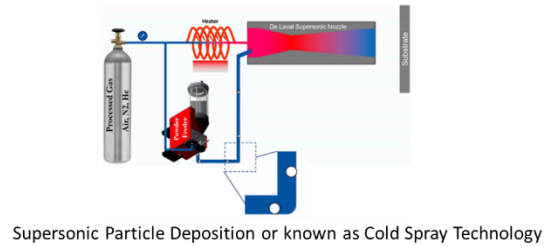
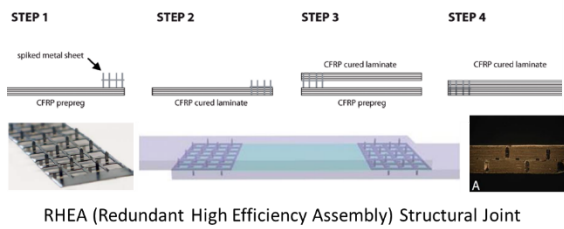


Figure 1: RHEA (Redundant High Efficiency Assembly) Structural Joint Design¹ (left) and Supersonic Particle Deposition also known as Cold Spray Process (right).

References:

- (1) Furfari, D.; Bisagni, C.; Pacchione, M. *ICAF Conference* **34**, (2015).
- (2) Hombergmeier, E.; Furfari, D.; Lucchini, R.; Rösler, T. *INCASE Conference* **1**, (2019).
- (3) Furfari, D.; *Advanced Materials Research* **891-892**, 992-1000 (2014).

Scientific and technological advances in India during COVID-19

J. P. Mittal

National Academy of Sciences, India
Chair Academic Board, UM-DAE CEBS, Mumbai
Email: mittaljp2003@yahoo.co.in

The COVID-19 crisis, which has descended upon the world with unimaginable swiftness, has brought much of the world to the halt. India, where there are several deep-seated problems which can increase the morbidity and mortality from COVID-19, took proactive measures to combat the virus.¹ Through its various national labs, expertise in diverse areas and involving private players in the fight against COVID, India quickly made giant forward leap in scientific and technological innovations. The country's rich R&D knowledgebase is manifested in the rapid testing, cost-effective diagnostic kits, virus culture, genome sequencing and disease surveillance. India's indigenously developed digital platforms (Aarogya Setu, COWIN, etc.) and vaccine development and manufacture program (Covaxin, Covishield, ZyCoV-D) has been a game changer.² It is also important to note that under *Vaccine Maitri* program, India has distributed ~70 million vaccine doses to 95 countries. Besides putting best scientific efforts to combat COVID-19 menace, India has also made tremendous progress in different science disciplines, from nuclear to space to robotics to energy.

References:

- (1) Radhakrishnan, N.; Gupta, D. K.; *The Lancet* **397**, 2464 (2021)
- (2) Kumar, V. M.; Pandi-Perumal, S. R.; Trakht, I.; Thyagarajan, S. P. *npj Vaccines* **6**, 60 (2021).

Promising Innovations in the Post-COVID world

Kikuo KISHIMOTO,* Satoshi ITOH, Akira MONKAWA

Technology Strategy Center, New Energy and Industrial Technology, Japan
 Email: kishimotokko@nedo.go.jp

The spread of the COVID-19 has forced us to realize a “new normal”, in which we continue our economic activities while preventing infection. In June 2020, NEDO published the report titled the “Social Changes and Promising Innovations in the Post-COVID World”⁽¹⁾ and released in it what social changes will become due to the Covid-19 crisis and what it is to be the image of innovations expected in the Post-Covid society. Many experts in Japan and abroad predict social changes and we analyzed this information and identified six major changes, as shown in Figure 1. Among them keys are digitalization and increased resilience.

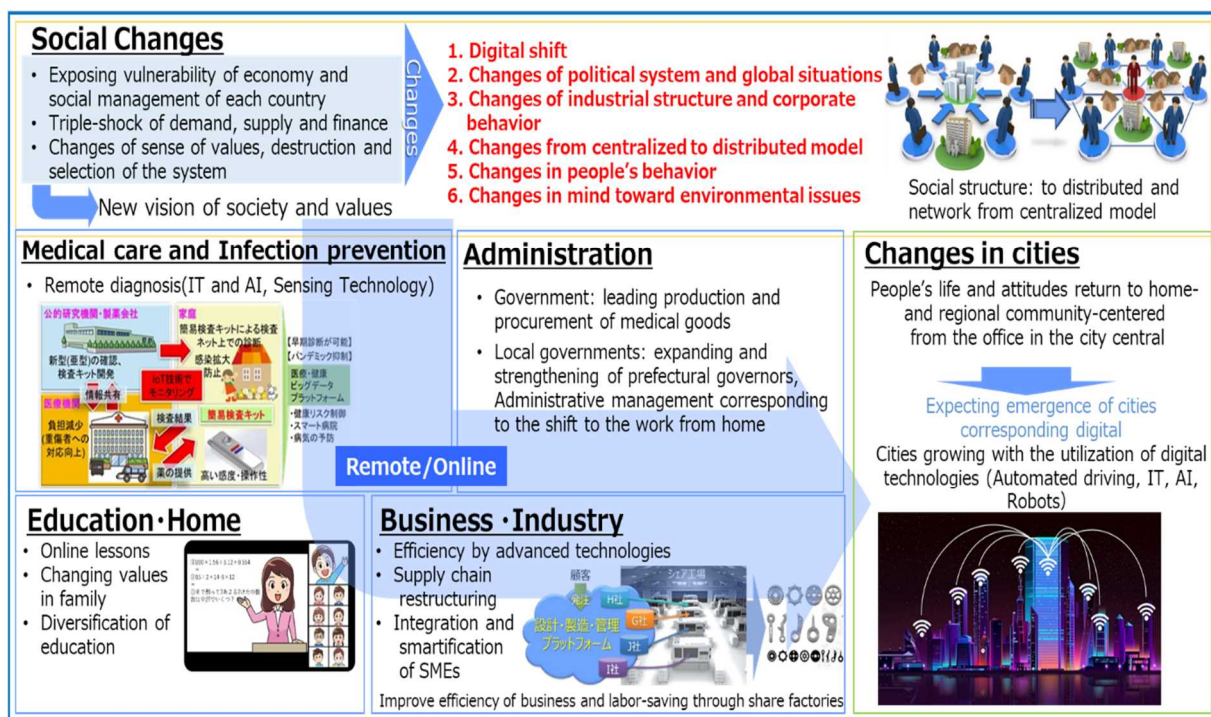


Figure 1: Social changes after the COVID-19 crisis and concrete examples.

In Post-Covid world, it is foreseen that further digitization will become popular and penetrate, and progress contactless and decentralized societies as new values. Awareness of environmental issues is also changing, and innovation is expected to help us shift to a sustainable society. “Well-being” has been drawing attention in recent years. We analyzed total 75-report concerning well-being domestic and overseas, white papers by government and reports of future forecast. Consequently, 6 universal values to keep in mind which should be strengthen and 12 visions of a society for realizing each value are clarified⁽²⁾. 40 examples of innovations through an overviewing analysis of the reports are also presented. The expected innovation is very broad and now a global social challenge. It is hoped that various parties will work together to create such innovation for prosperous future.

References:

- (1) TSC Foresight brief report, Social Changes and Promising Innovation in the Post-COVID-19 World, NEDO/TSC, <https://www.nedo.go.jp/content/100919493.pdf> (2020)
- (2) TSC Foresight, The "Prosperous Future" to be pursued beyond Innovation - What is the axis of value to cherish and the vision of society to realize?, NEDO/TSC, <https://www.nedo.go.jp/content/100934289.pdf> & [100934288.pdf](https://www.nedo.go.jp/content/100934288.pdf) (2021)

All you need is not only the facts
- Analysis of the Infodemic during the COVID-19 pandemic -
Fujio TORIUMI

Graduate School of Engineering, The University of Tokyo Japan
Email: tori@sys.t.u-tokyo.ac.jp

Social network services (SNSs) such as Twitter and Facebook are used by hundreds of millions of people worldwide for information gathering and communication [1]. Also, People are obtaining more and more information from social media and other online sources, but the spread of misinformation can lead to social disruption. In particular, social networking services (SNSs) can quickly spread information of uncertain authenticity and factuality.

In the pandemic of COVID-19 in 2020, a phenomenon called infodemics, in which a large amount of unverified information is spread, caused confusion in society. How should we respond to the spread of misinformation and disinformation?

We collected and analyzed misinformation spread on Twitter, one social media, in Japan under the COVID-19 pandemic and analyzed how it spread and its characteristics. In Japan, misinformation about a "shortage of toilet paper" spread, which leads to the hoarding of toilet paper. We analyzed what kind of tweets were spread at this time and compared them with the sales of toilet paper [2]. The results showed that the misinformation was not diffused widely. On the other hand, we found that tweets that correct misinformation spread on a large scale at the timing of the hoarding. The hoarding was not synchronized with misinformation but information that corrected misinformation. This fact suggests that the cause of the buyout is not the diffusion of misinformation but information that corrects misinformation. In other words, the diffusion of corrections rather than misinformation increased the social disorder.

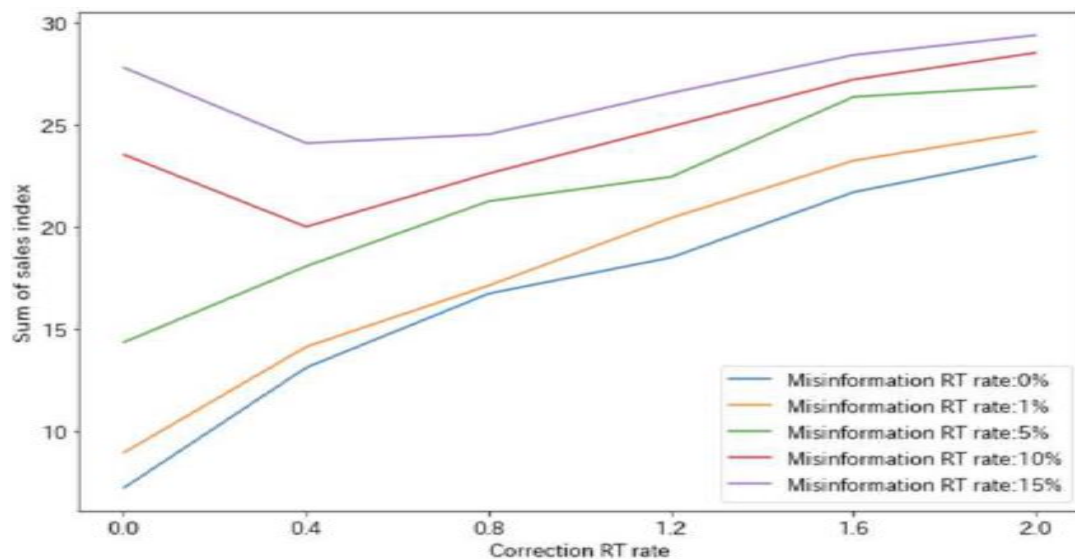


Figure 1: Suitable spread rate of correction tweets for misinformation

Based on this result, we estimated the optimal diffusion of the corrected information by simulation. The results show that there is an optimal diffusion rate depending on the diffusion of the original misinformation.

References:

- [1] Kemp S. Digital 2020: 3.8 billion people use social media. We are social.30. (2020)
- [2] Iizuka, R., Toriumi, F., Nishiguchi, M., Takano, M., & Yoshida, M. Corrective Information Does Not Necessarily Curb Social Disruption. arXiv preprint arXiv:2101.09665. (2021)

DNA nanodevices for single-molecule optical detection of various biomolecules

Akinori KUZUYA*

Department of Chemistry and Materials Engineering, Kansai University, JAPAN

Email: kuzuya@kansai-u.ac.jp

We have recently developed DNA origami pinching devices; DNA Pliers with two lever portions in 2D conventional DNA origami design, and DNA Chopsticks with 3D tubular levers (Figure 1).¹ These devices can take three forms; open cross, parallel closed, and antiparallel closed forms. When the lever portions are modified with a specific ligand, these devices can pinch exactly one target molecule between the levers and turn into parallel closed form. This structure change can be visualized by AFM. Various targets of a quite wide range of molecular weights from metal ions (a few tens of Da) to proteins (hundreds of kDa) can trigger such structural change. Real-time monitoring of the structure change was also possible with fluorescently modified DNA origami pinching devices, but this observation was not in single-molecular resolution.

In this study, we examined suitable conditions for DNA Origami devices to have sufficient mobility on mica for target binding and structure change, without coming off from the substrate, and successfully observed their movement with high-speed AFM in real-time.

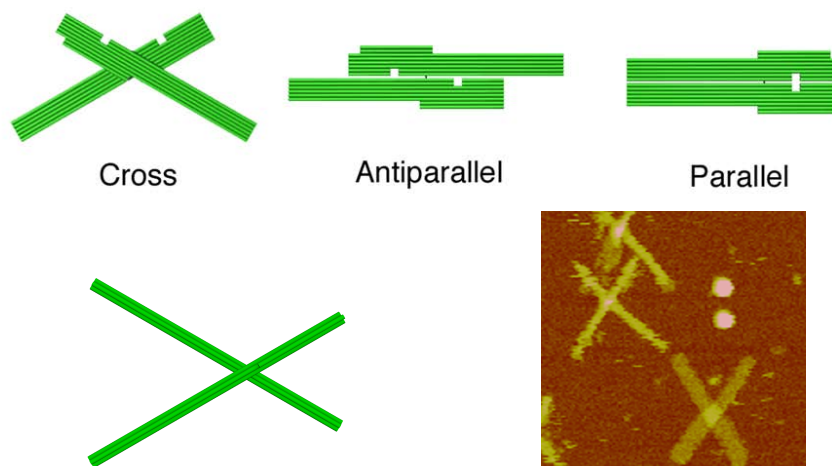


Figure 1: Schematic illustration and AFM images of DNA Pliers (top) and DNA Chopsticks (bottom).

We have also succeeded in observing DNA origami immobilized on glass surface, inspired by a pioneering work by Green et al.,² both with AFM and TIRF microscope (Figure 2).

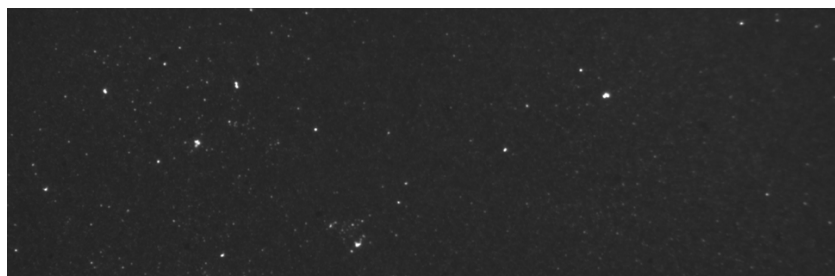


Figure 2: A TIRF image of fluorescein-modified DNA origami on glass surface.

References:

- (1) Kuzuya, A.; Sakai, Y.; Yamazaki, T.; Xu, Y.; Komiyama, M.; *Nat. Commun.* **2**, 449 (2011).
- (2) Green, C. M.; Hughes, W. L.; Graugnard, E.; Kuang, W. *ACS Nano.* **15**, 11597 (2021).

Fundamentals of laser peening and its industrialization through quantum beam technology

Yuji SANO

SANKEN, Osaka University, Japan
Email: yuji-sano@sanken.osaka-u.ac.jp



Quantum beams are not only an indispensable tool for basic science, but also induce various innovations in society. We have studied the interaction of intense laser pulses with engineering materials to enhance their properties. When metal materials are subjected to laser-induced shock, dislocations are generated on a microscopic level and hardening on a macroscopic level, which greatly increases the durability.^{1,2} This phenomenon is called "laser peening" or "laser shock peening" and we are using quantum beams to understand the underlying physics in laser peening, optimize the process and maximize the benefits. This is because the interaction occurs in the blink of an eye and it is impossible to observe the interaction inside opaque materials by usual methods.³ Here, we present our strides towards the understanding of laser peening and its real-world applications through quantum beams, such as neutron, X-ray, synchrotron radiation, or X-ray free electron laser (XFEL).

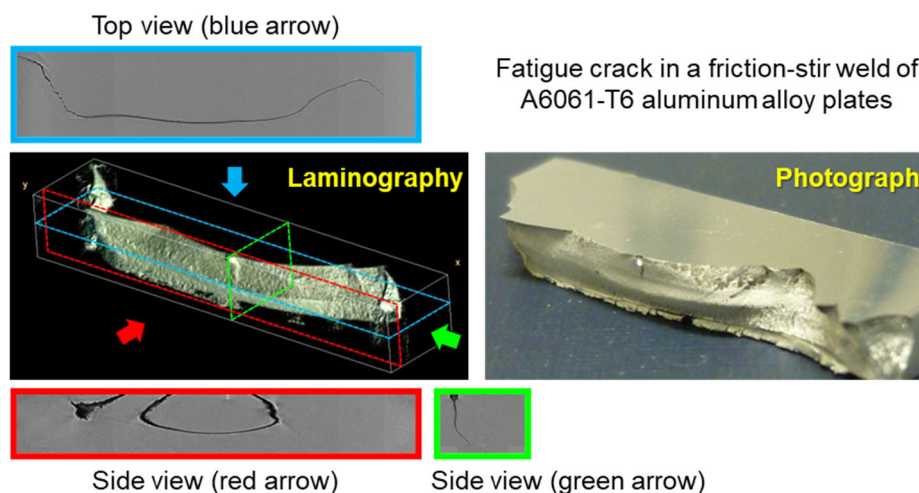


Figure 1: Fatigue crack in a friction-stir weld imaged by synchrotron radiation laminography

Reference:

- (1) Sano, Y.; Mukai, N.; Okazaki, K.; Obata, M. *Nucl. Instrum. Methods Phys. Res. B* **121**, 432 (1997).
- (2) Sano, Y. *Metals* **10**, 152 (2020).
- (3) Sano, Y.; Akita, K.; Sano, T. *Metals* **10**, 816 (2020).

Single molecule analysis and diagnosis by measuring chemical reaction rates

Kiyohiko KAWAI,^{a*} Atsushi MARUYAMA,^b Mamoru FUJITSUKA^a

a: SANKEN (The Institute of Scientific and Industrial Research), Osaka University, Japan.

b: Department of Life Science and Technology, Tokyo Institute of Technology, Japan

Email: kiyohiko@sanken.osaka-u.ac.jp

In order to achieve an ultra-sensitive analysis, one strategy would be to focus on an analytic method that relies on the properties of molecules that become highlighted when we look at molecules at the single-molecule level. In our recent studies, we have focused on the phenomenon so called fluorescence blinking. Fluorescent signals from a single fluorophore often blink, reflecting time-dependent fluctuations between bright “ON” and dark “OFF” states.

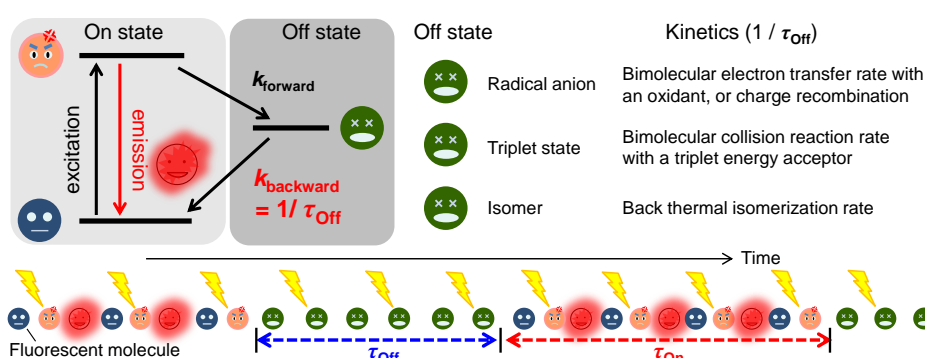


Figure 1: Schematic representation of KACB method.

During the repetitive cycles of excitation and emission, fluorescent molecules may occasionally enter non-fluorescent off states, such as: (a) the reduced or oxidized state triggered by photo-induced electron transfer, (b) the triplet state resulting from intersystem crossing, (c) the isomerized state formed by photo-triggered *trans-cis* isomerization as typically seen in cyanine dyes. Reversible formation of such off states causes a fluorescence blinking. The kinetics of a chemical reaction concomitant with blinking can be followed by the duration of the ON state (τ_{ON}) and that of the OFF state (τ_{OFF}). Based on the understanding of factors that affect the blinking, single fluorescent molecules can serve as reporters of their local microenvironment. We developed a method, termed **K**inetic **A**nalysis based on the **C**ontrol of fluorescence **B**linking (KACB). The blinking kinetics or patterns were controlled to reflect the microenvironment changes around the fluorophore. In this study, KACB method was adapted for detection of target DNA and RNA, and for investigation of antigen-antibody interactions at the single molecule level.

References:

- (1) Xu, J.; Fan, S.; Xu, L.; Maruyama, A.; Fujitsuka, M.; Kawai, K. *Angew. Chem. Int. Ed.* **60**, 12941 (2021).
- (2) Kawai, K.; Fujitsuka, M.; Maruyama, A. *Acc. Chem. Res.* **54**, 1001 (2021).
- (3) Kawai, K.; Maruyama, A. *Chem. Eur. J.* **26**, 7740 (2020).
- (4) Miyata, T.; Shimada, N.; Maruyama, A.; Kawai, K. *Chem. Eur. J.* **24**, 6755 (2018).
- (5) Kawai, K.; Miyata, T.; Shimada, N.; Ito, S.; Miyasaka, H.; Maruyama, A. *Angew. Chem. Int. Ed.* **56**, 15329 (2017).

About KACB please see <https://www.sanken.osaka-u.ac.jp/labs/mec/kawairesearch-e.pdf>
日本語 <https://www.sanken.osaka-u.ac.jp/labs/mec/kawairesearch.pdf>

Nanotechnology Platform at SANKEN

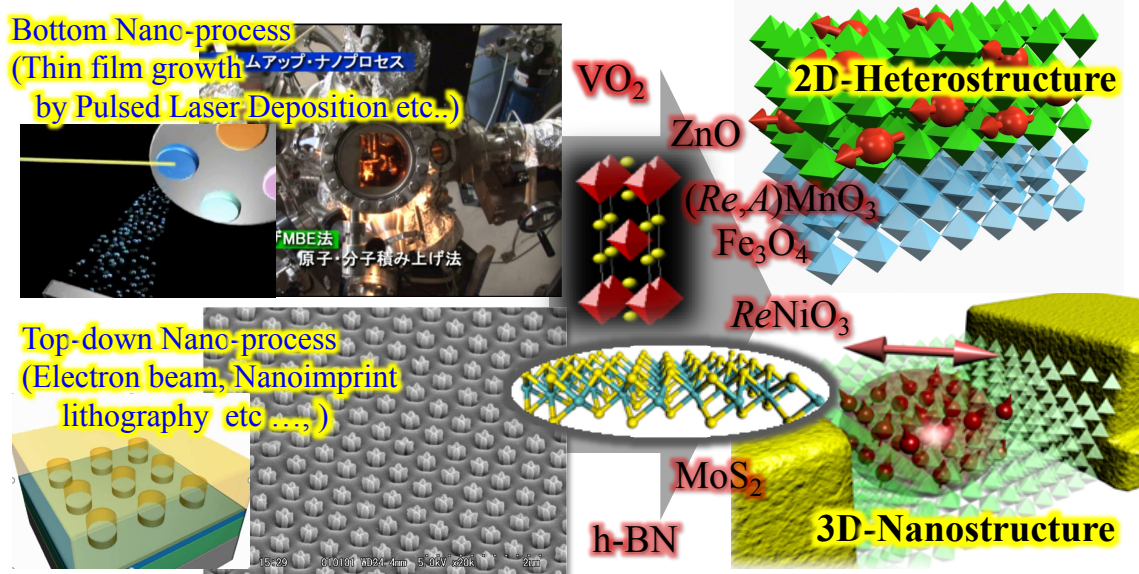
~ Current and Future beyond Covid-19 ~

Hidekazu TANAKA

Sanken (Institute of Scientific and Industrial Research), Osaka University,
8-1 Mihogaoka, Ibaraki, Osaka, 567-0047, Japan

Email: h-tanaka@sanken.osaka-u.ac.jp

Nanotechnology Open Facilities (NOF) at SANKEN is managed in close collaboration with Nanofabrication Platform, with Top-down nano-process and Molecule & Material Synthesis Platform with bottom up nano-process, as the "Nanotechnology Platform Japan" project by the MEXT. The mission is to establish a reliable research infrastructure (Platform) for scientific innovation by the alliance of the institutes which have cutting edge equipment and research know-how. Our "Molecule & Material Synthesis" platform supports developments of organic/inorganic/oxidative nanomaterials with synthesis of original thin films, artificial superlattice materials, nanowires/boxes and so on. "Nanofabrication Platform" supports the developments and evaluation of the resist materials for EUV lithography and the processing of nanoscale devices constructed by organic, inorganic, oxide, 2 dimensional materials. Nanotechnology research facilities at SANKEN supporting Top-down nano-process such as electron beam lithography, focus ion beam lithography and Bottom-up nano-process, such as thin film growth technologies of pulsed laser deposition system will be introduced. Each nano-process and their fusion nano-process have been producing excellent nano-materials and devices, such as functional oxide 2 dimensional materials /nanodevices^{(1), (2), (3)}.



Coming 10 years, Nanotechnology Open Facilities renew as "Advanced Research Infrastructure for Materials and Nanotechnology (ARIM) project" for Enhancing Material Innovation Power⁽⁴⁾ beyond Covid-19 with the assistance of remote control and informatics. Promoting digital transformation of materials R&D is an important direction, and ARIM project at Osaka University will be introduced.

References:

- (1) R. Rakshit, A. N. Hattori, Y. Naitoh, H. Shima, H. Akinaga, H. Tanaka, Nano Lett., 19(2019) 5003-5010.
- (2) S. Genchi, A. I. Osaka, A. N. Hattori, K. Watanabe, T. Taniguchi, and H. Tanaka, ACS Appl. Electron. Mater. 3 (2021) 5031-5036
- (3) A. N. Hattori, M. Ichimiya, M. Ashidai and H. Tanaka., Appl. Phys. Exp. 5 (2012) 125203.
- (4) <https://www.nanonet.go.jp/pages/arim/index.html>

Introducing machine learning to semiconductor single-spin quantum computation

Takafumi FUJITA,^{a,b,c,d} Yuta MATSUMOTO,^a Genki FUKUDA,^a Haruki KIYAMA,^{a,b,c}
Arne LUDWIG,^e Andreas D. WIECK,^e Akira OIWA^{a,b,c,d,*}

a: SANKEN, Osaka University, Japan

b: Center for Quantum Information and Quantum Biology, Osaka University, Japan

c: Center for Spintronics Research Network, Osaka University, Japan

d: Artificial Intelligence Research Center, SANKEN, Osaka University, Japan

e: Lehrstuhl für Angewandte Festkörperphysik, Ruhr-Universität Bochum, Germany

Email: oiwa@sanken.osaka-u.ac.jp

Unlike modern computers, quantum computation relies on fragile quantum coherence. Since the proposal of the physical implementation of single spins in quantum dots,¹ vast physical properties of quantum devices have been the main topic of research to make single spins reliable enough for quantum operational experiments.² New generations require more spins and operations that can actually run calculations on a quantum circuit even if there is a lot of noise on output signals and qubits.

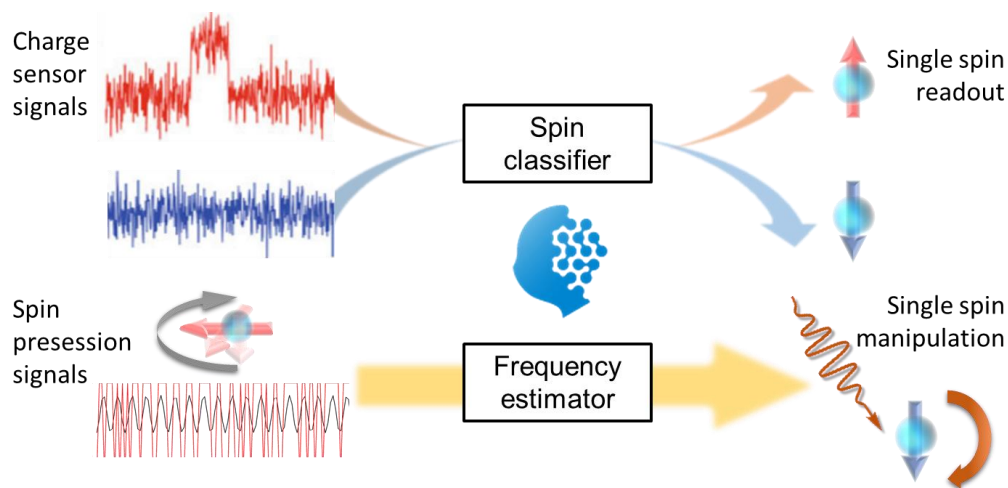


Figure 1: Example applications of neural networks to single-spin operation.

Nowadays, machine learning has emerged as a promising approach to unveil properties of semiconductor single-spin systems. Recently proposed as a tool to classify features of quantum dots, we experimentally demonstrated machine learning approaches to improve accuracies of classifying single-spin information from noisy real-time charge sensor signals³ and estimating spin resonance frequencies from sparse spin precession signals. These implementations trigger usage of machine learning in quantum dot experiments in general, leading to high-fidelity operations on large-scale arrays of qubits in future quantum-computers and -internet.

References:

- (1) Loss, D.; DiVincenzo, D. P. *Phys. Rev. A* **57**, 120 (1998).
- (2) Hanson, R.; Kouwenhoven, L. P.; Petta, J. R.; Tarucha, S.; Vandersypen, L. M. K. *Rev. Mod. Phys.* **79**, 1217 (2007).
- (3) Matsumoto, Y.; Fujita, T.; Ludwig A.; Wieck. A. D.; Komatani K.; Oiwa A. *npj Quantum Inf.* **7**, 136 (2021).

Flexible Sensor Sheet for Healthcare Monitoring

Teppei ARAKI,^{a,b,*} Takafumi UEMURA,^{a,b} Tsuyoshi SEKITANI^{a,b}

a: SANKEN (The Institute of Scientific and Industrial Research), Osaka University, Japan

b: Advanced Photonics and Biosensing Open Innovation Laboratory, National Institute of Advanced Industrial Science and Technology, Japan

Email: araki@sanken.osaka-u.ac.jp

An ultra-flexible sensor integrated with a lightweight wireless logger is ultimate flexible hybrid electronics (FHEs) to reduce inflammation and damage to body tissue. We have developed sheet-type sensors using stretchable conductors and ultra-flexible circuits to improve biocompatibility and acquire electrocardiogram^[1], electroencephalogram^[2], electrocorticogram^[3], pulse rate^[4], tracing of human body^[5], etc. This sensor connected with a small wireless measurement device realized long-term monitoring as FHEs. Furthermore, a transparent sensor sheet was developed to allow the visual inspection of an object through devices^[2,6], reducing vital stress/nervousness to monitor natural responses of biosignals in daily life. Simultaneous physical sensing and optical inspection of the targets can accelerate the development of the cyber-physical system to achieve a streamlined inspection process and solve various problems that hinder medical and healthcare applications.

References:

- [1] M. Sugiyama *et al.*, “An Ultraflexible Organic Differential Amplifier for Recording Electrocardiograms” *Nature Electronics*, 2, 351–360, 2019.
- [2] T. Araki *et al.*, “Wireless Monitoring Using a Stretchable and Transparent Sensor Sheet Containing Metal Nanowires” *Advanced Materials*, 32, 1902684, 2019.
- [3] T. Araki *et al.*, “Long-Term Implantable, Flexible, and Transparent Neural Interface Based on Ag/Au Core–Shell Nanowires” *Adv. Healthcare Mater.*, 8, 1900130, 2019.
- [4] A. Petritz *et al.*, “Imperceptible energy harvesting device and biomedical sensor based on ultraflexible ferroelectric transducers and organic diodes” *Nature Communications*, 12, 2399, 2021.
- [5] M. Kondo *et al.*, “Imperceptible magnetic sensor matrix system integrated with organic driver and amplifier circuits” *Science Advances*, 6, eaay6094, 2020.
- [6] A. Takemoto *et al.*, “Printable Transparent Microelectrodes toward Mechanically and Visually Imperceptible Electronics” *Advanced Intelligence Systems*, 2000093, 2020.

Toward end-to-end unsupervised classification of animal vocalization

Takashi MORITA^{a,*}

a: SANKEN, Osaka University
Email: tmorita.sanken@osaka-u.ac.jp

Development of deep learning methods in the past decade significantly improved machine learning performance in various fields. Automatic speech recognition (ASR) is no exception to those developments; deep learning enabled robust recognition of human speech against various noises and the achievements are already in empirical use, as exemplified by voice assistant systems installed in smartphones/speakers.

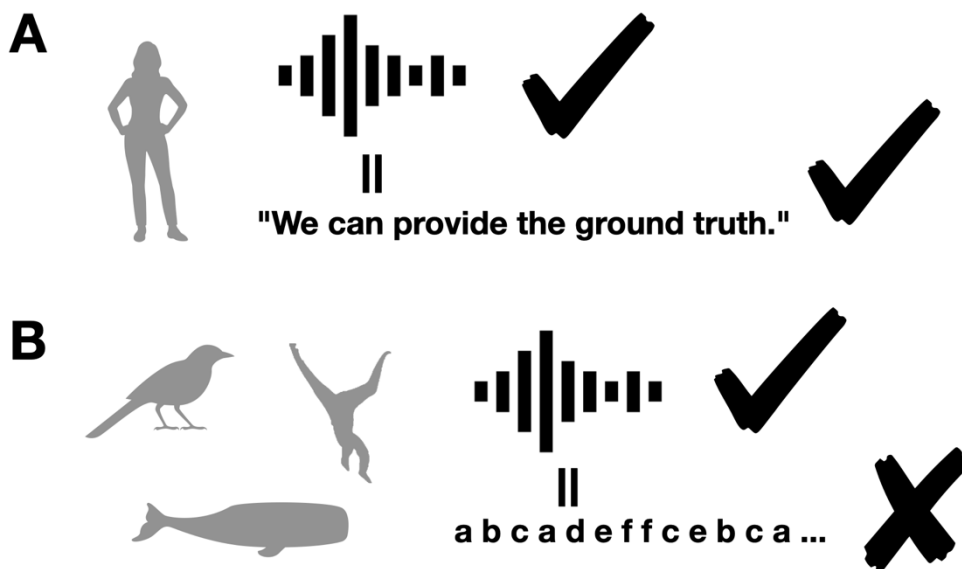


Figure 1: Difference in data available for human and animal ASR. (A) Human ASR can exploit the ground truth interpretation of speech sound via supervised learning. (B) By contrast, ground truth annotation/interpretation is not available in animal ASR and we need unsupervised machine learning to objectively infer discrete representation.

In contrast to the prosperity of today's ASR, however, its application to non-human animals is extremely limited. No artificial intelligence is yet able to reliably help us understand emotions or other latent states of our pets behind their vocalization. This limitation is due to the unavailability of ground-truth interpretation of animal vocalization (Figure 1). Even appropriate segmentation of vocalized sound and classification of the segmented vocal units can be unknown and non-trivial, and must be inferred solely from raw waveform data (i.e., animal ASR needs *unsupervised* machine learning).

In this talk, I will review recent attempts to classify animal vocalizations^{1,2} using modern unsupervised machine learning techniques^{3,4}, as well as more classical approaches based on annotations by human researchers.

References:

- (1) Sainburg, T.; Thielk, M.; Gentner, T. Q. *PLOS Comp. Biol.* **16** (10), 1-48 (2020).
- (2) Morita, T.; Koda, H.; Okanoya, K.; Tachibana, R. O. *bioRxiv*. 2020.05.09.083907 (2020).
- (3) Chorowski, J.; Weiss, R. J.; Bengio, S.; van den Oord, A. *IEEE IEEE/ACM Trans. Audio Speech Lang. Process.* **27** (12), 2041-2053 (2019).
- (4) Morita, T.; Koda, H.; *Interspeech*, 4856-4860 (2020).

Facilitating Computed-Tomography-based Diagnosis using Deep Learning Techniques

SHUQIONG WU1*

Department of Intelligent Media, SANKEN (The Institute of Scientific and Industrial Research), Osaka University, Suita, Osaka 565-0871, Japan
Email: wu@am.sanken.osaka-u.ac.jp (email address of corresponding author)

Obtaining intrafraction operative 3D organ information is important to diagnose disease and localize tumor positions. However, CT (computed tomography) scanning is difficult during beam delivery. Recently, planning CT and cone beam CT prior to beam delivery were used to localize the 3D positions of tumors. Nevertheless, the accuracy of information from planning CT declines when organ deformation exists, and the cone beam CT prior to beam delivery

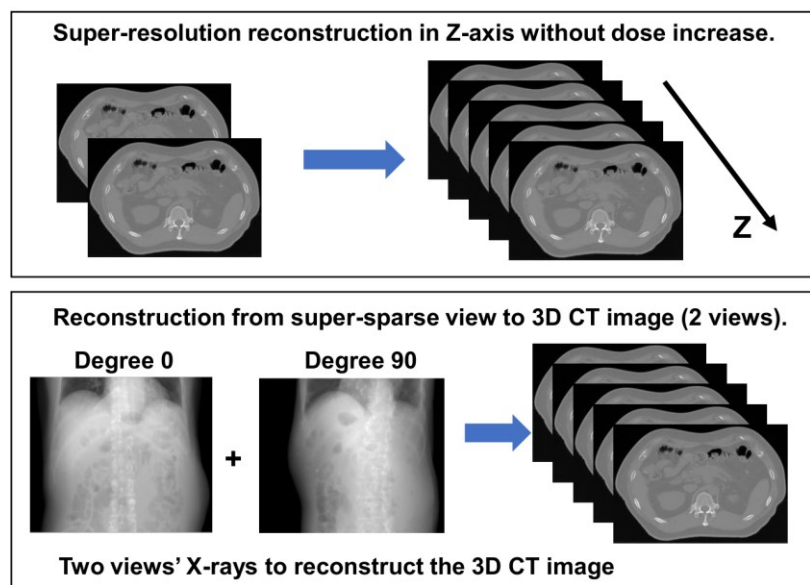


Figure1. The main architecture of this research

often suffers from artifacts [1]. To address these issues, we exploited deep learning models to achieve super-resolution reconstruction of CT data in the longitudinal direction for less artifacts, as well as to reconstruct 3D CT data from multi-view X-ray images for surgery navigation. In the super-resolution CT reconstruction in the longitudinal direction, multiple middle slices were reconstructed from each pair of adjacent slices, which reduced the slice thickness and increment without any dose increase. A U-net architecture [2] was adopted to reconstruct these middle slices. Finally, 22% improvement was obtained compared with a traditional linear interpolation. On the other hand, we exploited 3D GAN (Generative Adversarial Network) models to reconstruct 3D CT for abdominal organs from 2 views' X-ray images, which could achieve precise navigation during a cancer-related radiation therapy [3].

References:

- (1) Soffer S.; Ben-Cohen A.; Shimon O.; and et al., "Convolutional neural networks 273 for radiologic images: a radiologist's guide," *Radiology*, vol. **290**, no. 3, pp. 590–606, 2019.
- (2) Ronneberger O.; Fischer P.; and Brox T., "U-net: Convolutional networks for biomedical image segmentation," *MIC-CAI*, pp. 234–241, 2015.
- (3) Ying X.; Guo H.; Ma K.; and et al., "X2CT-GAN: Reconstructing CT from Biplanar X-Rays with Generative Adversarial Networks," *CVPR (Conference on Computer Vision and Pattern Recognition)*, pp. 10619–10628, 2019.

Development of octacalcium phosphate-based functional biomaterials

Taishi YOKOI,^{a,*}

a: Institute of Biomaterials and Bioengineering, Tokyo Medical and Dental University (TMDU)
 Email: yokoi.taishi.bcr@tmd.ac.jp

Octacalcium phosphate (OCP) is an inorganic substance that is critical for hard tissue formation and regeneration in the human body. Hydroxyapatite (HAp) is a well-known inorganic mineral present in the bones and teeth of mammals, including humans. OCP is regarded as a precursor of HAp in those hard tissues. Additionally, because of its excellent affinity towards bone tissues, OCP is used in surgery as a filler material for bone repair. Therefore, a deeper understanding of the physicochemical and biological properties of OCP is essential for the development of novel medical devices.

OCP exhibits a unique crystallographic property due to its layered structure composed of apatitic and hydrated layers. It was found in a previous study that hydrogen phosphate ions in the hydrated layers of OCP can be substituted by carboxylic acids.¹ Additionally, it has been reported that OCP with an organically-modified layered structure at the molecular level enables various applications including bone repair. The aim of our research is to create new ceramic biomaterials that have never before existed, by incorporating functional carboxylate ions into the OCP interlayer region.

Since some aromatic carboxylic acids exhibit fluorescent properties, OCP with incorporated aromatic carboxylate ions is also expected to have fluorescent functions. We attempted the incorporation of such carboxylate ion into OCP. From the successfully obtained OCPs, those with incorporated pyromellitate ions exhibited the strongest fluorescence. The 3D fluorescent spectrum of OCP with incorporated pyromellitate ions is shown in Figure 1. This organically-modified OCP was excited by UV light ranging between 260–330 nm and emitted visible light around 450 nm.

We successfully achieved the incorporation of specific aromatic carboxylic acids into OCP. In addition, we demonstrated that incorporating these carboxylic acids imparts fluorescent properties to OCP. As OCP has a high affinity for hard tissues in the human body and can be used as a material for artificial bones, its fluorescent properties could be used in the development of a theranostic material enabling the repair of bones and teeth, as well as fluorescence diagnosis. The developed organically-modified OCPs thus provide unique functionalities that could enable the development of biofriendly functional materials for artificial bones, dental implants, biosensors, and theranostic applications in the future.

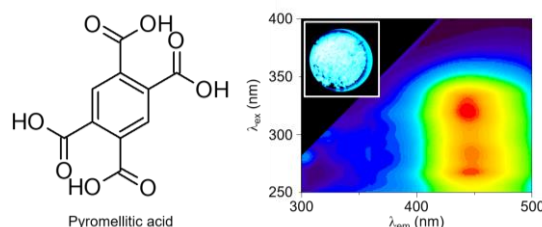


Figure 1: Molecular structures of pyromellitic acid and 3D fluorescent spectrum of OCP with incorporated pyromellitate ions. Insert: Image of OCP with incorporated pyromellitate ions under UV light.

Acknowledgments: This study was financially supported by JSPS KAKENHI (JP20H05181), and the Institute of Biomaterials and Bioengineering, TMDU [Project: Design & Engineering by Joint Inverse Innovation for Materials Architecture²] under the Ministry of Education, Culture, Sports, Science, and Technology, Japan. In addition, our work was supported by the Research Program for CORE lab of 'Dynamic Alliance for Open Innovation Bridging Human, Environment and Materials' under the 'Network Joint Research Center for Materials and Devices', and a research grant from The Murata Science Foundation.

References:

- (1) Yokoi, T.; Nakamura, J.; Ohtsuki, C.; *Incorporation behavior and biomedical applications of inorganic-layered compounds*, in *Bioceramics: from macro to nanoscale*, 139 (2020).

Charge-Discharge Reactions of Aqueous Energy-Storage Devices

Yasuyuki KONDO^{a,*} Kohei MIYAZAKI,^b Takeshi ABE,^b Yuki YAMADA^a

a: SANKEN(The Institute of Scientific and Industrial Research), Osaka University, Osaka

b: Graduate School of Engineering, Kyoto University, Kyoto

Email: yasuyuki.kondo@sanken.osaka-u.ac.jp

Recently, large-size energy-storage devices with high safety and high power are increasingly demanded for electric vehicles (EVs). Hybrid capacitors utilizing both non-faradaic (ion adsorption/de-sorption in electric double layer) and faradic reactions (redox reactions) are among the promising devices due to their higher power than lithium-ion batteries. For example, they use an activated carbon negative electrode and a graphite positive electrode (Figure 1). During charge, cations are adsorbed on the activated carbon, and anions are intercalated into the graphite; the reactions are reversed during discharge. As electrolytes, non-flammable water-based electrolytes are desired to ensure the safety.

However, the major problem of such water-based electrolytes is the low voltage stability (potential window) of water (only 1.23 V), which limits the operation voltage of the hybrid capacitors. To solve this problem, concentrated aqueous electrolytes have been researched to modify the electronic states of water molecules, thus expanding the potential window¹. Hence, concentrated aqueous electrolytes will enable hybrid capacitors to deliver higher voltage. In this talk, we will present the charge-discharge reactions of activated carbon negative electrodes and graphite positive electrodes in concentrated aqueous electrolytes.

First, for the negative electrode side, the charge-discharge behavior of two-electrode cells consisting of two activated carbon electrodes was studied. Stable charge-discharge could proceed up to the high-voltage of 2.6 V in sodium bis(fluorosulfonyl)amide (NaFSA) concentrated aqueous electrolytes by preventing water electrolysis². Second, as for the positive electrode side, electrochemical anion intercalation behaviors of graphite electrodes in dilute or concentrated NaFSA aqueous electrolytes are presented. Reversible charge-discharge reactions were achieved in concentrated electrolytes due to the prevented oxygen evolution reactions³. Lastly, the effects of difference in cation and anion structures on the charge-discharge reactions of aqueous hybrid capacitors were discussed.

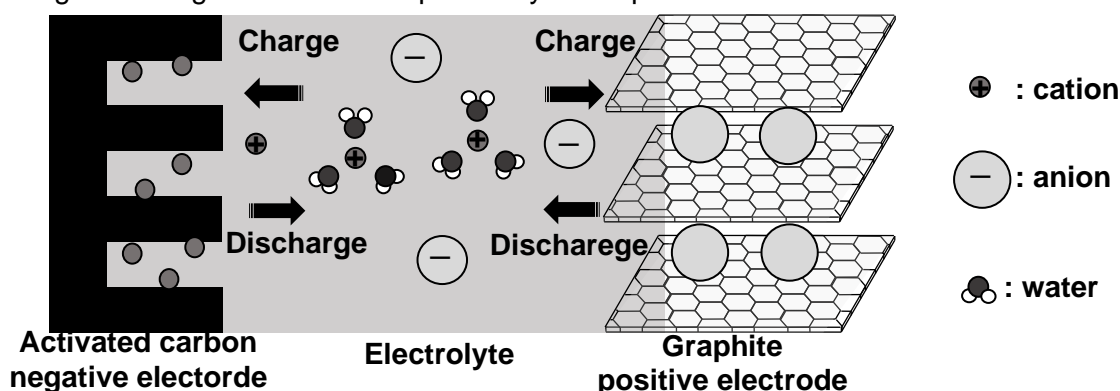


Figure 1: A schematic illustration of an aqueous hybrid capacitor.

References:

- (1) Yamada, Y. *et al.*, *Nat. Energy* **1**, 16129 (2016).
- (2) Kondo, Y.; Abe, T. *et al.*, *Electrochemistry* **88(3)**, 91 (2020).
- (3) Kondo, Y.; Miyazaki, K.; *et al.*, *Electrochem. Commun.* **100**, 26 (2019).

Development of seaweed-like sodium titanate as a sorbent material for environmental purification

Tomoyo GOTO,^{a,b,*} Yoshifumi KONDO,^{a,c} and Tohru SEKINO^a

a: SANKEN (The Institute of Scientific and Industrial Research), Osaka University, 8-1 Mihogaoka, Ibaraki, Osaka 567-0047, Japan

b: Institute for Advanced Co-Creation Studies, Osaka University, 1-1 Yamadaoka, Suita, Osaka 565-0871, Japan

c: Division of Materials and Manufacturing Science, Graduate School of Engineering, Osaka University, 2-1 Yamadaoka, Suita, Osaka 565-0871, Japan

**Email: goto@sanken.osaka-u.ac.jp*

Water pollutants such as heavy metals or radionuclides are one of the serious problem in realizing the sustainable society, and various materials of environmental purification such as sorbents are widely studied as one of the technologies to purify contaminated water. Among them, we are focusing on the layered sodium titanate as inorganic sorbents for cation removal from wastewater. Layered sodium titanates show the various unique morphology such as tube-like structure and have the cation-exchange property¹. The higher-order structure from nano- to macro-scale of sorbent affects the sorption reaction that includes the ion-exchange and surface adsorption, and therefore the design of crystal structure and morphology is important to enhance the sorption properties. In this study, seaweed-like sodium titanate mat (SST) were synthesized by hydrothermal process that excels as morphological control technique of inorganic compounds (Fig. 1), and the sorption property of divalent cations by SST were investigated.

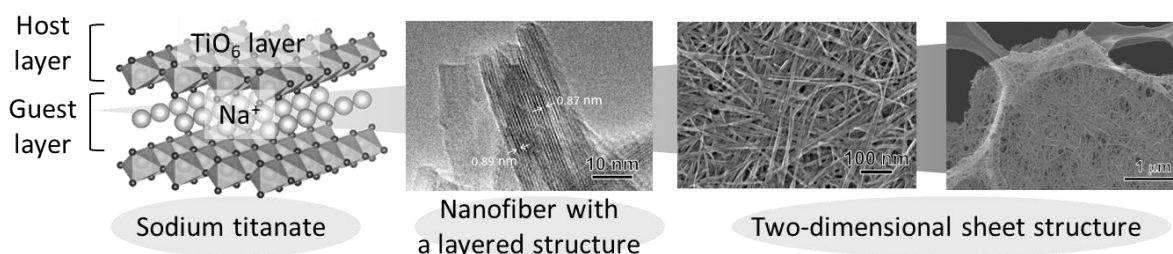


Figure 1: Higher-order structure of a seaweed-like sodium titanate mat (SST)^{2,3}

In the case of Co²⁺ sorption test using cobalt(II) nitrate solution, SST indicated the maximum sorption capacity of 1.85 mmol·g⁻¹ that was higher than that of chemical reagent of sodium metatitanate as a control sample². The sorption reaction of SST showed the mainly caused by the ion-exchange reaction, while the sodium metatitanate showed caused by the ion-exchange and the precipitation of hydroxide due to pH increase. These differences in sorption behavior are due to the selectivity of ion exchange reaction due to the crystal structure of sodium titanate sorbent. These results indicated that SST, which has high surface area and crystal structure suitable for ion exchange of target cation, is a good candidate as novel sorbent for water purification.

References:

- (1) Goto, T.; Cho, S. H.; Lee, S. W.; Sekino, T.; *J. Ceram. Soc. Japan.* **126**, 801 (2018)
- (2) Kondo, Y.; Goto, T.; Sekino, T. *RSC Adv.* **10**, 41032 (2020).
- (3) Kondo, Y.; Goto, T.; Sekino, T. *RSC Adv.* **11**, 18676 (2021).

Going fast and nano: Rediscoveries of the fluorescent protein toolbox for thermometry and nanoscopy in biological cells

Kai LU,^a Tetsuichi WAZAWA,^a Tomoki MATSUDA,^a Cong Quang VU,^{a,b} Masahiro NAKANO,^a
Vladislav V. VERKHUSHA,^{c,d} Takeharu NAGAI^{a,b,*}

a: SANKEN (The Institute of Scientific and Industrial Research), Osaka University, Japan

b: Graduate School of Frontier Biosciences, Osaka University, Japan

*c: Department of Anatomy and Structural Biology and Gruss-Lipper Biophotonics Center,
Albert Einstein College of Medicine, USA*

d: Medicum, Faculty of Medicine, University of Helsinki, Finland

Email: ng1@sanken.osaka-u.ac.jp

Fluorescent proteins (FPs) are bioimaging tools that visualize the inner workings of the cell. To serve such purpose, FPs are either used to label protein target *in situ* or engineered into biosensors to monitor functional parameters in physiologies and diseases. This FP toolbox is constantly expanding in parallel with advances in fluorescence microscopy techniques, which gives new possibilities of imaging at higher speed and resolution. Here, we will share two such examples of applying FP-based tools to observe the very fast and the very small in mammalian cells. In the first example, we tackled the problem of imaging intracellular heat diffusion, a transient event that demands the recording of temperature with kilohertz framerate. To this end, we developed a FP-based nanothermometer that excels in such department. Using this sensor, the sub-millisecond temperature dynamics during intracellular heat diffusion was successfully resolved and thermal conductivity of the cell was estimated. In the second example, we demonstrated the application of spontaneously switching FPs in single-molecule localization microscopy to resolve the nanoscopic structures of organelles. Low spectrum occupancy of the spontaneously switching FPs enabled multiplexed super-resolution microscopy with reduced complexity in optics. Our findings suggested that FPs still hold much unraveled potential even after decades of development since the advent of the original green fluorescent protein (GFP).

References:

- (1) Shinoda, H.; et al. *Cell Chem. Biol.* **26**, 1469 (2019).
- (2) Lu, K.; et al. *Int. J. Mol. Sci.* **20**, 5784 (2019).
- (3) Vu, C. Q.; et al. *Sci Rep* **11**, 16519 (2021).

Analysis of intracellular trafficking of extracellular vesicles for cytoplasmic biomacromolecule delivery

Masaharu SOMIYA*

SANKEN, Osaka University, Japan
Email: msomiya@sanken.osaka-u.ac.jp

Extracellular vesicles (EVs) are nanoparticles secreted by virtually all kinds of cells. Since EVs contain various biomolecules such as RNA and proteins, EVs are considered to serve as a shuttle to deliver cargo between cells. Although EV-mediated cargo delivery may contribute to intercellular communication, direct evidence demonstrating the cargo transfer between cells has been scarce. This is largely due to the lack of an appropriate experimental tool to understand the cargo delivery mechanism of EVs.

We have established two bioassays to assess the intracellular trafficking and cargo delivery mechanism of EVs; (1) real-time cargo delivery assay based on the complementation of two fragments of highly bright luciferase NanoLuc (HiBiT and LgBiT)¹ and (2) reporter gene assay to assess the membrane fusion of EVs.² The former assay can quantitatively measure the cytoplasmic cargo delivery of EVs in living recipient cells (Figure 1a). This assay is also capable to visualize the cargo delivery process by using a luminescence microscope. The latter assay can evaluate the membrane fusion efficiency of EVs after the uptake into recipient cells. Upon the membrane fusion between EVs and cell membrane, the transcription activator domain is released to the cytoplasm of the recipient cell and induces the reporter gene expression (Figure 1b).

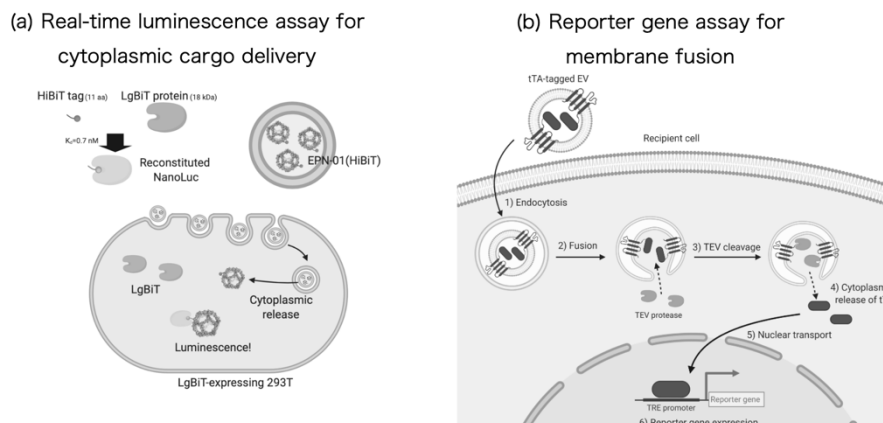


Figure 1: Novel bioassays to study intracellular trafficking of EVs.

By using these novel bioassays, we confirmed that authentic EVs derived from multiple human cell lines are capable of neither fusing with cell membrane nor delivering the cargo into the cytoplasm. On the other hand, we found that EVs conjugated with a virus-derived membrane fusion protein (vesicular stomatitis virus G protein, VSV-G) induced membrane fusion and cytoplasmic cargo delivery.

Since the modification of EVs with VSV-G significantly enhanced the cargo delivery, we applied this concept for the delivery of bioactive proteins. After the active loading of model proteins into EVs by using a rapamycin-mediated heterodimerization system, we succeeded in the functional cargo delivery into the recipient cells.³

References:

- (1) Somiya, M; Kuroda, S. *Anal. Chem.* **93**, 5612 (2021).
- (2) Somiya, M; Kuroda, S. *J. Extracell. Vesicles* **10**, e12171 (2021).
- (3) Somiya, M; Kuroda, S. *bioRxiv* 2021.11.04.466099 (2021).

Development of photo-functional nanomaterials with new properties and their application to bioscience

Yasuko OSAKADA^{a,b,*}

a: Institute for Advanced Co-Creation Studies,

b: SANKEN (The Institute of Scientific and Industrial Research), Osaka University, Japan

Email: yosakada@sanken.osaka-u.ac.jp

The development of synthetic organic nanomaterials, such as nanoparticles and two dimensional polymers, offers an attractive means to preset their unique photochemical properties, as well as potential their use in bioscience, such as cellular imaging and functional regulation. Based on the principals of photochemistry and radiation chemistry, we developed novel imaging and energy conversion methods, to control their photo-functional properties.

The fast part of this presentation will focus on the development of noble imaging methods using light. The X-ray excited imaging nanomaterials and photo-switchable fluorescence materials will be discussed in this presentation.¹⁻³ In the second part, our focus will shift to two dimensional polymer materials for photocatalytic reaction.⁴ These studies establish a starting points for the design of unique photo-functional organic nanomaterials toward biological science.

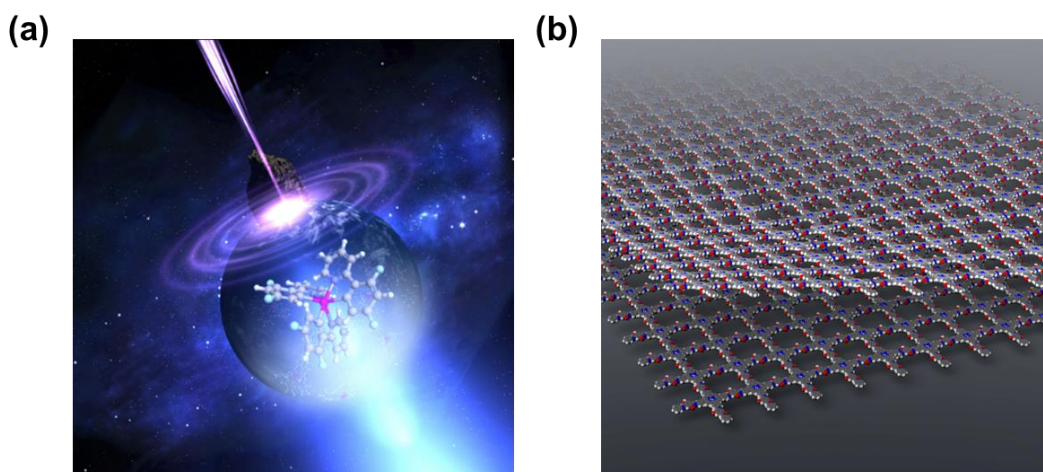


Figure 1: (a) X-ray excitable polymer nanoparticles using iridium complexes as doping molecules. (b) Synthesis of ultrathin two-dimensional porphyrin nanodisks via covalent organic framework exfoliation for photocatalytic reactions.

References:

- (1) (a) Osakada, Y.; Pratx, G.; Sun, C.; Sakamoto, M.; Ahmad, M.; Volotskova, O.; Ong, Q.; Teranishi, T.; Harada, Y.; Xing, L.; Cui, B., *Chem. Commun.* **50**, 3549 (2014); (b) Osakada, Y.; Pratx, G.; Hanson, L.; Solomon, P. E.; Xing, L.; Cui, B., *Chem. Commun.* **49**, 4319 (2013). (c) Liu, Z.; Jung, K. O.; Takahata, R.; Sakamoto, M.; Teranishi, T.; Fujitsuka, M.; Pratx, G.; Osakada, Y. *RSC Adv.* **10**, 13824 (2020).
- (2) (a) Osakada, Y.; Fukaminato, T.; Ichinose, Y.; Fujitsuka, M.; Harada, Y.; Majima, T., *Chem. Asian J.* **12**, 2660 (2017); (b) Osakada, Y.; Hanson, L.; Cui, B., *Chem. Commun.* **48**, 3285-3287 (2012).
- (3) (a) Tanaka, A.; Liu, Z.; Osakada, Y., *Bioorg. Med. Chem. Lett.* **29**, 1899 (2019); (b) Osakada, Y.; Zhang, K., *Bull. Chem. Soc. Jpn.* **90**, 714 (2017).
- (4) (a) Fan, Z.; Nomura, K.; Zhu, M.; Li, X.; Xue, J.; Majima, T.; Osakada, Y., *Commun. Chem.* **2**, 55 (2019). (b) Li, X.; Goto, T.; Nomura, K.; Zhu, M.; Sekino, T.; Osakada, Y., *Appl. Surf. Sci.* **513**, 145720 (2020). (c) Li, X.; Kawai, K.; Fujitsuka, M.; Osakada, Y. *Surfaces and Interfaces* 101249 (2021). (Review)

Synthesis of highly reduced strongly correlated oxide SrCoO₂

Hao-Bo LI^a, Shunsuke KOBAYASHI^b, Chengchao ZHONG^a, Morito NAMBA^a, Yu CAO^a, Daichi KATO¹, Yoshinori KOTANI^c, Qianmei LIN^a, Maokun WU^d, Wei-Hua WANG^d, Masaki KOBAYASHI^e, Koji FUJITA^e, Cédric TASSEL^a, Takahito TERASHIMA^f, Akihide KUWABARA^b, Yoji KOBAYASHI^a, Hiroshi TAKATSU^{a,*}, Hiroshi KAGEYAMA^{a,*}

a: Department of Energy and Hydrocarbon Chemistry, Graduate School of Engineering Kyoto University, Kyoto, 615-8510 Japan.

b: Nanostructures Research Laboratory, Japan Fine Ceramics Center, Nagoya, 456-8587 Japan.

c: Japan Synchrotron Radiation Research Institute, 1-1-1, Kouto, Sayo-cho, Sayo-gun, Hyogo, 679-5198 Japan.

d: Department of Electronic Science and Engineering, and Tianjin Key Laboratory of Photo-Electronic Thin Film Device and Technology, Nankai University, Tianjin 300071 China.

e: Department of Material Chemistry, Graduate School of Engineering, Kyoto University, Katsura Nishikyo-ku, Kyoto 615-8510, Japan.

f: Department of Physics, Graduate School of Science, Kyoto University, Kyoto 606-8502, Corresponding author: kage@scl.kyoto-u.ac.jp takatsu@scl.kyoto-u.ac.jp

Controlling oxygen deficiencies is essential for the development of novel chemical and physical properties in strongly correlated oxides. In the recent decades, low-temperature topochemical reactions using metal hydrides (e.g., CaH₂) are known as a powerful method to lead to highly reduced oxides such as SrFeO₂¹ and LaNiO₂², although their applicability is limited due to uncontrollable product. In this work we use a combination of electrochemical protonation and thermal dehydration to synthesize highly reduced oxide. SrCoO_{2.5} thin film is converted to SrCoO₂ by dehydration of HSrCoO_{2.5} at 350 °C (Figure 1). SrCoO₂ represents the first perovskite-derived compound consisting only of tetrahedra, forming a four-legged spin tube. Upon heating, HSrCoO_{2.5} with distorted octahedra gradually dehydrates (H_{1-x}CoO_{2.5-x/2}) and then switches to the one-dimensional spin tube structure. This suggests that ‘destabilization’ of the SrCoO_{2.5} precursor by protonation drastically alters the reaction energy landscape. Given that electrochemical protonation has been applied to a variety of transition metal oxides, this simple process opens new avenues for exploring novel oxides.

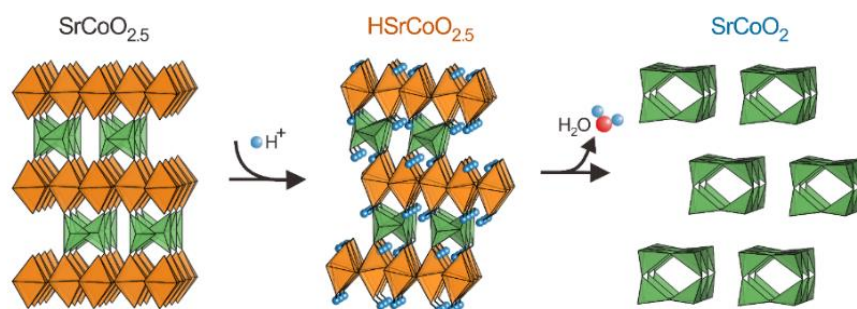


Figure 1. The structure evolution of electrochemical protonation and dehydration.

References:

- (1) Tsujimoto, Y.; Tassel, C.; Hayashi, N.; Watanabe, T.; Kageyama, H.; Yoshimura, K.; Takano, M.; Ceretti, M.; Ritter, C.; Paulus, W. Infinite-layer iron oxide with a square-planar coordination. *Nature* **450**, 1062-1065 (2007).
- (2) Hayward, M. A.; Green, M. A.; Rosseinsky, M. J.; Sloan, J. Sodium hydride as a powerful reducing agent for topotactic oxide deintercalation: synthesis and characterization of the nickel(I) oxide LaNiO₂. *J. Am. Chem. Soc.*, **121**, 8843-8854 (1999).

Piezoelectricity of wurtzite materials: A first-principles study

Hiro Yoshi Momida,^{a,*} Tamio Oguchi^b

a: Institute of Scientific and Industrial Research (SANKEN), Osaka University, Japan

b: Center for Spintronics Research Network, Osaka University, Japan

Email: momida@sanken.osaka-u.ac.jp

Piezoelectric wurtzite materials such as ZnO and GaN have received a lot of attention as energy-harvesting and piezotronics device materials. The wurtzite materials, especially AlN, have another advantage of applicability in high-temperature environments such as sensors in automobile engines, because of the good thermodynamic stability of their noncentrosymmetric crystal structures even at high temperatures. However, the piezoelectric constants of wurtzite-type materials are generally much smaller than those of the perovskite-type materials such as $\text{Pb}(\text{Zr}_x\text{Ti}_{1-x})\text{O}_3$ by a few orders. It remains a challenge to explore better piezoelectric materials. Among the wurtzite materials, the highest piezoelectricity has been experimentally discovered for $\text{Sc}_x\text{Al}_{1-x}\text{N}$ (about 25 pC/N for $x \sim 0.5$). Novel materials superior to $\text{Sc}_x\text{Al}_{1-x}\text{N}$, have not been synthesized yet as there are no clear and general materials-design criteria practically usable for enhancing the piezoelectricity of wurtzite materials.

In this study, we calculate longitudinal piezoelectric constants (e_{33}) of more than a dozen binary wurtzite materials, which are listed in the crystal structure databases, by the first-principles methods, and we study relations between the piezoelectric constants and several material parameters using the statistical-learning methods (1). The results show that the wurtzite materials with high e_{33} generally have small lattice constant ratios (c/a) almost independent of constituent elements, and approximately expressed as $e_{33} \propto c/a - (c/a)_0$ with the ideal lattice constant ratio $(c/a)_0$. We find that this simple relation also holds for highly-piezoelectric ternary materials such as the calculated e_{33} values of $\text{Sc}_x\text{Al}_{1-x}\text{N}$ (2). Therefore, this material-design criterion can be applicable to the case in doped ternary materials. Based on the insight above, we have conducted a computational search for highly-piezoelectric wurtzite materials by identifying materials with smaller c/a . Effects of in-plane strain on piezoelectricity of AlN, element-combination effects in LiX ($X = \text{halogen elements}$), and element-doping effects into ZnO are examined. The result shows that the piezoelectricity of ZnO can be significantly enhanced by partial substitutions of Zn with Ca. Though the calculated value of e_{33} of $\text{Ca}_x\text{Zn}_{1-x}\text{O}$ is still smaller than that of $\text{Sc}_x\text{Al}_{1-x}\text{N}$, we expect that $\text{Ca}_x\text{Zn}_{1-x}\text{O}$ is at a definite advantage in materials cost and natural resource in abundance of constituent elements.

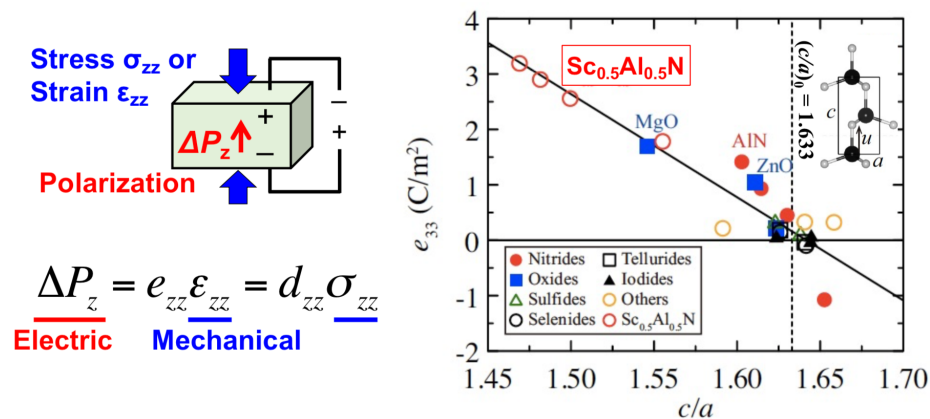


Figure 1: Calculated piezoelectric constants (e_{33}) vs. lattice constant ratio (c/a) of several wurtzite materials.

References:

- (1) Momida, H.; Oguchi, T. *Appl. Phys. Express* **11**, 041201 (2018).
- (2) Momida, H.; Teshigahara, A.; Oguchi, T. *AIP Adv.* **6**, 065006 (2016).

Nanostructure of Rh/SnO₂ catalyst under CO oxidation reaction

Naoto KAMIUCHI,^{a,*} Hideto YOSHIDA,^a

a: Sanken, Osaka University, Japan
Email: kamiuchi@sanken.osaka-u.ac.jp

Catalyst, which assists chemical reactions, is one of the most significant materials not only in the chemical industry but in solving environmental problems. For instance, solid catalysts are effective to purify harmful gases such as volatile organic compounds (VOCs) and automotive exhaust gases including hydrocarbon (HC), carbon monoxide (CO) and nitrogen oxide (NO_x). Precious metal catalysts supported on tin oxide (SnO₂) are well-known to catalyze the total oxidation of VOCs¹, and rhodium (Rh) catalysts are applied to purification of automotive exhaust gases². In this work, the nanostructure of Rh/SnO₂ in CO oxidation reaction are studied by environmental TEM (ETEM) observation and FT-IR measurement.

The catalyst of Rh/SnO₂ was prepared by the conventional impregnation method. The obtained powder was calcined at 400°C in air and was pretreated at 200°C in H₂ gas. The catalyst exhibits high activity for CO oxidation reaction even at room temperature.

The nanostructure was carefully observed using a Cs-corrected ETEM, which is a powerful tool to understand the nanostructure of catalysts in gaseous atmospheres. In the catalyst pretreated at 200°C in H₂, nanoparticles with the size of about 5 nm are stably supported on SnO₂ particles. On the other hand, Rh nanoparticles gradually disintegrate and diffuse to the surface of SnO₂ under the reaction environment of CO oxidation (1vol.% CO/air, 100 Pa) (Fig. 1). The disintegration is important because it leads to the increase of catalytically active sites.

FT-IR measurement was carried out for Rh/SnO₂ catalyst in CO and O₂ to understand the interaction between Rh and CO. Two types of Rh-CO species (Rh⁰(CO) and Rh⁺(CO)₂) are clearly confirmed under the CO atmosphere. The linearly CO-adsorbed Rh species decreases with the introduction of O₂. The result implies that one of the active sites for CO oxidation reaction can be the metallic Rh. The findings will contribute to the progress in the development of superior environmental catalysts.

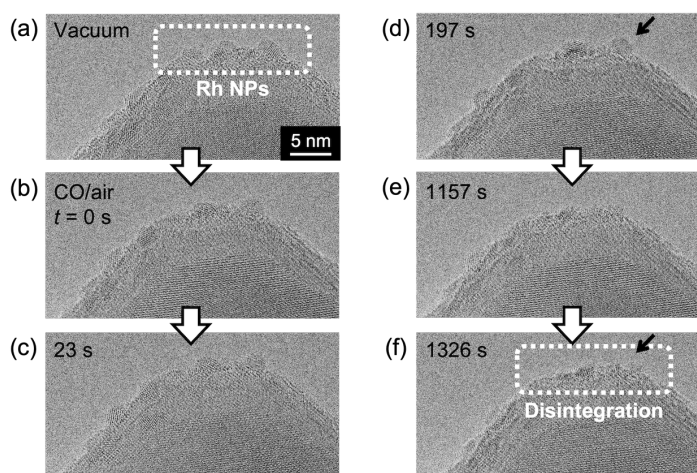


Figure 1: A series of ETEM images of Rh/SnO₂ catalyst under 1vol.% CO/air (100 Pa) at room temperature.

Acknowledgements

This work was supported by a Grant-in-Aid for Scientific Research (C), Grant No. 18K05201, a Grant-in-Aid for Young Scientists (B), Grant No. 26870332 and “Dynamic Alliance for Open Innovation Bridging Human, Environment and Materials” from the Ministry of Education, Culture, Sports, Science, and Technology, Japan (MEXT).

References:

- (1) Kamiuchi, N.; Mitsui, T.; Yamaguchi, N.; Muroyama, H.; Matsui, T.; Kikuchi, R.; Eguchi K. *Catal. Today* **157**, 415 (2010).
- (2) Haneda, M.; Sawada, H.; Kamiuchi, N.; Ozawa, M. *Chem. Lett.* **42**, 60 (2013).

DNA detection and discrimination using of nanogap single-molecule measurement

Yuki KOMOTO^a, Takahito OHSHIRO^a, Masateru TANIGUCHI^a.

*a: SANKEN (The Institute of Scientific and Industrial Research), Osaka University, Japan
Email: komoto@sanken.osaka-u.ac.jp*

Among the many biomolecules, DNA is extremely important in biology and medicine. There is a need for DNA sequencing technology with higher throughput and readability of modified bases. Single molecule measurement is a promising candidate as a novel DNA sequencing technique. Single molecule measurements can directly measure the conductance of a single molecule passing through a metal nanogap. Therefore, it is expected to achieve a higher throughput sequencing technique that can read modified bases. We have performed single molecule measurements of DNA and RNA using the Mechanically Controllable Break Junction method which is one of single-molecule measurement. The obtained single molecule signals were assigned to bases based on the current level. By assembling the fragment sequences, quantitative analysis of miRNAs was performed with single-molecule measurement.[1] Furthermore, we performed single molecule measurements of one of the modified bases, ethylated guanine (N^2 -Et-dG) and guanine to show that our method can read modified bases. The modified bases showed higher conductance due to their electronic states. The obtained single-molecule signals were used to build a machine learning model. The machine learning model succeeded in correctly discriminate modified base with an accuracy of 0.77.[2] Single molecule measurement can be applied to various biomolecules because the conductance of a single molecule is directly measured. We utilized single molecule measurement to detect modified bases of fluorinated DNA used as anti-cancer drugs [3] and methylated DNA associated with cancer.[4] Single molecule measurement can be applied not only to modified bases but also to the identification of neurotransmitters diffused from brain [5] and amino acids.[6] Thus, single molecule measurement has shown potential as a novel method for biomolecule detection.

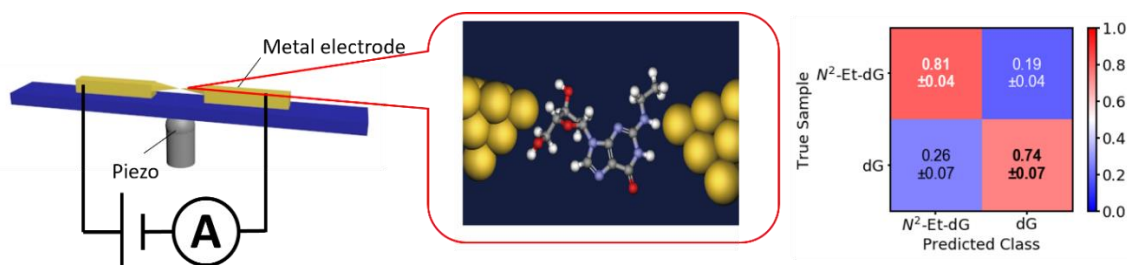


Figure 1: Schematic view of single-molecule measurement of modified DNA base, N^2 -Et-dG and discrimination result of the modified DNA.

References:

- (1) T. Oshiro et al., *Sci. Rep.*, 8, 1(2018)
- (2) Y Komoto et al., *Chem. Commun.*, 56, 14299 (2020)
- (3) T. Oshiro et al., *Sci. Rep.*, 9, 3886(2019)
- (4) T. Oshiro et al., *Sci. Rep.*, 11, 19304(2021)
- (5) Y Komoto et al., *Sci. Rep.*, 10, 1 (2020)
- (6) T. Ohshiro et al., *Nat. Nanotech.*,9,835(2014)

Improvement of water repellency of fluoroalkyl (meth)acrylate-based polymer with chemical and physical approaches

Hiroki YAMAGUCHI^{a,*}

a: Technology and Innovation Center, Daikin Industries, Ltd., Japan

Email: hiroki.yamaguchi@daikin.co.jp

Water repellency is one of the important surface properties that is closely related to many industries and our lives. Higher performance of water repellent material is expected to become a customer requirement as its range of applications expand as we understand better and better the occurring phenomenon. Therefore, in this presentation, we report an example of improving the water repellency of an (meth)acrylate-based polymer having a fluoroalkyl (Rf) groups at the side chain by a chemical and a physical approach.

As a chemical approach, we designed a copolymer that introduces comonomer so that the main chain becomes rigid¹. Figure 1 (a) shows the relationship among the ratio of the comonomer in the copolymer, the sliding angle, which is an index for evaluating dynamic water repellency and is deeply related to actual use, and the glass transition temperature (T_g) of the copolymer calculated from the differential scanning calorimeter (DSC). It was confirmed that the sliding property of copolymer was improved as the T_g of the copolymer increased. We assume that the higher T_g of the prepared material reduces the original molecular motion of the polymer chains as well as the surface reorientation occurring when water comes into contact with the polymer surface.

In the chemical approach, there is a certain limit to the improvement of water repellency, for example, static water repellency is reported to be 119° ². A popular approach is to combine chemical approach to have a good starting repellency and then add fine structures as physical approach to improve water repellency. However, the mechanical strength is usually weak due to these fine surface structures making the final material unsuitable for practical applications. We have demonstrated hereby that a coating thin film using fine silicone particles modified with Rf-methacrylate (SiPRf) could potentially solve the physical vulnerability issue. It was possible to produce a coating film that provides so-called superhydrophobicity with a static contact angle of over 150° with improved wear resistance by adjusting SiPRf/resin ratio in the coating film as demonstrated in Figure 1 (b).

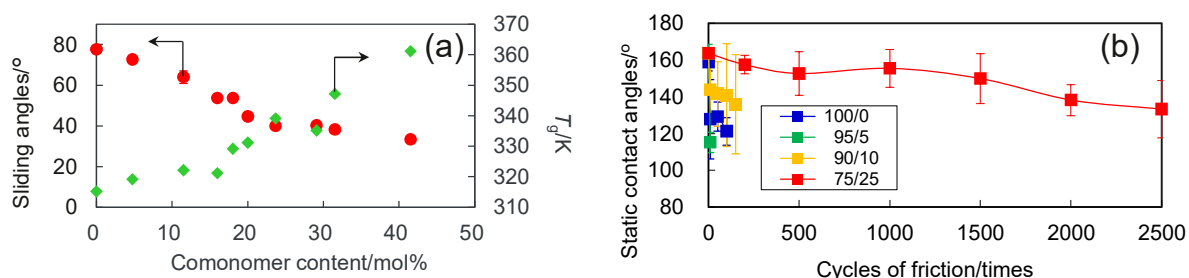


Figure 1: (a) Water sliding angle and values of T_g measured by DSC and (b) Performance of wear resistance for SiPRf/resin = 100/0, 95/5, 90/10, 75/25 (w/w) thin film by spin coat.

References:

- (1) Yamaguchi, H.; Hiraga, K.; Kubota, K.; Inamasu, R.; Morita, M. *Chem. Lett.* **50**, 1714 (2021).
- (2) Nishino, T.; Meguro, M.; Nakamae, K.; Matsushita, M.; Ueda, Y. *Langmuir* **15**, 4321 (1999).

Development of Perovskite Solar Cells

Taisuke MATSUI*, Hiroshi HIGUCHI, Takayuki NISHIHARA, Teruaki YAMAMOTO and Yukihiro KANEKO

Technology Division, Panasonic Corporation

Email: matsui.taisuke@jp.panasonic.com

Perovskite solar cells have recently attracted great interest for next generation solar cells such as low-cost, light-weight, and/or flexible solar cells. While power conversion efficiency has reached as high as conventional widely used crystal Si solar cells¹, long-term stability and large area module production need to be improved for practical use. We found stability and crystal quality of perovskite films are improved by addition of small amount of alkaline metals such as Cs and Rb²⁻⁴, which enables to achieve highly stable and large area perovskite solar cells.

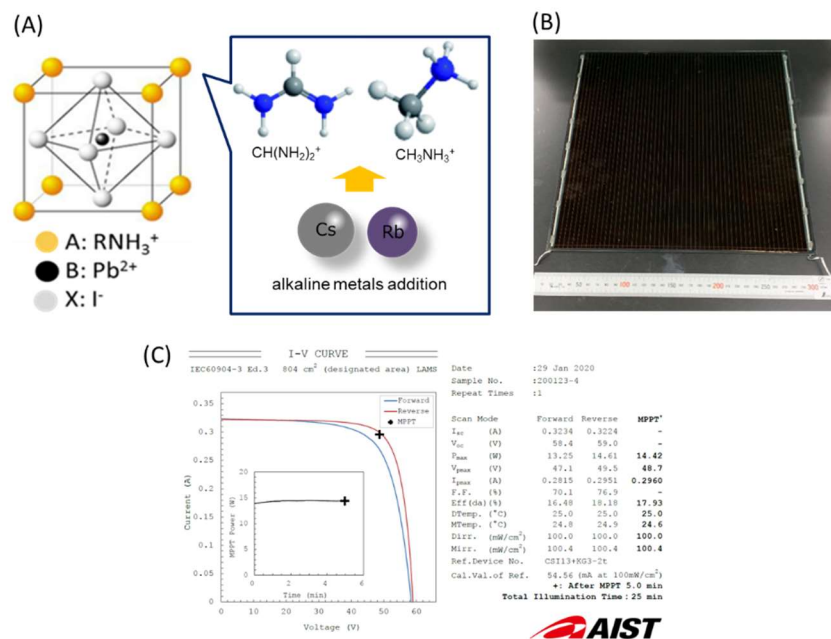


Figure 1: (A)structure of a perovskite material (B)appearance of perovskite a photovoltaic module, (C)certified efficiency of a perovskite photovoltaic module.

As a result, we achieved more than 90% retention in power conversion efficiency after dump-heat test (85°C-85%, 1000h) and world highest power conversion efficiency of 17.9% at the area of 804cm² among large-area perovskite photovoltaic modules⁵. These results show great potential for practical use in near future.

References:

- (1) Best Research-Cell Efficiency Chart
<https://www.nrel.gov/pv/assets/pdfs/best-research-cell-efficiencies-rev211117.pdf>
- (2) M. Saliba, T. Matsui, J.-Y. Seo, K. Domanski, J.-P. Correa-Baena, M. K. Nazeeruddin, S. M. Zakeeruddin, W. Tress, A. Abate, A. Hagfeldt, M. Grätzel, Energy Environ. Sci. 9, 1989–1997 (2016).
- (3) M. Saliba, T. Matsui, K. Domanski, J.-Y. Seo, A. Ummadisingu, S. M. Zakeeruddin, J.-P. Correa-Baena, W. R. Tress, A. Abate, A. Hagfeldt, M. Grätzel. Science 354, 206–209 (2016).
- (4) T. Matsui, T. Yamamoto, T. Nishihara, R. Morisawa, T. Yokoyama, T. Sekiguchi, T. Negami, Adv. Mater. 31, e1806823 (2019)
- (5) Champion Photovoltaic Module Efficiency Chart
<https://www.nrel.gov/pv/assets/pdfs/champion-module-efficiencies.pdf>

Wafer-Scalable Graphene Sensors for Biochemical Detection in Ionic Liquids

Hiroko MIKI, Atsunobu ISOBAYASHI, Tatsuro SAITO, Yoshiaki SUGIZAKI, Hideyuki TOMIZAWA*

Corporate Research & Development Center, Toshiba Corporation
Email: hideyuki1.tomizawa@toshiba.co.jp

Demands on biosensors are growing as significantly powerful tools for quick medical diagnostics. Development of a number of biosensors with surface plasmon resonance (SPR),¹ immunochromatography,² and graphene field effect transistors (GrFETs)³⁻⁴ are reported. Graphene is a material which has two dimensional sp² bonded carbons with exceptionally high carrier mobility.⁵ With these properties, GrFETs are expected to constitute highly sensitive sensors. Ionic liquids are liquids that are composed of solely ions, and a various kinds of cations and anions are known to form ionic liquids. Due to their unique properties such as non-volatility, high viscosity and hygroscopicity, ionic liquids are widely studied in the field of basic science and engineering.^{6,7} Structure of ionic liquids are suggested to be heterogeneous, and local structures may exist.⁸ Recently, a number of studies on biological application are also reported⁹⁻¹⁰. Streptavidin-biotin binding in ionic liquids studied with SPR biosensors are reported.¹¹ Ionic liquids with biotinylated imidazolium cations were used in the study. The enzymatic activity and its long-term retention of urease in several kinds of ionic liquids were found to be superior to conventional buffers.¹² In this study, we measured I_d (drain current) - V_g (gate voltage) characteristics during the hydrolysis of urea catalyzed by urease and the streptavidin-biotin binding in ionic liquids by using GrFET sensors that were fabricated on silicon substrates by semiconductor process. GrFETs are highly sensitive to the surface condition of graphene. Since the I_d - V_g characteristics strongly reflects the surface condition of graphene, GrFET has strong potential to enable highly sensitive biosensing. We selected the hydrolysis of urea by urease as a model system for enzymatic reactions and streptavidin-biotin binding for the interaction of protein with probe molecules. The observed I_d - V_g characteristics were evaluated whether biosensing was possible in ionic liquids.

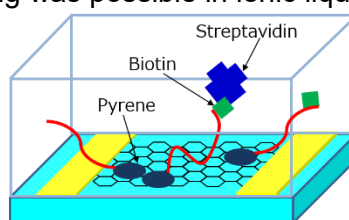


Figure 1: Schematic figure of the graphene sensor for streptavidin-biotin binding detection.

References:

- (1) Singh P. *Sensors and Actuators B: Chemical*, **229**, 110 (2016).
- (2) Endo F. *et al. PLoS One.*, **12**, 2 (2017).
- (3) Ohno Y. *et al. Jpn. J. Apply. Phys.*, **50**, 070120-1-4 (2011).
- (4) Mohanty N.; Berry V. *Nano Lett.*, **8**, 4469 (2008).
- (5) Novoselov K.S. *et al. Nature*, **438**, 197 (2005).
- (6) Welton T. *Chem. Rev.*, **99**, 2071 (1999).
- (7) Seddon K.R. *J. Chem. Technol. Biotechnol.*, **68**, 351 (1997).
- (8) Triolo A. *et al. J. Phys. Chem. B*, **111**, 4641 (2007).
- (9) Patel R.; Kumari M.; Khan A. *Appl. Biochem. Biotechnol.* **172**, 3701 (2014).
- (10) Benedetto A.; Ballone P. *ACS Sustainable Chem. Eng.*, **4**, 394 (2016).
- (11) Ratel M. *et al. Anal. Chem.*, **85**, 5770 (2013).
- (12) Kaneko K.; Kawai K. presented at Consortium of Biological Science, Kobe, Japan, December, 2017.

Atomic Scale Simulations for Pseudocapacitive MXene electrode

Yasuaki OKADA,^{a*} James M. GOFF,^{b,c} Francisco Marques dos SANTOS VIEIRA,^b
Nathan D. KEILBART,^{b,d} and Ismaila DABO,^b

a: Murata Manufacturing Co., Ltd., Japan

*b: Department of Materials Science and Engineering, Materials Research Institute,
The Pennsylvania State University, United States*

c: Sandia National Laboratory, United States

d: Lawrence Livermore National Laboratory, United States

Email: okd_y@murata.com

MXenes have gathered much attention as a novel class of two dimensional materials, discovered by Barsoum and Gogotsi^{1,2}. Their large specific surface area and high tunability of electrochemical properties as a function of the transition metal and surface terminal group make them excellent candidates for pseudocapacitor and battery electrodes. In this study, we performed first-principles and grand canonical Monte Carlo calculations^{3,4} combined with voltage-dependent two dimensional cluster expansion models and predicted charge storage behavior of MXene electrodes as pseudocapacitor for a range of transition metal compositions⁵. We found that $M_3C_2O_2$ MXene electrodes consist of group-VI transition metals have up to 80% larger areal energy densities than typical $Ti_3C_2O_2$ electrodes owing to their larger Faradaic voltage window. The size of the pseudocapacitive voltage window is affected by the range of oxidation states of transition metals in MXene electrodes.

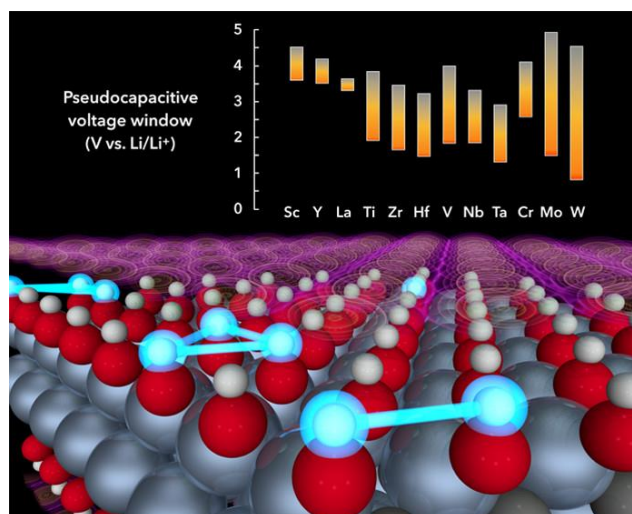


Figure 1: Schematic of MXene electrode surface and pseudocapacitive voltage windows

References:

- (1) Naguib, M.; Come, J.; Dyatkin, B.; Presser, V.; Taberna, P.; Simon, P.; Barsoum, M. W.; Gogotsi, Y. *Electrochemistry Communications* **16**, 61-64 (2012).
- (2) Anasori, B.; Lukatskaya, M. R.; Gogotsi, Y. *Nature Reviews Materials* vol. **2**, 16098 (2017).
- (3) Keilbart, N.; Okada, Y.; Feehan, A.; Higai, S.; Dabo, I. *Phys. Rev. B.* 2017, **95**, No. 115423.
- (4) Okada, Y.; Keilbart, N.; Goff, J. M.; Higai, S.; Shiratsuyu, K.; Dabo, I. *MRS Adv.* 2019, **4**, 1833–1841.
- (5) Goff, J. M.; dos Santos Vieira, F. M.; Keilbart, N. D.; Okada, Y.; Dabo, I. *ACS Appl. Energy Mater.* 2021, **4**, 3151–3159.

Laboratory Automation for High-level Expression of Recombinant Protein-A in Escherichia coli

Daichi Suemasa,^a Eiji Hayashi,^{a,*} Isao Aritome,^a Akiko Sato^b
Takeshi Asano,^c Atsushi Shibai,^d Saburo Tsuru,^c Chikara Furusawa,^{c,d}

a: Tsukuba Research Laboratories, JSR Corporation, Japan

b: JSR-UTokyo Collaboration Hub, CURIE, JSR Corporation, Japan

c: Graduate School of Science, The University of Tokyo, Japan

d: Center for Biosystems Dynamics Research, RIKEN, Japan

Email: eiji_hayashi@jsr.co.jp

pET expression system in combination with Escherichia coli BL21(DE3) is one of the organisms of choice for the production of recombinant protein A and it has become the most popular expression platform.¹ In this system, it is known that isopropyl-D-1-thiogalactopyranoside (IPTG) and glucose play important roles.^{2,3} Both materials are essential for the production of protein and growth of E.coli. However, since these substances interfere with each other's functions,²⁻⁵ it is necessary to confirm the optimum value of each addition amount in advance.

In this study, we used automated culture system (Fig.1) in order to search the optimum condition of IPTG and glucose amount by automatic parallel experiment. This system which is designed by Chikara Furusawa's group⁶, can automatically culture cells and measure the growth rate of E. coli over time.

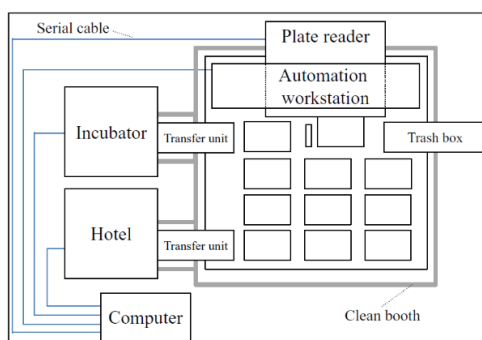


Figure 1: The automated culture system consists of Biomek® NX span8 laboratory automation workstation connected to a microplate reader, shaker incubator, and microplate hotel.⁶

Protein A producing E. coli BL21(DE3) under the pET expression system were cultured in an automated experiment in which IPTG and glucose were combined at various concentrations. As a result of this automated experiment, optimal concentrations of IPTG and glucose for high yields of protein A were obtained. Further information about the experimental results will be reported in the conference.

This study was performed in the course of our research & development activities on protein A.

References:

- (1) Studier, F. W.; Moffatt, B. A. *J Mol. Biol.* **189**, 113 (1986).
- (2) Neubauer, P.; Hofmann, K.; Holst O.; Mattiasson, B.; Kruschke, P. *Appl. Microbiol. Biotechnol.* **36**, 739 (1992).
- (3) Wurm, D. J.; Veiter, L.; Ulonska, S.; Eggenreich, B.; Herwig, C.; Spadiut, O. *Appl. Microbiol. Biotechnol.* **100**, 8721 (2016).
- (4) Magasanik, B. *Cold Spring Harb. Symp. Quant. Biol.* **26**, 249 (1961).
- (5) Ullmann, A. *Res. Microbiol.* **147**, 455 (1996).
- (6) Horinouchi, T.; Minamoto, T.; Suzuki, S.; Shimizu, H.; Furusawa, C. *J Lab. Autom.* **19**, 478 (2014).

High-sensitive strain sensing using tunnel magnetoresistance effect

Kenta SAITO,^a Akiko IMAI,^a Tomohiro KOYAMA,^{a,b*} and Daichi CHIBA^{a,b*}

a: SANKEN, Osaka University, Japan

b: Center for Spintronics Research Network, Osaka University, Japan

Email: saiken11@sanken.osaka-u.ac.jp

Development of magnetoresistive random access memory (MRAM) and high-density hard disk drive has been realized by the progress of spintronics, where both the electron charge and spin are utilized. Following the giant magnetoresistance (GMR) effect firstly discovered in 1988,^{1,2} the tunnel magnetoresistance (TMR) effect showing much higher MR ratio at room temperature has been the subject of research.³ The TMR effect is observed in the system consists of two ferromagnets separated by a thin insulator layer, called magnetic tunnel junction (MTJ), and the tunnel resistance changes dramatically depending on the relative angle between the magnetization directions of two ferromagnets.

So far, the main target of spintronics has been magnetic recording. In this study, we aim to utilize the magnetoresistance effect for mechanical strain sensing, which is completely new route of spintronics application. Our group has demonstrated the spintronics strain sensor using the GMR device fabricated on a flexible substrate.^{4,5} When the tensile strain is applied to the flexible substrate, the magnetization of the free layer rotates through the magnetoelastic effect and the relative angle between the free layer and pinned layer changes. Thus, the strain can be detected as the resistance change. The purpose of this study is to improve the sensitivity of spintronics strain sensor using not the GMR effect but the TMR effect that shows 20-50 times higher MR ratio. In this study, we have successfully fabricated the MTJ structure on the flexible substrate. Moreover, in the present flexible TMR device, we have observed the strain-induced resistance change much larger than the GMR device, suggesting that more effective strain sensing is possible using it.

The authors thank S. Ota and A. Ando for his technical help. This work was partly supported by JST A-Step (Grant No. JPMJTR20T7), and Spintronics Research Network of Japan.

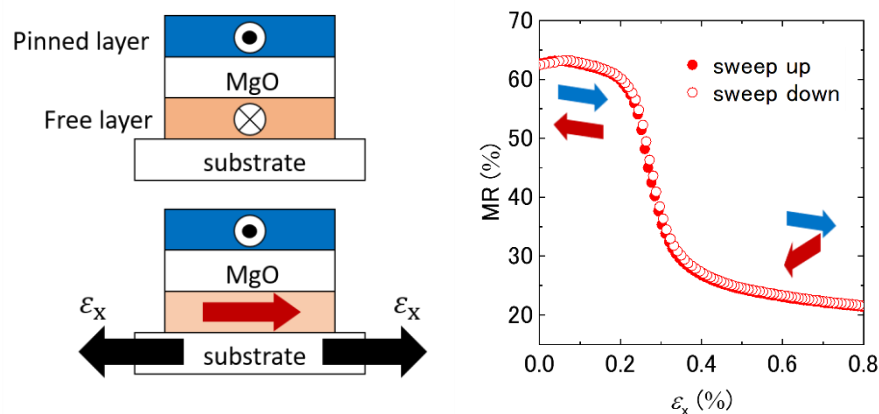


Figure 1: The tensile strain (ε_x) dependence of MR. The magnetization of the free layer rotates toward the direction of strain. When $\varepsilon > 0.24$, the resistance changes linearly.

References:

- (1) Baibich, M. N.; Broto, J. M.; Fert, A.; Van Dau, F. N.; Petroff, F.; Eitenne, P.; Creuzet, G.; Friederich, A.; Chazelas. *J. Phys. Rev. Lett.* **61**, 2472 (1988).
- (2) Binasch, G.; Grünberg, P.; Saurenbach, F.; Zinn, W. *Phys. Rev. B* **39**, 4828 (1989).
- (3) Miyazaki, T.; Tezuka, N. *J. Magn. Magn. Mater.* **139**, 231 (1995).
- (4) Ota, S.; Ando, A.; Chiba, D. *Nat. Electron.* **1**, 124 (2018)
- (5) Matsumoto, H.; Ota, S.; Ando, A.; Chiba, D. *Appl. Phys. Express* **114**, 132401 (2019).

Temperature Dependence of Spin-Orbit Torque in Ferromagnet/Antiferromagnet-insulator/Heavy-metal Tri-layer Structure

Toshiaki Morita,^a Kento Hasegawa,^{a,b} Tomohiro Koyama,^{a,c,d} Daichi Chiba,^{a,c}

a: SANKEN, Osaka University, Japan

b: Department of Applied Physics, The University of Tokyo, Japan

c: Center for Spintronics Research Network, Osaka University, Japan

d: PRESTO, JST, Japan

Email: tmorita11@sanken.osaka-u.ac.jp

Spintronics, which was opened by the discovery of the giant magnetoresistance effect in 1988, is electronics that utilizes the spin degree of freedom of electrons¹⁻³. Spintronic memory devices are attracting attention as one of the basic technologies supporting highly-advanced-information society. For example, a magnetic tunnel junction (MTJ), which composed of two ferromagnetic (FM) layers separated by a thin insulator layer, is used as a storage element in magnetic random access memory (MRAM). In MRAM, information is nonvolatily stored as a magnetization direction of the FM layer in a MTJ element. Thus, MRAM may open a route to a realization of normally-power-off computing.

Current MRAM mainly uses spin transfer torque (STT) for writing information, where the magnetization switching is driven by the transfer of angular momentum between conduction and localized electrons. STT-driven magnetization switching is known to have a problem of durability because a charge current flows through the insulator layer⁴. To cope with this problem, magnetization switching induced by a new type of current-induced torque, called spin-orbit torque (SOT), in FM/heavy-metal (HM) bilayer structure has been vigorously studied⁵. In the SOT method, the spin current is generated by an in-plane charge current in HM layer through the spin-orbit interaction. This spin current flows into the FM layer, exerting a torque on the magnetization. SOT probably achieve high durability of MRAM devices, along with a high-speed information writing. However, the current density required for the SOT switching is extremely large. One of the solutions for this problem is to enhance the transmittance of the spin current at the FM/HM interface. It has been reported that the spin current transmittance is improved by inserting NiO, which is an antiferromagnet (AFM) insulator, at the FM/HM interface. To investigate the effect of NiO insertion on SOT, we focus on the temperature dependence of SOT in FM/NiO/HM tri-layer structure because the magnetic property of NiO is easily controlled by temperature.

The work is supported by Program for Leading Graduate Schools: "Interactive Materials Science Cadet Program", the PRESTO from JST (Grant No. JPMJPR21B5), and the Spintronics Research Network of Japan. A part of this work was conducted using facilities at the Low Temperature Center, Osaka University.

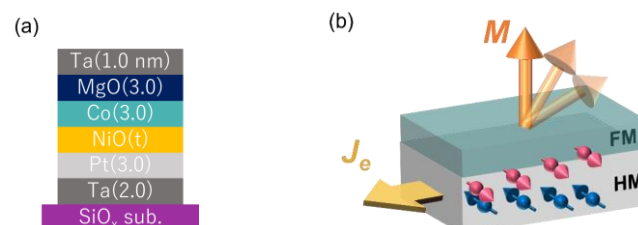


Figure 1: (a) Structure of the sample. (b) Schematic illustration of SOT.

References:

- (1) Baibich, M. N. *et al.*, *Phys. Rev. Lett.* **61**, 2472 (1988).
- (2) Grunberg, P. *et al.*, *Phys. Rev. Lett.* **57**, 2442 (1986).
- (3) Binasch, G. *et al.*, *Phys. Rev. B* **39**, 4828 (1989).
- (4) Huai, Y. *et al.*, *Appl. Phys. Lett.* **84**, 3118 (2004).
- (5) Miron, I. M. *et al.*, *Nature* **476**, 189 (2011).

Noise Characterization of Organic Transistor Circuit for Light Sensor Array

Rei KAWABATA,^{a,b,*} Teppei ARAKI,^{a,b} Mihoko AKIYAMA,^a Naoko KURIHIRA,^a
Takafumi UEMURA,^a Tsuyoshi SEKITANI^{a,b}

a: SANKEN (The Institute of Scientific and Industrial Research), Osaka University, Japan

b: Graduate School of Engineering, Osaka University, Suita, Osaka, Japan.

Email: araki@sanken.osaka-u.ac.jp, sekitani@sanken.osaka-u.ac.jp

Flexible sensors are mechanically bendable and stretchable to follow the surface of an object, allowing for continuous detection under event^[1,2]. In particular, organic materials have been studied in the development of flexible sensors for applications of medical and healthcare, robotics and infrastructure^[3]. Light is useful for non-destructive and non-invasive detection from the surface of the object^[4]. If a flexible optical sensor can be adapted to a wide range of wavelengths, molecular information can be detected instantaneously. Furthermore, a large-area flexible optical sensor can be realized by arraying a single cell comprising a photodetector and a transistor switch. The light sensor array enables a two-dimensional imaging and would contribute to abnormality detection from a chemical perspective.

However, organic transistors are susceptible to electromagnetic noise. Electromagnetic waves (visible light, infrared rays, radio waves) that exist around us reduce the signal-to-noise ratio of the light sensor cell. Therefore, it is important to evaluate the characteristic of organic transistors and their circuits under the illumination of the electromagnetic waves, and to examine concrete methods to reduce the noise.

In this study, an evaluation system was established to characterize the organic transistors and their circuits under illumination of visible light, infrared light, and terahertz. An organic transistor circuit was affected by all electromagnetic waves, changing the output characteristics by up to about 20%. In the evaluation using an inverter circuit as an amplifier, the hum noise exceeded a signal amplitude in an output signal. Noise reduction less than 1% was achieved with a barrier structure under illumination of visible light. The details will be presented in this symposium. We are going to establish noise reduction methods to a wide range of wavelengths (visible ~ THz) for the development of the imager of molecular information in the flexible optical sensor.

References:

- (1) Kaltenbrunner, M., et al. *Nature* **499**, 458–463 (2013).
- (2) Sugiyama M., et al., *Nature Electronics* **2**, 351–360 (2019).
- (3) Jiang, C., et al. *Science* **363**, 719-723 (2019)
- (4) Suzuki, D., et al. *Nature Photonics* **10**, 809–813 (2016).

End-to-end Model-based Gait Recognition using Synchronized Multi-view Pose Constraint

Xiang LI^{a,*}, Yasushi MAKIHARA^a, Chi XU^a, Yasushi YAGI^a

a: SANKEN, Osaka University, JAPAN

Email: li@am.sanken.osaka-u.ac.jp

We propose an end-to-end model-based cross-view gait recognition¹ which employs pose sequences and shapes extracted by human model fitting. Specifically, we consider a problem setting where gait sequences from single different views are given as a pair to match in a test phase, while asynchronous multi-view gait sequences are given for each subject in a training phase. This work exploits multi-view constraint in the training phase to extract more consistent pose sequences from any views in the test phase, unlike the existing methods do not consider them. For this purpose, as shown in Figure 1, given asynchronous multi-view gait sequences, we introduce a phase synchronization step in the training phase so that we can impose pose consistency at each synchronized phase in a temporally up-sampled phase domain. We then train our network by minimizing a loss function based on the synchronized multi-view pose constraint as well as shape consistency, temporal pose smoothness, recognition accuracy, etc in an end-to-end manner. We also introduce the synchronization step in a test phase to reduce intra-subject variations caused by asynchronous pose features. Experimental results on the OU-MVLP and CASIA-B datasets show that the proposed method achieves the state-of-the-art performance for both gait identification and verification scenarios, especially a great improvement in terms of the pose representations.

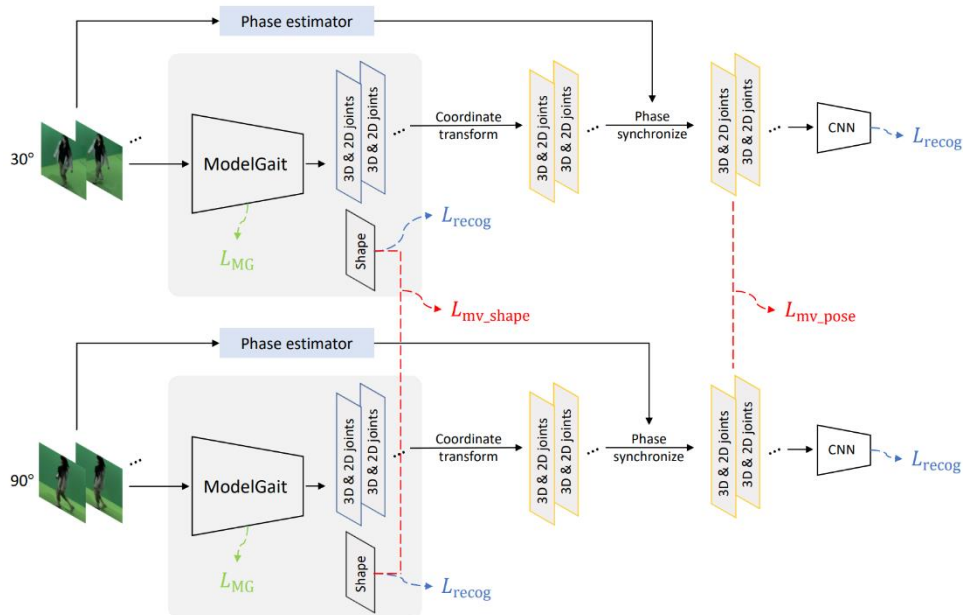


Figure 1: Overall framework of the proposed method. The backbone network, ModelGait², independently extracts initial pose and shape features for multi-view RGB input sequences. The phase estimator estimates the phase information of the input sequences for the latter synchronization. Networks parameters are shared for different view angles.

References:

- (1) Li, X.; Makihara, Y.; Xu, C.; Yagi, Y. "End-to-end Model-based Gait Recognition using Synchronized Multi-view Pose Constraint," Int. Workshop on Human-centric Trustworthy Computer Vision: From Research to Applications, online, pp. 4106-4115, Oct. 2021.
- (2) Li, X.; Makihara, Y.; Xu, C.; Yagi, Y.; Yu, S.; Ren, M. "End-to-end Model-based Gait Recognition," ACCV, online, pp. 3-20, Dec. 2020.

Real-Time Gait-Based Age Estimation and Gender Classification from a Single Image

Chi XU^{a,*}, Yasushi MAKIHARA^a, Ruochen LIAO^a, Hiroataka NIITSUMA^a, Xiang LI^a,
Yasushi YAGI^a, and Jianfeng LU^b

a: SANKEN, Osaka University, Japan

b: Nanjing University of Science and Technology, China

Email: xu@am.sanken.osaka-u.ac.jp

We propose a unified real-time framework for gait-based age estimation and gender classification that uses just a single image¹, which reduces the latency in video capturing compared with the existing methods based on a gait cycle. To cope with the problem of lacking motion information in the input single image, we first reconstruct a gait cycle of a silhouette sequence from the input image via a gait cycle reconstruction network (i.e., PA-GCR in Fig. 1). The reconstructed gait cycle is then fed into a state-of-the-art gait recognition network (i.e., GaitSet in Fig. 1) for feature representation learning, which is further used to obtain the class of the gender and the estimated probability distribution of integer age labels.

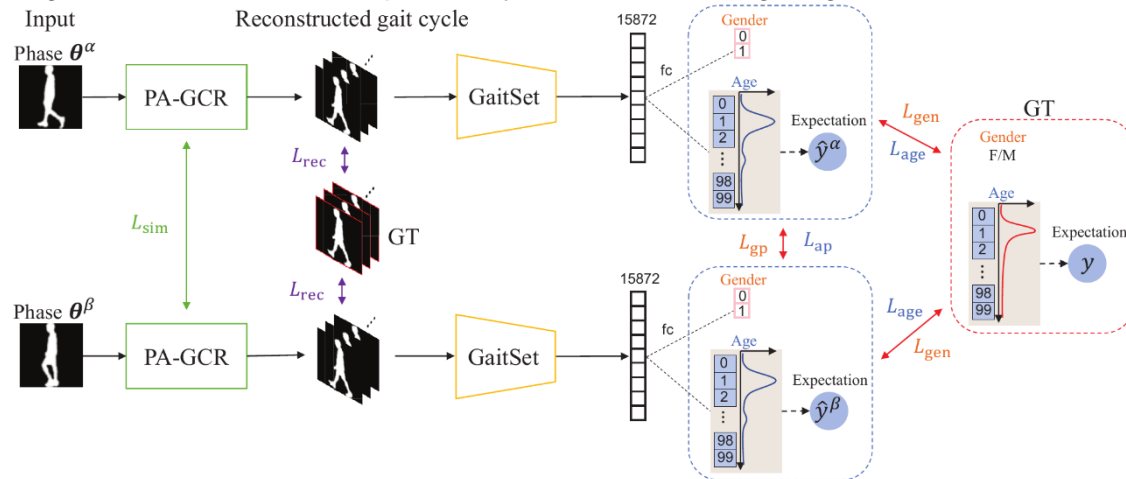


Figure 1: Overview of the proposed method. The digits represent the dimension of the features. GT and fc denote the ground truth and fully connected layer, respectively. In the training phase, a pair of single images from the same subject is used as the inputs, and the network parameters are shared; in the test phase, only a single image is fed into the network to output the estimated gender class and age label distribution, and the expectation of the label distribution is computed as the final estimated age value.

Unlike the existing methods focusing on the gait sequences captured from the side view, the proposed method is applicable to the gait images from an arbitrary view with a single trained model, which is more suitable for real-world application scenarios (e.g., automatic access control). Stand-alone and client-server online systems were implemented based on the proposed method, which validates the real-time/online property in actual scenes. The experiments on the world's largest multi-view gait dataset demonstrate the effectiveness of the proposed method, which achieves performance improvement compared with the benchmark algorithms.

References:

- (1) Xu, C.; Makihara, Y.; Liao, R.; Niitsuma, H.; Li, X.; Yagi, Y.; Lu, J. "Real-Time Gait-Based Age Estimation and Gender Classification from a Single Image," Proc. of the IEEE Winter Conf. on Applications of Computer Vision 2021 (WACV 2021), online, pp. 3460-3470, Jan. 2021.

Towards Open-domain Chatbot Talking from Explainable Behaviors

Hayato FUTASE* and Kazunori KOMATANI

SANKEN, Osaka University, Japan
 Email: h-futase@ei.sanken.osaka-u.ac.jp

Open-domain chatbots are systems that have been constructed based on neural networks in recent years and talk with human users via text on various topics. It needs to consider behavior, knowledge, and emotion to build a friendly relationship with the user.^{1,2} The behaviors in such systems have been defined as a set of several sentences. We focus on the chatbot that talks based on behaviors representing a person's experiences and habits. We enable the chatbot to talk consistently by acquiring many behaviors through its utterance and selecting the appropriate behaviors corresponding to the topics at that time. There are two types of behaviors: behaviors that a user gives in advance and behaviors that the chatbot can guess from its utterance. Some contradiction that cannot be explained appears during a conversation, and it would degrade the user's trust. However, by simply removing almost all behaviors that contradicted the chatbot's behaviors, we only leave with a few behaviors. Then the chatbot does not tend to give utterances that supported a behavior at that time topic to a user. In this study, we investigate the relationship between the behaviors of open-domain chatbots and the contradiction to having the chatbot take many behaviors corresponding to a topic. Furthermore, we evaluate the contradiction regarding explainability and human likeness.

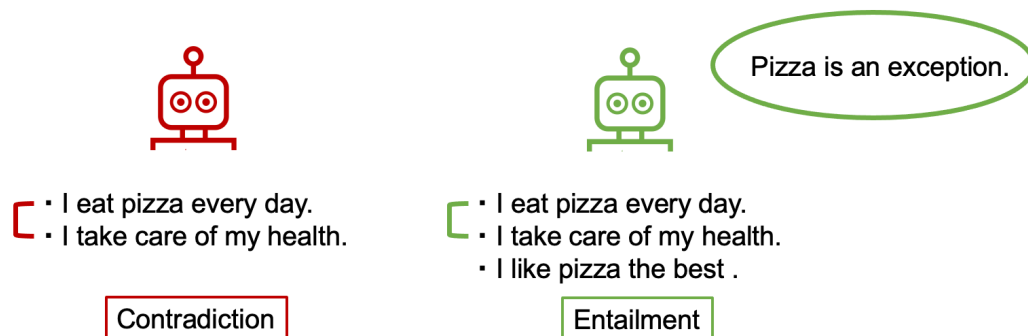


Figure 1: Example of a contradiction that can be resolved by adding a single behavior. The two behaviors of the red (left) chatbot are contradictory. The green (right) chatbot, on the other hand, also has a contradictory relationship between the two behaviors. Its contradiction is justified in eating pizza every day even though it is concerned about its health; because it has the behavior "I love pizza.". Therefore, there is no contradiction, and the two behaviors coexist from both the chatbot's and the user's points of view.

References:

- (1) Minlie Huang and Xiaoyan Zhu. ACM Transactions on Information Systems, Vol. 1, No. 1, Article 1 (2020).
- (2) Jing Xu, Arthur Szlam, and Jason Weston. arXiv2017.07567v1 (2021).

Skin-Adhesive, -Breathable and -Compatible Cellulose Nanopaper for Comfortable On-Skin Biosignal Measurement

Yintong HUANG,*

Teppei ARAKI, Kojiro UETANI, Tsuyoshi SEKITANI, Masaya NOGI, Hirotaka KOGA

SANKEN, Osaka University, Japan

Email: huangyt15@sanken.osaka-u.ac.jp

On-skin electronics, that can transfer biosignal from skin surface to machines through the electrodes mounted on flexible substrates, is an emerging research field in flexible electronics. Recently, the rapid developments of on-skin electronics have been observed in a wide spectrum of applications¹, especially in home healthcare which becomes a remarkably important technology during the international crisis of COVID-19. To date, many efforts have been made towards human-friendly on-skin electronics for efficient biosignal transfer by creating skin-adhesive substrates, ultra-thin substrates, and breathable substrates, etc. to optimize the conformal contact with skin and skin-comfortability.

Wood-derived cellulose nanopapers, a class of natural polymer-based materials, provide various attractive properties including human-friendliness, flexibility, disposability, and reusability,² demonstrating their possibility as substrate materials towards the trends of human-friendly and sustainable electronics. However, although cellulose nanopapers have been widely used for flexible electronics, cellulose nanopaper-based on-skin electronics remains unexplored. The major reasons are the unavailable skin-adhesion and the limited breathability resulting from the densely packed structures within cellulose nanopapers, which are serious drawbacks for comfortable on-skin biosignal measurement.

Herein, a skin-adhesive, -breathable, and -compatible cellulose nanopaper was fabricated by tailoring porous structures for on-skin biosignal measurement (Figure 1). The porous cellulose nanopaper gains high skin-adhesion strength of 2.3 N cm^{-2} with re-adhesive ability, without adding additional chemicals. Besides, it has outstanding breathability (water vapor transmission rate: $2912 \pm 101 \text{ g m}^{-2} \text{ day}^{-1}$) resulting from the high porosity of 44.1%, and also shows good skin-compatibility. To confirm its performance for on-skin electronics, the porous cellulose nanopaper was mounted with gold electrode and successfully applied for electroencephalogram (EEG), electromyography (EMG), and electrocardiogram (ECG) signals monitoring. The gold electrode-mounted nanopaper showed wrinkle-resistance, possibility for long-term, and reusability after detaching from skin. This porous cellulose nanopaper provides an ideal platform for human-friendly and sustainable on-skin biosignal measurement.

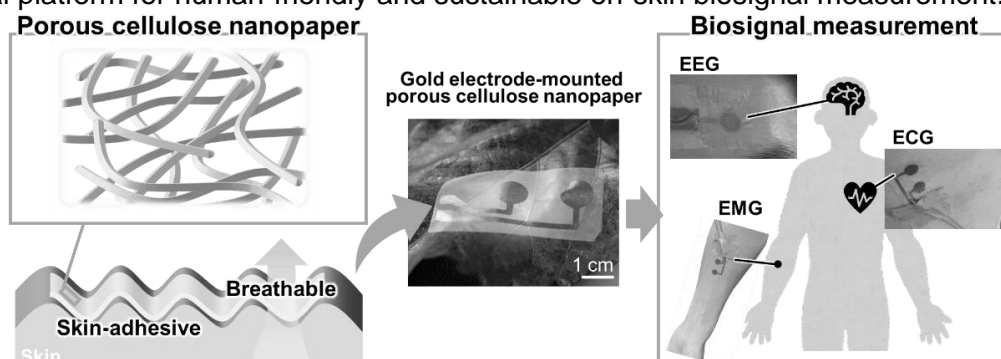


Figure 1: Schematics of the cellulose nanopaper with porous structures providing skin-adhesion and -breathability, and its applications for biosignal measurements.

References:

- (1) Liu, U.; et al. *ACS Nano* **11**, 9614 (2017).
- (2) Jiang, F.; et al. *Adv. Mater.* **30**, 1703453 (2018).

Acknowledgments: This work was supported by JSPS Grant-in-Aid for JSPS Fellows (JP21J21971 to Y. H.) and by JST FOREST Program (JPMJFR2003 to H. K. and JPMJFR2022 to T.A). The authors thank Ms. N. Kurihira.

Tuning of the electrical properties of carbonized cellulose nanopaper

Kazuki OMOTE,^a Kojiro UETANI,^b Masaya NOGI,^b Hirotaka KOGA^{b,*}

a: Graduate School of Engineering, Osaka University, Japan

b: SANKEN, Osaka University, Japan

Email: hkoga@eco.sanken.osaka-u.ac.jp

Rapid increase in the global usage of electronic products has accelerated the consumption of non-renewable resources, leading to a growing emphasis on the active use of renewable resources in future electronics. The cellulose nanofiber paper (nanopaper) has recently shown great promise as renewable wood-derived substrate materials for green electronics, owing to its high optical transparency and biodegradability. However, the use of cellulose nanopaper in electronic applications is limited to insulating and dielectric components, because the electrical conductivity of nanocellulose is very low (ca. 10^{-13} S cm^{-1}).

Here we report the tuning of the electrical properties of the cellulose nanopaper by a carbonization. The cellulose nanopaper was carbonized at different temperatures (650, 750, 1000, and 1100 °C). Then, the electrical properties of the carbonized cellulose nanopaper, such as electrical conductivity, and carrier concentration and mobility, were evaluated the Hall effect measurement. The electrical conductivity of the cellulose nanopaper was significantly increased by carbonization; the electrical conductivity was increased from ca. 10^{-3} to 10^2 with an increase of the carbonization temperatures from 650 to 1100 °C (Fig. 1a). As shown in Fig. 1b and c, the carrier concentration was increased from $\sim 10^{15}$ to 10^{20} cm^{-3} by increasing the carbonization temperature, while the carrier mobility were not largely affected by carbonization temperatures (0.235–0.673 $\text{cm}^2 \text{V}^{-1} \text{s}^{-1}$). These results suggested that the electrical conductivity of the carbonized cellulose nanopaper can be tuned by changing its carrier concentration rather than mobility. Notably, the major carrier types were n-rich at 650 °C and p-rich at ≥ 750 °C, suggesting that electrons and holes dominated the electrical conduction of the cellulose nanopapers carbonized at 650 and ≥ 750 °C, respectively. From the results of FT-IR and Raman analyses, it was suggested that the progressive growth of sp^2 -hybridized carbon domains gradually increases the carrier concentration and electrical conductivity of carbonized cellulose nanopaper, while the major carrier type can be determined by the chemical state of the disordered carbon regions. This study will pave the way for the renewable cellulose nanopaper semiconductor.

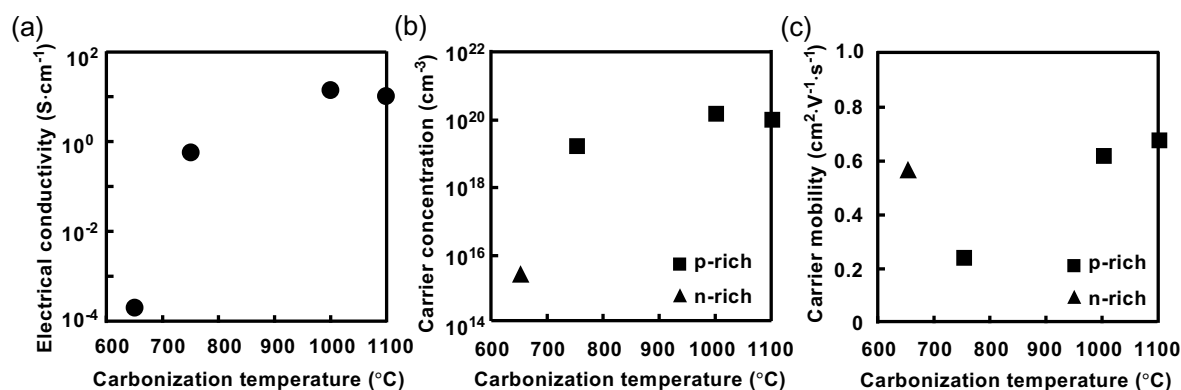


Figure 1: (a) Electrical conductivity, (b) carrier concentration, and (c) carrier mobility of the nanocellulose papers carbonized at different temperatures.

Acknowledgement: This work was partially supported by the JST FOREST Program (JPMJFR2003 to H. K.).

Redispersed and aggregation behavior of surface-modified TEMPO-oxidized cellulose nanofibers as anticorrosion layers on electrodes

Chenyang LI, * Takaaki KASUGA, Kojiro UETANI, Hiroataka KOGA, Masaya NOGI

SANKEN, Osaka University, Japan
Email: lichenyang@eco.sanken.osaka-u.ac.jp

Electrochemical migration, as one of the most severe reliability issues for electronics, will occur once an electronic device is powered on with water present inside.¹ This process causes the growth of metallic dendrites thus short circuit failure for electronics (Fig 1a). Waterproofing sealings have been utilized on electronics for preventing water going inside for decades, but this conventional corrosion protection is usually petrochemical-based which does not meet the requirement of sustainable society. Therefore, developing a new coating formulation that based on sustainable resources is of great importance for development of electronics with high-reliability.

Our group's previous work has tried to coat TEMPO-oxidized cellulose nanofibers (with sodium carboxylate groups, TOCN-Na), a wood-derived renewable nanomaterial, on copper electrodes for electrochemical migration inhibition, and it exhibited a totally new inhibition strategy. Submersing the coated electrodes into water, instead of waterproofing, the dried film dispersed into water and formed hydrogel layers at anodes due to the negatively charged TOCN-Na nanofibers (Fig 1b). The dense network of hydrogel enabled cross-link with copper ions to prevent dendrites growing thus inhibiting electrochemical migration.² The previous work has shown the basic concept of short circuit inhibition by TOCN-Na, however, a deeper understanding of the mechanism involved is needed to optimize the effect.

The carboxylate groups on TOCNs can provide places to modify their surface structures by converting the counter-ions of carboxylate groups to other ions. In this work, surface-modified TOCNs with different alkyl ammonium carboxylates were coated on copper electrodes for testing their electrochemical migration inhibition performances (Fig 1c). The hydrogel formation processes of surface-modified TOCNs were studied by *in situ* observation and *ex situ* characterization. With high redispersion ability, the TOCNs were more easily/quickly dispersed into water; while with high conductivity, the dispersed TOCNs showed more attraction by electric fields and tended to form dense hydrogel at anode for effective inhibition. These results will help to understand using TOCNs coating for anticorrosion protection of electronics more clearly, which can be expanded to other cellulose nanofibers and sustainable hydrophilic polymers for the use of improving electronics' reliability.

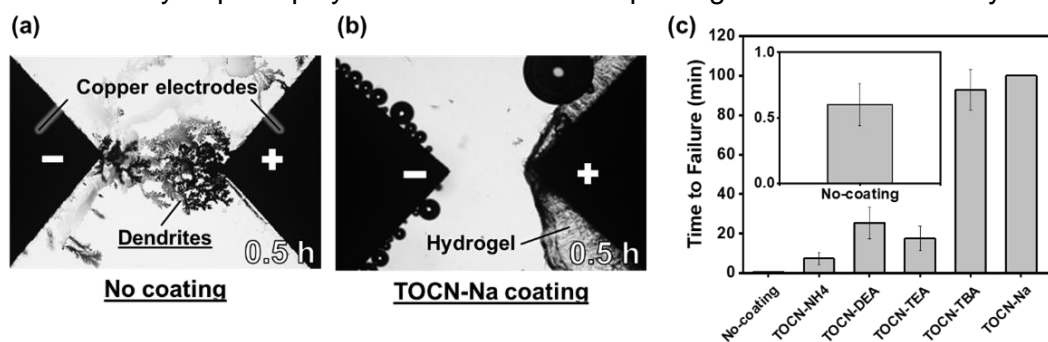


Figure 1: Water submersion test of copper electrodes. (a) Without and coating, dissolved copper ions formed dendrites to cause a short circuit failure; (b) While with a TOCN-Na coating, nanofibers formed a hydrogel layer at the anode, providing protection against short circuit failure; (c) Protection time by different types of TOCN coatings.

References:

- (1) Minzari, D., et al., *Corros. Sci.* **53**(10), 3366-3379 (2011).
- (2) Kasuga, T., et al., *ACS Appl. Nano Mater.* **4**(4), 3861-3868 (2021).

Chitin nanofiber-derived elastic carbon aerogel for frequency-tunable microwave absorption

Xiang LI,* Luting ZHU, Kojiro UETANI, Masaya NOGI, Hirotaka KOGA

SANKEN, Osaka University, Japan
Email: xian.li@eco.sanken.osaka-u.ac.jp

Electromagnetic pollution has been a severe environmental problem that interferes the operation of precise devices.¹ Carbon aerogels have been actively investigated as promising materials to prevent electromagnetic pollution, due to their light weight and effective microwave absorption (less than -10 dB). With the frequency expansion of the next-generation wireless devices, the carbon aerogels are desired to afford frequency-tunable absorption. However, the absorption frequency of the carbon aerogels is depended on their intrinsic dielectric properties, leading to the difficulty in the frequency-tunable absorption. Thus, it remains a challenge to tune the absorption frequency of a single carbon aerogel in accordance with the situation.

To overcome this challenge, herein, a chitin nanofiber-derived elastic carbon aerogel (CCA) and its compression strategy are proposed. The CCA was fabricated by unidirectional freeze-drying of the crab shell-derived chitin nanofibers/water dispersion and the subsequent carbonization. Owing to the uniform honeycomb-like structures with thin nanofibrous channel walls, the CCA showed super elastic properties; it can withstand 100,000-cycles compression (40% strain) and recovery in the vertical direction of the honeycomb-like channels (Figure 1a). The CCA offered the strong microwave absorption of -80.4 dB at 11.1 GHz, which was much superior to the effective absorption level (-10 dB). It should be noted that the strongest microwave absorption could be tuned from 11.1 to 11.6 and 11.8 GHz by changing the compression strain from 0 to 20 and 40%, respectively (Figure 1b). These results were provided by the tunable thicknesses of the elastic CCA by reversible compression; the decreased thicknesses of the CCA by compression (within 40% strain) were well-matched with the 1/4 wavelength of the increased microwave frequency, thus affording the frequency-tunable microwave absorption. Further compression (60 and 80% strain) led to drastic weakening the microwave absorption performance of the CCA due to the impedance mismatching, which was caused by its increased electrical conductivity. The CCA exhibited the frequency-tunable microwave absorption property even after 1000-cycles compression fatigue treatment (Figure 1c), indicating the mechanical stability and super elasticity after fatigue treatment. Thus, this study provides a new guidance for designing strong and frequency-tunable microwave absorption materials.

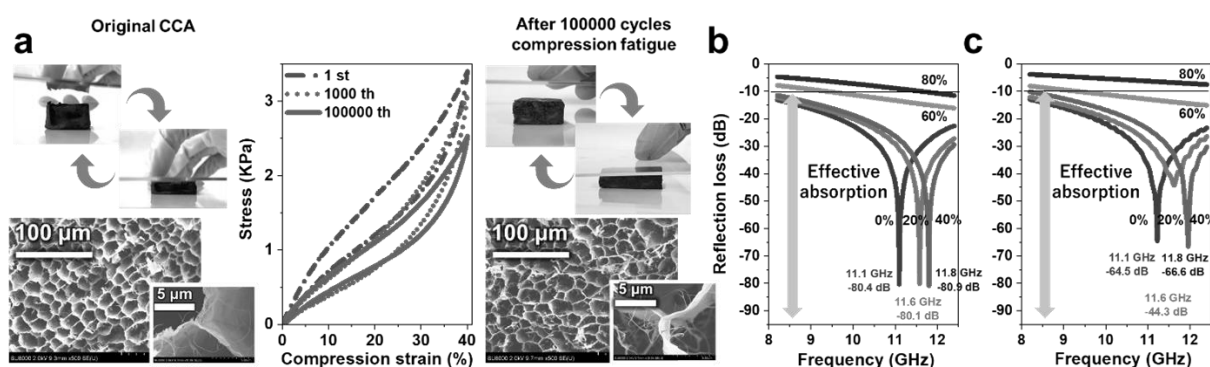


Figure 1: (a) Optical and cross-sectional FE-SEM images, and 1-100,000 cycles stress-strain curves of the CCA. Reflection loss values of the CCA at the different compression strain (0-80%) (b) before and (c) after 1000 cycles compression fatigue treatment.

Reference:

(1) Balci, O.; Polat, E.; Kakenov, N.; Kocabas, C. *Nat. Commun.* **6**, 6628 (2015).

Acknowledgements: This work was partially supported by the JST SPRING Program (JPMJSP2138 to X. L.), and by the JST FOREST Program (JPMJFR2003 to H. K.).

Carbonized Chitin Nanopaper and Its Photothermal Heating Performance

Thanakorn YEAMSAKSAWAT, Jun SHIRAHAMA, Xiang LI, Luting ZHU,
Kojiro UETANI, Masaya NOGI, Hiroataka KOGA *

SANKEN, Osaka University, Japan
Email: hkoga@sanken.osaka-u.ac.jp

Photothermal materials, which can absorb and convert light into thermal energy, have attracted much attention toward utilization of renewable solar energy. Among many photothermal materials, porous carbons are intensively attractive, owing to their advantages of broadband light absorption¹. From the viewpoint of sustainable development, renewable biomass-derived porous carbons are desired, and the exploration of their suitable molecular structure for photothermal performances has become one of the crucial challenges.

Here we report fabrication and photothermal performances of the cellulose and chitin nanofiber-derived porous carbons. Cellulose and chitin, which are the two most abundant biomass resources on earth, can be extracted as nanofibers from wood and crab shell, respectively. In this study, cellulose and chitin nanofibers were fabricated into the paper with porous nanostructures and then carbonized at 500 °C under nitrogen atmosphere. We found that the carbonized chitin nanopaper exhibits a superior photothermal performance than the carbonized cellulose nanopaper; the temperature of the carbonized chitin nanopaper was increased from room temperatures to ca. 73 °C under solar light irradiation (1 sun, AM1.5) for 700 s, which was higher than those of the carbonized cellulose nanopaper (ca. 69 °C) (Fig. 1a). The high photothermal performance was mainly attributed to the higher light absorption property of the carbonized chitin nanopaper at 250–2500 nm, which represents the wavelength range of solar light (Fig. 1b). According to the XRD and UV-vis-NIR analyses, these results would be derived from the molecular structure of the carbonized chitin, including more graphitized carbon structures for broadband light absorption and nitrogen-doped carbon structures for the reduced bandgap (0.60 and 0.71 eV for carbonized chitin and cellulose, respectively). Thus, the chitin nanofibers are expected as a promising precursor to fabricate the biomass-derived porous carbons with high photothermal performances.

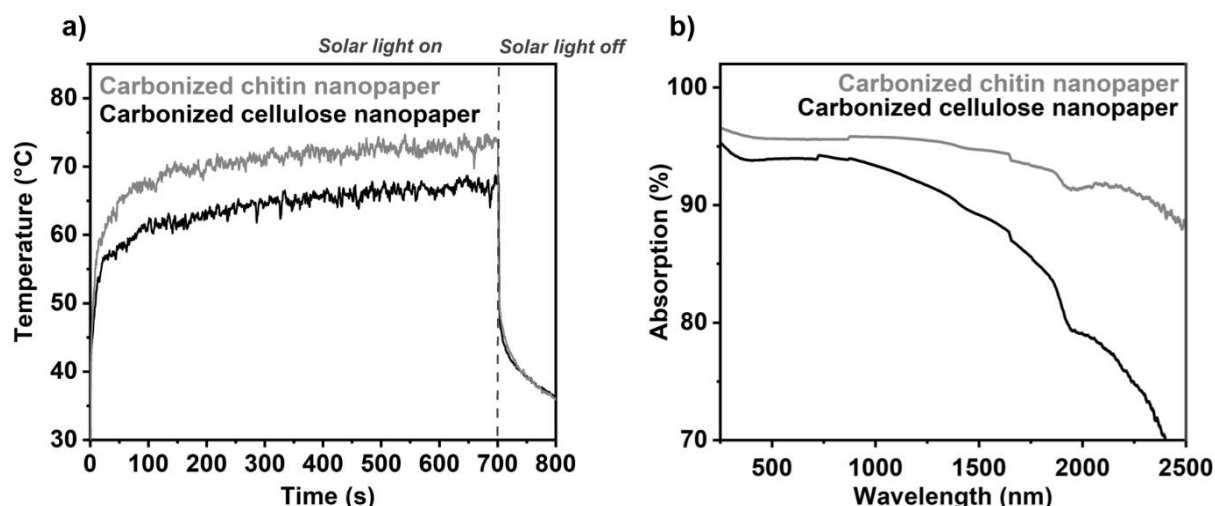


Figure 1: (a) Surface temperature versus time under solar light irradiation (1 sun) for 700 s and (b) UV-vis-NIR adsorption spectra of the carbonized cellulose and chitin nanopapers.

Reference:

(1) Han, B.; Zhang, Y. L.; Chen, Q. D.; Sun, H. B.; *Adv. Funct. Mater.* **28**, 1802235 (2018).

Anisotropic Thermally Conductive Papers with Uniaxially Aligned Carbon Fibers Embedded in Cellulose Nanofiber Matrix

Kosuke TAKAHASHI,^{a,*} Hiroataka KOGA,^b Masaya NOGI,^b Kojiro UETANI^{b,*}

a: Graduate School of Engineering, Osaka University, Japan

b: SANKEN, Osaka University Japan

Email: uetani@eco.sanken.osaka-u.ac.jp

Since the heat generation density in electronic devices has been increasing as the devices became smaller, heat removal measures have become an urgent issue.¹ In particular, there is a need to develop anisotropic thermally conductive base materials that conduct and dissipate heat in a specific direction in order to reduce thermal interference between adjacent elements. In this study, we focused on two fibrous materials, cellulose nanofiber (CNF) and pitch-based carbon fiber (CF), to develop the anisotropic thermally conductive base material. The tunicate-derived CNFs have the inherent self-agglomeration property and show 3~10 times higher thermal conductivity (2.5 W/mK) than polymers. Moreover, the CNF paper has been used as the heat dissipation substrate for the cutting-edge kirigami electronics.² The CF has been chosen as the thermal conductive filler because of its very high thermal conductivity (800 W/mK) and large structural anisotropy. By combining the physical advantages of CNFs and CFs and further aligning CFs in the specified direction, we expected that a base material with anisotropic heat conduction could be developed.

The randomly aligned CF/CNF papers were first prepared through the wet filtration method with the CF contents of 0, 5, 10, 15, and 20 wt%. As shown in Fig. 1a, with increasing the CF contents, the in-plane thermal diffusivity of the paper was significantly increased, whereas those in the through-plane direction remained almost the same. It is clear that the addition of CF to CNF paper improves the in-plane direction heat transfer property.

In order to further align CFs in the paper in one direction, the liquid phase 3D patterning method³ was employed (Fig. 1b). When the amount of CF added is 5%, the thermal diffusivities of uniaxially aligned CF/CNF paper showed 5.03, 1.78, and 0.15 mm²/s in the x, y, and z direction, respectively. We have succeeded in developing a paper having the in-plane anisotropic thermal diffusivity with an anisotropy of about three times in the x and y directions.

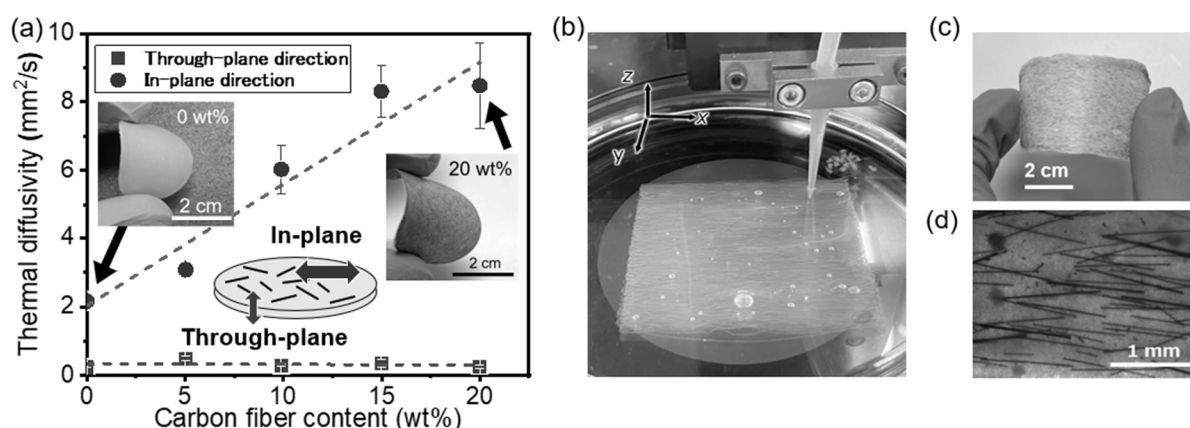


Figure 1: (a) The in-plane and through-plane thermal diffusivities of randomly aligned CF/CNF papers. (b) Formation process of the uniaxially aligned CF/CNF paper with the size of $\sim 7 \times 6$ cm² by the liquid phase 3D patterning. Typical appearance of uniaxially aligned CF/CNF paper (c) and a micrograph of the paper surface (d).

References:

- (1) Danowitz, A.; Kelley, K.; Mao, J.; Stevenson, J. P. *et al. ACM Queue* **10**, 10 (2012).
- (2) Uetani, K.; Kasuya, K.; Wang, J.; Huang, Y. *et al. NPG Asia Mater.* **13**, 62 (2021).
- (3) Uetani, K.; Koga, H.; Nogi, M. *Nanomaterials* **10**, 958 (2020).

Structure analyses of cellulose nanofibers prepared by TEMPO-mediated oxidation and potassium permanganate oxidation

Manabu MIZUKAMI, Takaaki KASUGA, Kojiro UETANI, Hirotaka KOGA, Masaya NOGI *

SANKEN, Osaka University, Japan
Email: nogi@eco.sanken.osaka-u.ac.jp

Pulp, the raw material for paper, is a 10-30 μm wide fiber composed of 3-15 nm wide cellulose nanofibers bundled together by hydrogen bonding. To disintegrate the pulp fibers into cellulose nanofibers, the pulp fibers are subjected to chemical pretreatments such as 2,2,6,6-tetramethylpiperidine 1-oxyl (TEMPO) -mediated oxidation¹, carboxymethylation², and potassium permanganate oxidation³ followed by minor mechanical disintegration. In this study, we focused on two of these chemical pretreatments, TEMPO-mediated oxidation and potassium permanganate oxidation, and prepared nanofibers with sodium carboxylate groups on the surface (Na^+ nanofibers) and nanofibers with carboxyl groups on the surface (H nanofibers). The morphology of the nanofibers and the transition of the functional groups on the surface of the cellulose nanofibers during the reaction process were investigated.

The cellulose nanofibers in softwood bleached kraft pulp are bundled by hydrogen bonds formed by C2, C3 and C6 hydroxyls on the surface of the nanofibers. Upon TEMPO-mediated oxidation of pulp fibers, the C6 hydroxyls on the surface of the nanofibers are converted to sodium carboxylate groups, and the nanofiber surface becomes negatively charged¹. As a result, the pulps were disintegrated into Na^+ nanofibers by electric double layer repulsion between the nanofibers (Fig. 1a). When the Na^+ nanofibers were immersed in hydrochloric acid, H nanofibers were obtained by protonation (Fig. 1b). On the other hand, potassium permanganate oxidation of pulp fiber yielded H nanofibers (Fig. 1c), and further immersion in sodium hydroxide solution was necessary to obtain Na^+ nanofibers. In the future, we plan to study the surface state of the nanofibers during TEMPO-mediated oxidation and potassium permanganate oxidation processes by FT-IR, zeta potential measurement, and XRD measurement.

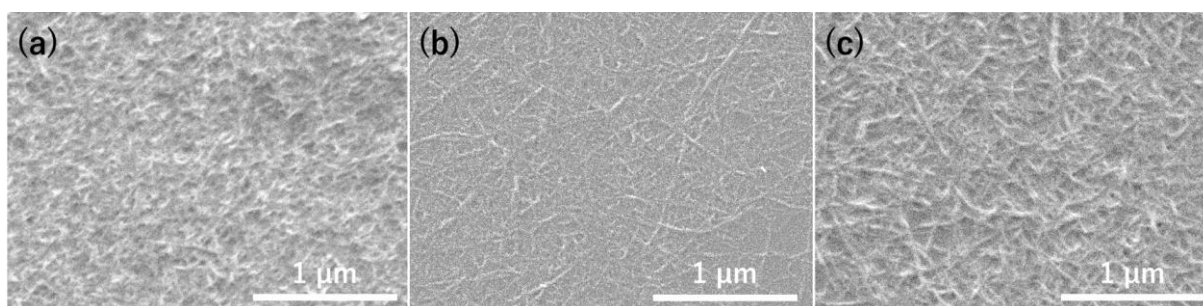


Fig. 1 FE-SEM images of (a) Na^+ cellulose nanofibers by TEMPO-mediated oxidation, (b) H cellulose nanofibers by TEMPO-mediated oxidation and (c) H cellulose nanofibers by potassium permanganate oxidation.

References:

- (1) Saito T. et al. *Biomacromolecules*, 2006, 7, 1687
- (2) Wågberg L. et al. *Langmuir*, 2008, 24, 784
- (3) Liu Y. et al. *Green Chem.*, 2021, 23, 8069

Acetylation of Cellulose Nanopapers Prepared by TEMPO-Mediated Oxidation

Yurika TERAOKA, Chenyang LI, Takaaki KASUGA, Hitomi YAGYU, Kojiro UETANI,
Hirotaka KOGA, Masaya NOGI*

SANKEN, Osaka University, Japan
Email: nogi@eco.sanken.osaka-u.ac.jp

As a novel material made of cellulose nanofibers, cellulose nanopaper exhibited high transparency, similar to that of glass. Among different types of cellulose nanopapers, cellulose nanopaper made of TEMPO-mediated oxidation of cellulose nanofibers shows high transparency and superior gas-barrier property, which makes it a potential food packaging material^{1,2}. However, the gas-barrier permeability of cellulose nanopaper can be reduced because of the high hygroscopicity of cellulose³. Chemical treatment methods, such as counterion exchange treatment to TEMPO-mediated oxidation of cellulose nanofibers, for reducing hygroscopicity have already been reported. In this study, we proposed an acetylation treatment for TEMPO-mediated oxidation of cellulose nanofibers, and the transmittance as well as hygroscopicity of the resulted nanopapers were evaluated.

TEMPO-mediated oxidation of cellulose nanofibers suspension with functional groups of sodium carboxylates was used as a starting material. Na⁺ type nanopaper was prepared by cast-drying the suspension onto an acrylic plate. For the preparation of H type nanopaper, the dried Na⁺ type nanopaper was soaked in 0.1M hydrochloric acid at room temperature for 2 h, then the wet nanopaper was washed thoroughly with water and re-dried. Acetylation treatment for nanopapers were prepared from the following procedure: Na⁺ type or H type nanopaper were dehydrated by acetone and placed in a mixture of 40 ml acetic acid, 50 ml toluene, and 2.5 ml perchloric acid. Then, 10 ml of acetic anhydride was added into the mixture with stirring for 1 h at room temperature, followed by washing thoroughly with isopropanol and re-drying. The obtained nanopapers were denoted as Acetylation-Na⁺ type nanopaper and Acetylation-H type nanopaper. All types of nanopaper were dried at 50 % relative humidity and 23 °C.

The obtained nanopapers (thickness: 50±10 μm) were clearly transparent (Fig 1a-1d), and the transmittance of nanopapers were improved by acetylation treatment. After acetylation, the total light transmittance (wavelength: 600 nm) increased from 90.6 to 92.5% for Na⁺ type nanopaper (Fig 2a) and from 90.6 to 92.3% for H type nanopaper, respectively (Fig 2b). The change of hygroscopicity after acetylation treatment will be future investigated by characterizing and comparing the density of nanopapers.

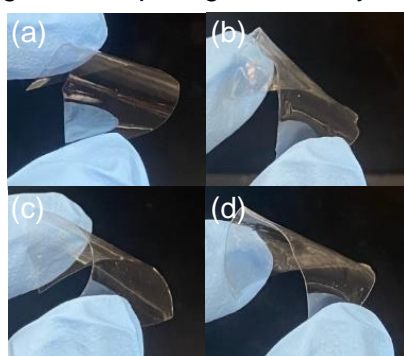


Figure 1: Appearance of nanopapers, (a) Na⁺ type, (b) H type, (c) acetylation-Na⁺ type, and (d) acetylation-H type.

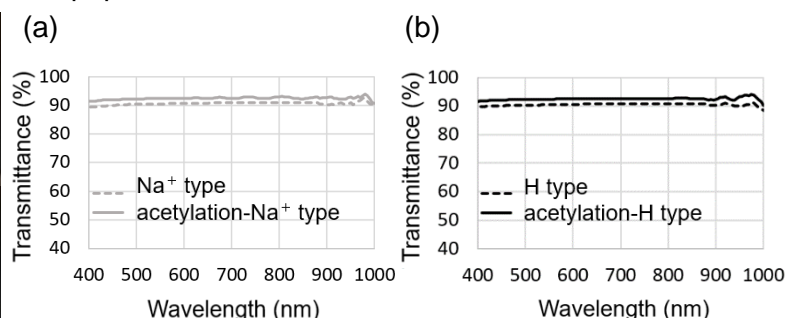


Figure 2: Change of total light transmittance after acetylation treatment for (a) Na⁺ type and for (b) H type.

References:

- (1) Shimizu, M. et al. *Biomacromolecules* **2014**, *15*, 4320–4325.
- (2) Fukuzumi, H. et al. *Cellulose* **2014**, *21*, 1553–1559.
- (3) Fukuzumi, H. et al. *Biomacromolecules* **2011**, *12*, 4057–4062.

Iodine-treated cellulose for photothermal heating

Jun SHIRAHAMA,^a Luting ZHU,^a Yintong HUANG,^a Thanakorn YEAMSUKSAWAT,^a
Kojiro UETANI,^b Masaya NOGI,^b Hiroataka KOGA^{b,*}

a: Graduate School of Engineering, Osaka University, Japan

b: SANKEN, Osaka University, Japan

Email: hkoga@eco.sanken.osaka-u.ac.jp

Carbonized biomass has recently attracted much attention as promising photothermal materials for efficient use of renewable solar-light energy as heat, due to light absorption in broad wavelength range and sustainability.¹ Cellulose is the most abundant and renewable biomass on earth. Because cellulose has poor photothermal heating performances due to its insufficient solar-light absorption, its carbonization has been attempted at high temperatures (over 500 °C) to ensure the broad-wavelength-range light absorption.² However, such high-temperature carbonization inevitably causes drastic carbon loss and volume shrinkage¹, leading to the solar-light absorption loss as well as the decreased heat capacity.

Here, we report the iodine (I₂)-mediated carbonization of cellulose to improve carbon yield and volume retention for effective photothermal heating. A cellulose fabric was treated at 200 °C with I₂ gas. Then, the formation of aromatic carbon rings was confirmed by the ¹³C nuclear magnetic resonance (NMR) analysis, while the cellulose treated at 200 °C without I₂ showed the similar molecular structure to the original cellulose (Fig. 1). In addition, elemental analyses indicated that the carbon content of the cellulose increased from 43 to 60 wt% and the hydrogen/carbon and oxygen/carbon ratios were decreased from 14 to 6 wt% and 117 to 50 wt%, respectively, after the treatment at 200 °C with I₂. These results suggested that the carbonization of cellulose can progress in the presence of I₂, possibly owing to the I₂-mediated dehydrogenation and deoxygenation reactions.

The cellulose fabric treated at 200 °C with I₂ showed the broad-wavelength light absorption from 250 to 2500 nm, which is consistent with the solar-light wavelength range, due to the carbonized molecular structure. Thereby, the treated cellulose fabric afforded photothermal heating from room temperatures to 70 °C under solar light (1 sun) irradiation, which was superior to that of the cellulose fabrics carbonized at 500 °C without I₂ (from room temperatures to 66 °C). While such conventional high-temperature carbonization at 500 °C caused low carbon yield (15 wt%), volume retention (44 vol%), and the resulting solar-light energy loss (2.37%), the I₂-mediated carbonization at 200 °C improved all of them (89 wt%, 74 vol%, 0.32%, respectively). Owing to the high carbon yield, the cellulose fabric treated at 200 °C with I₂ also provided higher heat capacity (40 mJ K⁻¹) than that carbonized at 500 °C without I₂ (6.2 mJ K⁻¹). Thus, our results highlight that the I₂-mediated carbonization of cellulose can improve its photothermal heating performances by its increased carbon yield and volume retention, paving a way for more effective utilization of biomass materials as photothermal materials.

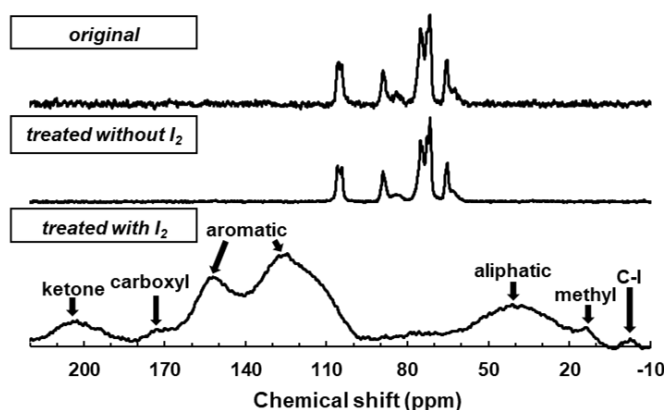


Figure 1: ¹³C NMR spectra of the original cellulose and the cellulose treated at 200 °C with I₂ and without I₂.

References:

- (1) Zhang, C.; Liang, H.; Xu, Z.; Wang, Z. *Adv Sci.* **6**, 1900883 (2019)
- (2) Huo, H.; Ma, Y.; Cheng, Y.; Cao, J. *Energy Environ. Sci Pollut Res.* (2021).

Large scale chemical bottom-up synthesis of nanostructured peroxo titanates

Do Hyung HAN,^a Hyunsu PARK,^a Tomoyo GOTO,^{a,b} Sunghun CHO,^a Tohru SEKINO^{a,*}

a: SANKEN (The Institute of Scientific and Industrial Research), Osaka University, 8-1 Mihogaoka, Ibaraki, Osaka, 567-0047, Japan

b: Institute for Advanced Co-Creation Studies, Osaka University, 1-1 Yamadaoka, Suita, Osaka, 565-0871, Japan

Email: sekino@sanken.osaka-u.ac.jp

Low dimension nanostructured titanate materials are interest in various fields due to their excellent physical and chemical properties, which mainly prepared through hydrothermal alkali treatment¹. However, this synthesis method has been carried out under high concentration alkali which has adversely affected the environmental aspects and productivity of materials. Recently, our research group reported an efficient method for synthesizing titanate nanostructures using a chemical bottom-up process². In this method, TiH₂ is used to prepare peroxo-titanium complex ion precursor and through previous research, conditions for NaOH concentration and pH for preparing the ion precursor have been established. In addition, it was confirmed that the synthesis of nanostructured titanate was possible from heating the prepared ion precursor at a low temperature of 100 °C under atmospheric pressure.

In this study, in order to investigate the effect of TiH₂ amount on the synthesis of peroxo-titanium complex ion precursor and titanate nanostructure used in our method, the synthesis was performed under various amounts of TiH₂. Compared to the previous study², it was possible to scale up to about 4 times, and at the same time, it led to the successful synthesis of peroxo-titanium complex ion within the corresponding area (10:1–2.5:1 of Na:Ti molar ratio). Figure 1. shows XRD patterns of titanate samples. It can be confirmed that layered sodium titanate was successfully formed through self-organization reaction between titanium-sodium ion species from the prepared ion precursor. Furthermore, samples synthesized under this Na:Ti molar ratio did not show any differences in crystalline structure and morphology. Interestingly, the precursor-derived peroxide bonding was detected in the synthesized titanate samples, which resulted in the optical band gap narrowing. Our results not only suggest an efficient synthetic route for mass production, but also the potential for application in photo-functional materials.

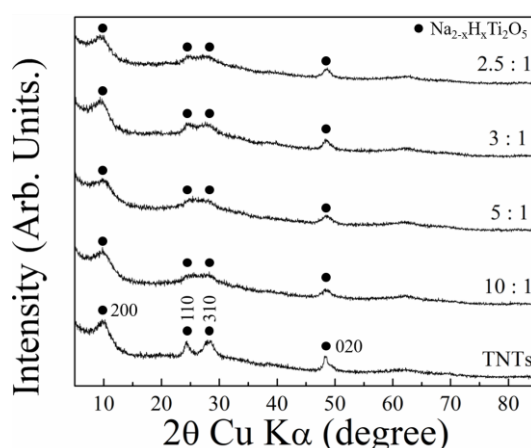


Figure 1: XRD patterns of titanate samples.

References:

- (1) Kasuga, T.; Hiramatsu, M.; Hoson, A.; Sekino, T.; Niihara, K. *Langmuir* **14**, 3160 (1998).
- (2) Park, H.; Goto, T.; Han, D.; Cho, S.; Nishida, H.; Sekino, T. *ACS. Appl. Nano Mater.* **3**, 7795 (2020).

Synthesis of one-dimensional nanostructures in low temperature

Sunghun Cho*, Hyunsu Park, Tomoyo Goto, Yeongjun Seo, Tohru Sekino

SANKEN, Osaka University, Japan
Email: shcho@sanken.osaka-u.ac.jp

One-dimensional (1D) nanostructures (e.g. wires, rods, ribbons and tubes) have received considerable attention owing to their distinct physical and chemical properties and potential applications in nanodevices.¹ Selenium, as an important elemental semiconductor, exhibits unique photoelectric and other promising properties, such as relatively high photoconductivity, low melting point, and it can be practically applied to solar cells, rectifiers, sensors, photographic exposure meters and serves as an ideal candidate for generating other functional materials.²

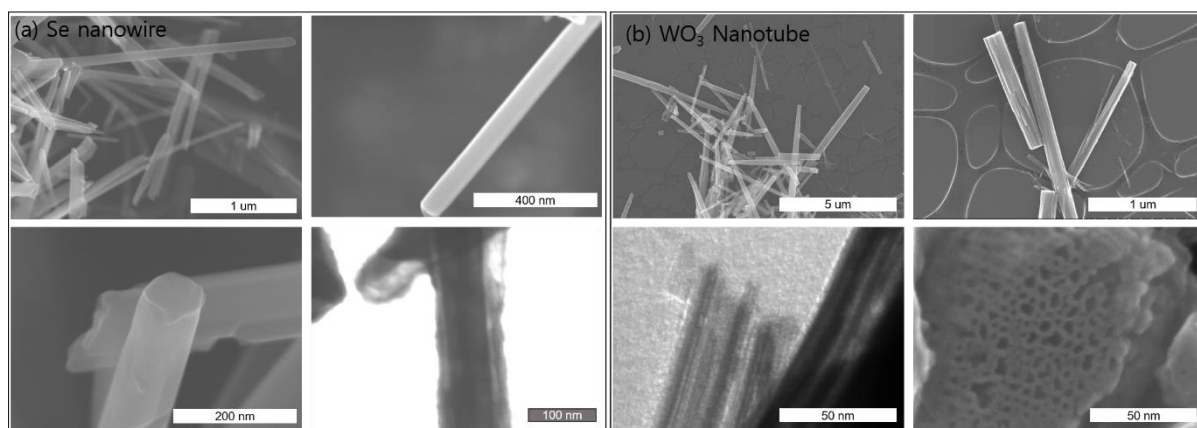


Figure 1: FESEM image of (a) Se nanowires and (b) WO_3 nanotubes.

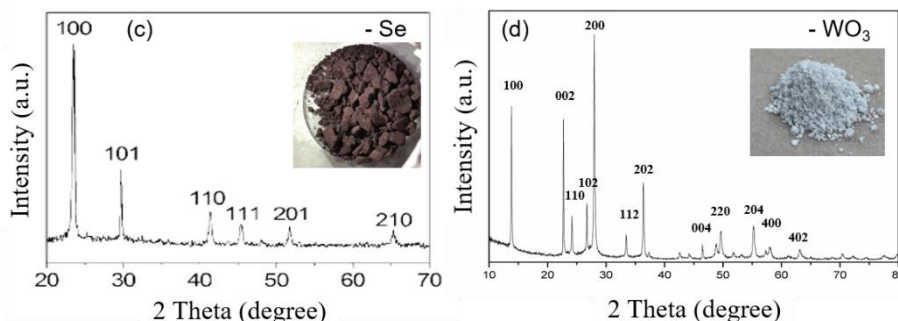


Figure 2: XRD pattern of the obtained (c) selenium nanowires and (d) WO_3 nanotubes.

WO_3 also received considerable attention owing to some outstanding properties. It is used for instance in electronic devices, catalysts, gas sensors, splitting water and rechargeable lithium-ion batteries, as well as in other fields.³ Selenium nanowires were prepared by water at room temperature, and WO_3 nanotubes were synthesized by hydrothermal processes. Selenium nanowires and WO_3 nanotubes have been used as a template for the synthesis of the functional metal oxide nanotubes. The obtained 1D nanostructures were composed of fine wires and tubes with sizes as 10–100 nm. These nanostructures were characterized by field emission scanning electron microscopy (FESEM), X-ray diffraction (XRD), transmission electron microscopy (TEM). Advantages of this method include that it is a simple and general process that can open new avenues for the synthesis of a variety of functional nanotube structures.

References:

- (1) Iijima, S. et al. *Nature*. **56**, 354 (1991).
- (2) Cooper, W. C. et al. *Van Nostrand Reinhold, New York*. (1974).
- (3) Zhang, J. P. et al. *J. Mater. Chem* **21**, 5492 (2011).

Momentum-resolved resonance photoelectron spectroscopic study on TiSe₂

Shin-ichiro TANAKA^{a*}, Keiji Ueno^b, Fumihiko Matui^c

a: SANKEN, Osaka University, Japan

b: Graduate School of Science and Engineering, Saitama University, Japan

c: UVSOR Synchrotron Facility, Institute for Molecular Science, Japan

Email: stanaka@sanken.osaka-u.ac.jp

Transition metal dichalcogenides attract interests for these years from the view point of not only the technological application but also the basic condensed-matter physics as their quasi two-dimensional character provides many interesting phenomena such as charge-density wave (CDW) transition. Among them, TiSe₂ is quite unique because it exhibits not the ordinal two-dimensional but three-dimensional transition. Thus, the electronic structure resolving the electron momentum is worthy to investigate in detail. Meanwhile, we are under developing the new electron analyzer; i.e. Momentum Microscope[1] which enables us to investigate the band dispersion in wide area within a short period. Here we show the investigation of the Momentum-resolved photoelectron spectroscopic study on TiSe₂.

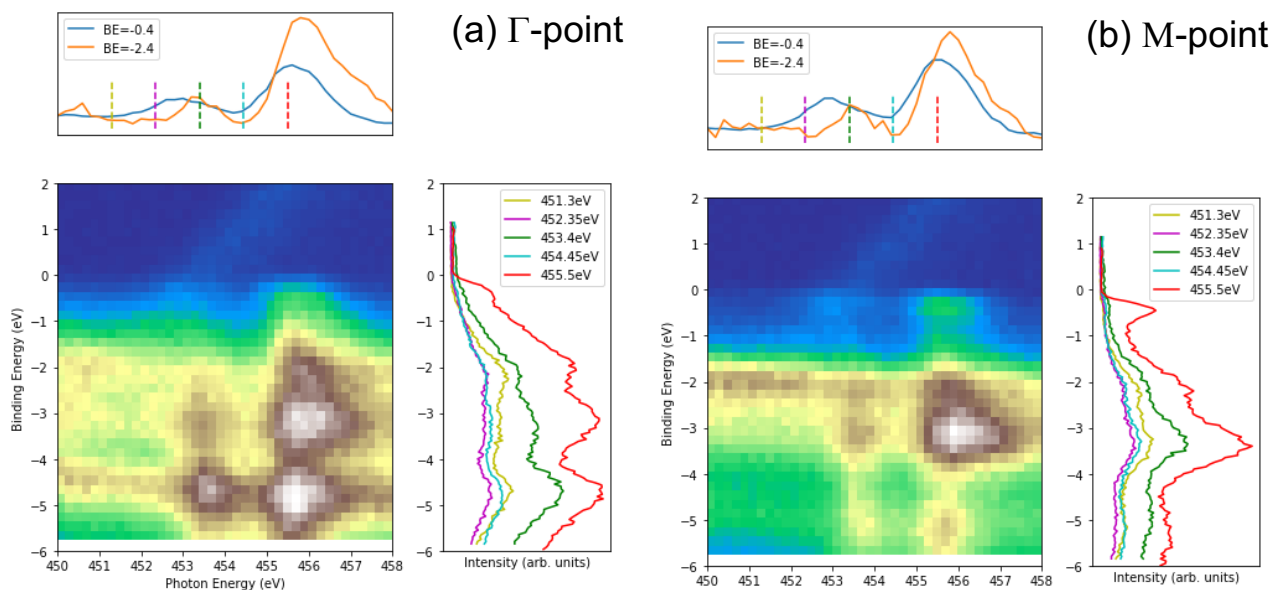


Figure 1: Photoelectron yields as functions of photon energy (top), binding energy (right), and both (middle) at the Γ (a) and M(b) points of TiSe₂. Photon energies correspond to the Ti-L_{2,3} edge.

Figure 1 shows the photoelectron yields as function of the photon and electron energies at the specific points (Γ -A and M-L) in the 2-dimensional (plane-projected) Brillouin zone of TiSe₂. The photon energy region corresponds to the Ti-L_{2,3} edge which is due to the excitation from the Ti2p core level to the Ti3d-derived conduction band. The most prominent feature is the resonantly enhancement of the photoelectron near the Fermi level at the M-point. This clearly indicate that electron-pocket-like valence-band-maximum is provided by the Ti3d orbital. The detail of the interpretation of the whole spectrum, together with the k_z -dependent (perpendicular to the crystal planes) behavior, will be discussed in the presentation.

References:

- (1) F. Matsui, S. Makita, H. Matsuda, T. Yano, E. Nakamura, K. Tanaka, S. Suga and S. Kera, Jpn. J. Appl. Phys. 59 079401 (2020).

Improvement of Residual stress and Fatigue Properties of Metal Materials Using a Compact Low-Energy Laser Peening Device

Yoshio MIZUTA ^a, Tomonao HOSOKAI ^a, Kiyotaka MASAKI ^b, Tomoharu KATO ^c,
Yoshihiro SAKINO ^c, Satoshi TAMAKI ^d, Yuji SANO ^{a,d,e,*}

a: Sanken, Osaka University, Japan

b: National Institute of Technology, Okinawa College, Japan

c: Kindai University, Japan

d: LAcubed Co., Ltd, Japan

e: Institute for Molecular Science, Japan

Email: yuji-sano@ims.ac.jp (email address of corresponding author)

Laser peening or laser shock peening introduces compressive residual stresses on the surface of metallic components covered with water by irradiating them with successive high-intensity laser pulses.¹⁻³ The advantage of laser peening is the possibility of fine execution management and the capability to introduce deep compressive residual stresses on the material surfaces. It is well known to be highly effective in inhibiting stress corrosion cracking and fatigue cracking on material surfaces. In addition, laser peening has an excellent effect on improving the fatigue strength of welds, which compensates for the disadvantage of high strength steels when welded. Laser peening has a high potential for enhancing material surface, but the high-power laser used requires clean room facilities, large equipment and severe operating conditions. Therefore, the application of the laser peening has been limited to high cycle fatigue of jet engine fan blades and stress corrosion cracking of nuclear reactor structures. If microchip lasers, which are small and easy to handle, could be used as a light source for laser peening, it would be possible to apply them not only to production processes in factories but also to existing steel structures such as bridges, to which conventional lasers have been difficult to apply for the above reasons. In this presentation, we report the results of the laser peening treatment of A7075 (aluminum alloy) and HT780 (high strength steel) with the laser pulse energy of less than 10 mJ. Even at such a low pulse energy, compressive residual stress was imparted (Figer.1) and fatigue properties were improved.

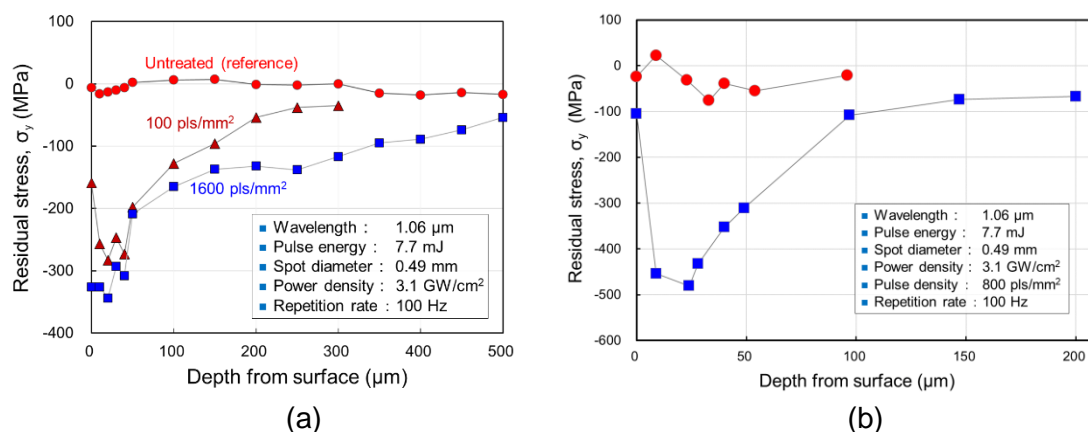


Figure 1: Residual stress depth profiles (a)A7075, (b)HT780

References:

- (1) Sano, Y., "Quarter Century Development of Laser Peening without Coating", *Metals*, Vol. 10 (2020), 152.
- (2) Clauer, A.H., "Laser Shock Peening, the Path to Production", *Metals*, Vol. 9 (2019), 626.
- (3) See, D.W., Dulaney, J.L., Clauer, A.H., and Tenaglia, R.D., "The Air Force Manufacturing Technology Laser Peening Initiative", *Surf. Eng.*, Vol. 18 (2002), pp. 32-36.

Electron beam chirp dexterity in staging laser wakefield acceleration

N. Pathak^{1,2,*}, A. Zhidkov^{1,2}, Z. Jin^{1,2}, Y. Mizuta¹, and T. Hosokai^{1,2}

¹ Institute of Scientific and Industrial research (SANKEN), Osaka University, Japan,

² Laser Accelerator R&D, Innovative Light Source Division, RIKEN SPring-8 Center, Japan.

Email: *naveenpathak@sanken.osaka-u.ac.jp

Laser WakeField Acceleration (LWFA) scheme has been widely accepted for its outstanding acceleration potential, however, its use in the real practical scientific and industrial applications is mainly limited by the relatively large energy spread of the accelerated beam. In general, the problem of energy spread in LWFA is associated with the three fundamental reasons: (i) an uncontrolled or continuous self-injection of the electrons in the laser wakefield, (ii) charge density of the injected electron beam beyond the beam loading limitation and (iii) the non-uniform profile of the wakefield strength in the longitudinal direction. Even in the idealistic case, where the electron self-injection is strictly controlled and localized both in space and time, and the electron beam density is kept well below the beam loading effect, the problem of the energy spread still persists. This is because of the non-uniformity in the longitudinal electric or acceleration field of the plasma wave. In this presentation we will discuss the usefulness of injecting a negatively chirped electron beam, in the context of multi-stage LWFA, in order to achieve very narrow energy-spread along with high charge density.

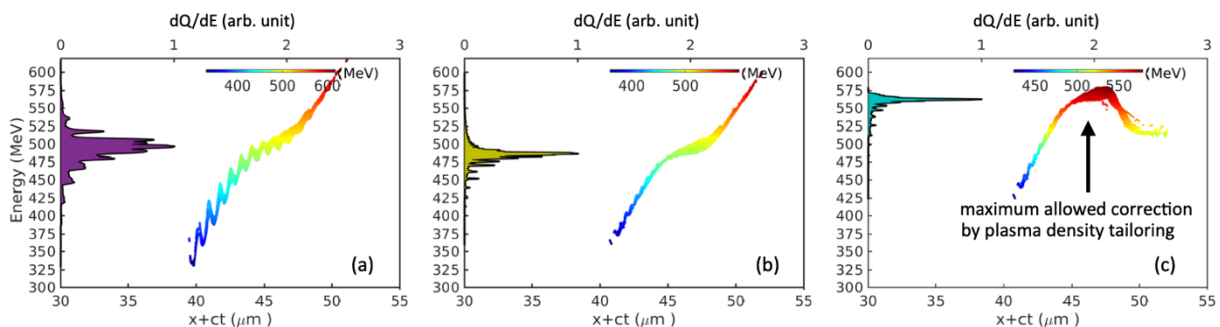


Figure 1: Electron beam phase space and corresponding energy spectrum evolution for (a) an unchirped electron beam, (b) negative energy chirped electron in uniform plasma density and (c) negative energy chirped electron beam in tapered plasma density.

References:

- (1) N. Pathak, A. Zhidkov, T. Hosokai, Phys. Plasmas **28**, 053105 (2021).
<https://doi.org/10.1063/5.0040897>
- (2) N. Pathak, A. Zhidkov, T. Hosokai, Phys. Letters A **425**, 127873 (2021).
<https://doi.org/10.1016/j.physleta.2021.127873>

Development of Laser-wakefield Acceleration Platform

Zhan Jin,^{a,b,*} Alexei Zhidkov,^{a,b} Naveen Pathak,^{a,b} Yoshio Mizuta,^{a,b} Kai Huang,^{b,c}
Nobuhiko Nakanii,^{b,c} Izuru Daito,^{b,c} Masaki Kando,^{b,c} Tomonao Hosokai^{a,b}

a: SANKEN, Osaka University, Mihogaoka 8-1, Ibaraki, Osaka 567-0047, Japan

b: Laser Accelerator R&D, Innovative Light Sources Division, RIKEN SPring-8 Center, Kouto 1-1-1, Sayo-cho, Sayo-gun, Hyogo 679-5148, Japan

c: Department of Advanced Photon Research, Kansai Photon Science Institute, National Institutes for Quantum and Radiological Science and Technology, 8-1-7 Umemidai, Kizugawa, Kyoto 619-0215, Japan

Email: jin@sanken.osaka-u.ac.jp

Laser-wakefield acceleration (LWFA), providing potentially jitter-free sources of radiation and electrons, is one of the rapidly developed scientific fields.¹ Staging LWFA is considered to be a necessary technique for developing full-optical high energy electron accelerators. Splitting of the acceleration length into several technical parts and with independent laser drivers allows not only the generation of stable, reproducible acceleration fields but also overcoming the dephasing length while maintaining an overall high acceleration gradient and a compact footprint.^{2,3}

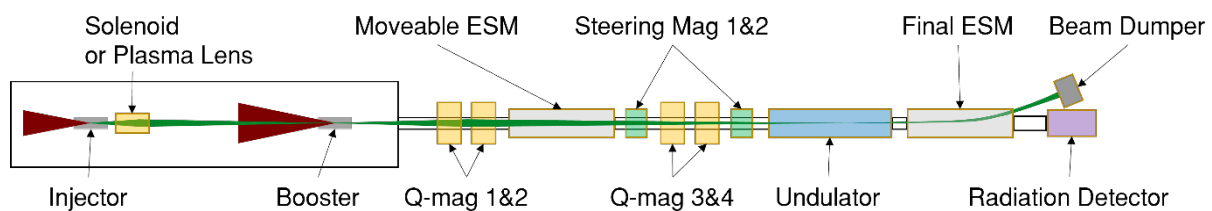


Figure 1: Schematic setup of the LWFA platform.

The Laser Acceleration Platform is a unique experimental platform specially designed for laser wake-field acceleration research, which is located in the RIKEN SPring-8 center, Harima, Hyogo Prefecture, next to the 8 GeV storage ring and SACLA linear accelerator and XFEL. In this presentation, we will introduce our recent progress in this platform, mainly on the staging LWFA and undulator radiation.

References:

- (1) Tajima, T; and Dawson, J. M. *Phys. Rev. Lett.* **43**, 267 (1979).
- (2) Steinke, S. et. al. *Nature* **530**, 190 (2016).
- (3) Jin, J. et. al. *Scientific Reports* **9**, 20045 (2019).

Investigation on the emission timings of electron bunches from laser wakefield acceleration via EO spatial decoding

K. Huang*, H. Kotaki, M. Mori, T. Esirkepov, J. K. Koga, Y. Hayashi, N. Nakanii, S. V. Bulanov, M. Kando

Kansai Photon Science Institute (KPSI), National Institutes for Quantum Science and Technology (QST), 8-1-7 Umemidai, Kizugawa-city, Kyoto, 619-0215, Japan

Email: huang.kai@qst.go.jp

Laser wakefield acceleration (LWFA)¹ has been studied intensively due to the inherent ultrashort bunch duration (fs) and larger acceleration gradient (GV/cm) over conventional accelerators. For application such as pump-probe experiment, knowledge of not only the electron pulse duration, but also the emission timings of electron bunches shot by shot are very important. Although it is of great importance, the real-time emission time detection of the electron bunch from LWFA had barely been conducted in experiment.

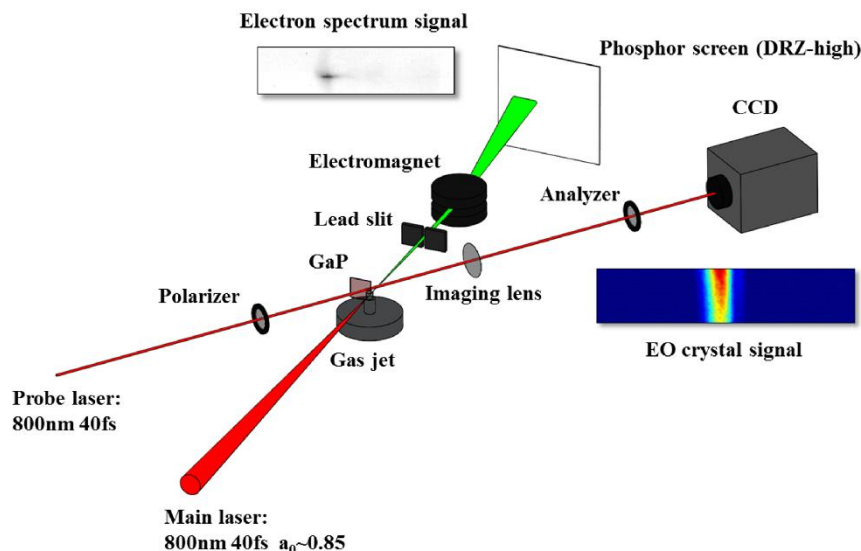


Figure 1: The experiment set-up of electro-optic spatial decoding in LWFA. This experiment was performed using the JLITE-X laser at KPSI, QST

Electro-optic (EO) spatial decoding is a convenient technique widely used in THz study². To measure the emission timing of electrons, we introduced the EO spatial decoding into LWFA. By setting the EO crystal very close to the gas target, we observed the spherical-wavefront coulomb field and derived a new formula describing the temporal mapping relationship³. We discovered that injection position of the electron beams became closer to the drive laser pulse with increased plasma density for Helium gas in the self-injection regime⁴. With superior data attainability and non-destructive single-shot characteristics, this method could be a candidate as electron emission timing monitor for LWFA experiments.

References:

- (1) Tajima, T.; Dawson, J. *Phys. Rev. Lett.* **43**, 267 (1979).
- (2) Shan, J. *Opt. Lett.* **25**, 426 (2000).
- (3) Huang, K. *Sci. Rep.* **8**, 2938 (2018).
- (4) Huang, K. *Phys. Rev. Accel. Beams* **22**, 121301 (2019) (Editors' suggestion).

THz source driven by femtosecond laser created plasma with applied transverse electric field in air

Kaoru Kobayashi, Akihiro Ichige, Hidetoshi Ito, Ren Kashihara,
Takamitsu Otsuka*, and Noboru Yugami

Graduate Program in Optical Engineering, Division of Engineering and Agriculture, Graduate
School of Regional Development and Creativity, Utsunomiya University, JAPAN

Email: takamitsu@cc.utsunomiya-u.ac.jp

High-power terahertz (THz) radiation sources have many potential applications in imaging, biological sensing, surface analysis, and condensed matter studies. Electron acceleration by the THz wave is also one of attractive new applications. Because of the empirical breakdown threshold scaling of the accelerating tube is given by $E_s \propto f^{1/2} \tau^{-1/4}$, where E_s is the surface electric field, f is the frequency of operation and τ is pulse duration, respectively, higher operation frequency and shorter pulse EM wave has an advantage for electron acceleration. Electromagnetic (EM) wave sources based on laser and plasma interactions is one of the most attractive methods for achieving such radiation sources.

We studied that the THz radiation from laser created plasma with the transverse electric field. Figure 1(a) shows the experimental setup. A Ti:sapphire laser system which has central wavelength of 800 nm with maximum energy of 40 mJ and 120 fs pulse duration (full width at half maximum: FWHM) was employed for creating an ionization front. The laser was focused in air using a plano-convex lens with focal length of 800 mm and its focal diameter was 40 μm . The maximum laser intensity was estimated to be $2.7 \times 10^{16} \text{ W/cm}^2$. A static electric field was applied to the focal region along the y -direction (perpendicular to the laser axis) by two copper plate electrodes. The electrodes length and gap were 1 cm each and were biased with a pulsed power supply up to 15.0 kV with the duration of 200 ns (FWHM). The maximum electric field E_0 at the center of the gap was estimated to be 15 kV/cm.

Figure 1(b) shows the example of the angular patterns of radiation measured in the xz plane with the detector sensitive from 0.33 to 0.5 THz. The THz radiation is emitted in the forward direction with the linear polarization which is parallel to the applied electric field. The radiation power is proportional to the square of applied electric field. From simulation results, the plasma diameter is determined the peak frequency of radiation. This indicates that the radiation frequency is controlled by the plasma diameter, in other words, focal diameter of the laser light. We also made a simple analytical model which consider the electron motion under the electric field decayed by the Debye shielding¹.

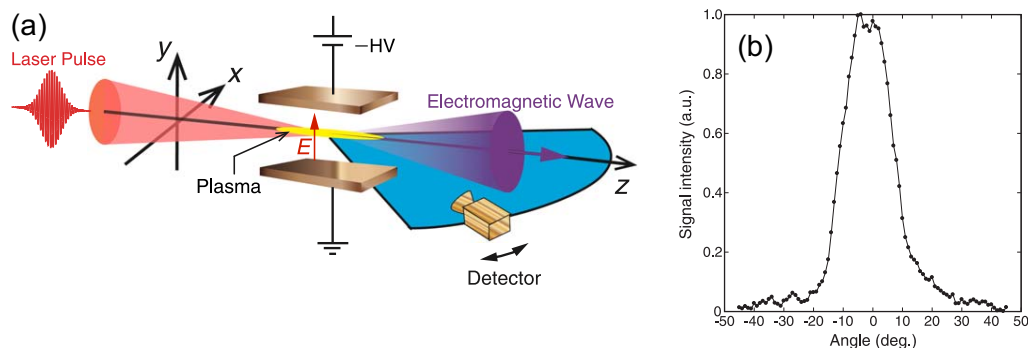


Figure 1 (a) Schematic diagram of experimental setup. (b) Angular distribution of radiation power by the detector which responds between 0.33 and 0.5 THz. Each dots are normalized by the maximum value at 0°.

References:

- (1) Fukuda, T. et al., *Jpn. J. Appl. Phys.* **59**, 020902 (2020).

Upcycling Silicon Swarf to Advanced Electrode Materials

Jaeyoung CHOI, Jiasheng WANG, Taketoshi MATSUMOTO*

SANKEN, Osaka University, Japan
Email: tmatsumo@sanken.osaka-u.ac.jp

Si swarf is generated during slicing Si ingots with wire saws. The weight of generated Si swarf is comparable to that of produced Si wafers for solar cells, and 100 kt of Si swarf are generated per year. Upcycling Si swarf is important from the viewpoint of the life cycle assessment because Si is generally produced from SiO₂ with carbon and a high thermal budget.

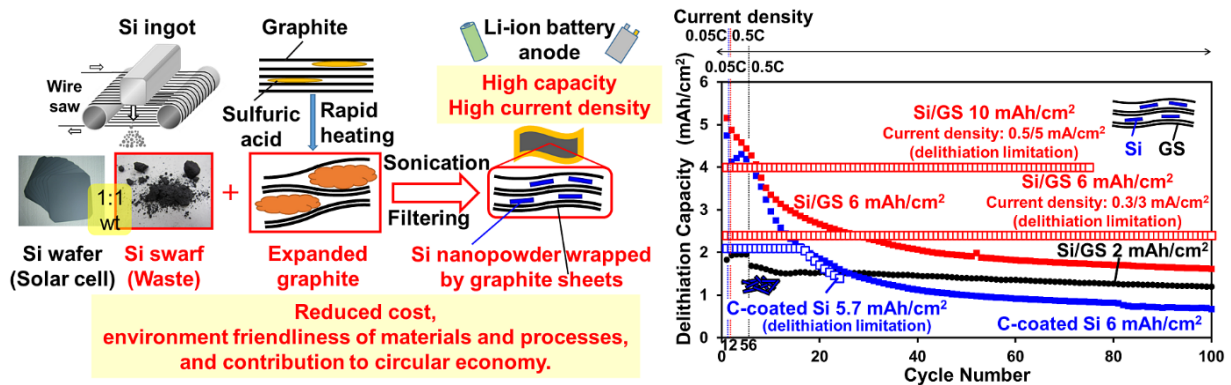


Figure 1 Application of Si swarf to anodes in Li ion batteries.

Si anodes in Li ion batteries possess a high theoretical capacity of 3578 mAh/g, compared to that of the current graphite anode (372 mAh/g). Si powder is destroyed due to large volume change during lithiation-delithiation cycles. 150 nm was reported to be the critical size to suppress the pulverization of Si powder.¹ 2D Si nanomaterials thinner than 150 nm are expected to address the degradation during cycles. In this study, anodes with flake-shaped Si swarf of 9–40 nm thickness and 60 nm–2 μ m lateral size are investigated.²

Anodes with Si swarf wrapped by graphite sheets (Si/GS, 5/1 wt.) and amorphous carbon coated Si swarf (C-Si, Si/C=10/1 wt.) are fabricated. GSs are produced from expanded graphite by sonication in N-methylpyrrolidone (NMP). Si/GS composites are fabricated by sonication of Si swarf and GSs in NMP and filtration. Coin cells are assembled with a Si anode, Li foil, polyethylene separator and 1 M LiPF₆ in ethylene carbonate/diethyl carbonate.

The Si/GS electrodes are stable, compared to the C-Si electrodes after 300 cycles. Aggregated GSs wrap Si/GS composites and play roles as stable frameworks during 300 cycles for the Si/GS electrodes as observed by scanning electron microscopy (SEM) and transmission electron microscopy (TEM). In the case of the C-Si electrodes, Si frameworks are found after the 100th cycle but fuse after the 300th cycle. The internal resistance for the Si/GS electrode is lower than that for the C-Si electrode as indicated by electrochemical impedance measurements. The cyclability, delithiation capacity and current density of the Si electrodes are greatly improved by wrapping Si with GSs, delithiation limitation of Si/GS electrodes after deep lithiation of Si and increases in the mass loading of Si electrodes.

References:

- (1) Liu, X. H.; Zhong, L.; Huang, S.; Mao, S. X.; Zhu, T.; Huang, J. Y. *ACS. Nano.* **6**, 1522 (2012).
- (2) Choi, J.; Wang, J.; Matsumoto, T. *J. Electrochem. Soc.* **168**, 020521 (2021).
- (3) Kimura, K.; Matsumoto, T.; Nishihara, H.; Kasukabe, T.; Kyotani, T.; Kobayashi, H. *J. Electrochem. Soc.* **164**, A995 (2017).

Pulse Duration Dependence of Dry Laser Peening Effects in the Femtosecond-to-Picosecond Regime

Itsuki Nishibata^{a*}, Masayuki Yoshida^a, Yusuke Ito^b, Naohiko Sugita^b, Akio Hirose^a, Tomokazu Sano^a

a: Division of Materials and Manufacturing Science, Osaka University, Japan

b: Department of Mechanical Engineering, The University of Tokyo, Japan

Email: i.nishibata@mapse.eng.osaka-u.ac.jp

Ultrashort pulse laser processing achieves precise machining. In order to control the processing characteristics by ultrashort pulse laser, it is necessary to clarify the dependence of pulse energy and pulse duration. As the laser intensity increases above 10^{13} W/cm², nonlinear phenomena such as the optical Kerr effect and ionization are more prominent. This leads to defocusing and changes in the laser intensity distribution¹. Therefore, when processing cannot be conducted due to nonlinear phenomena, the pulse duration can be extended to reduce the laser intensity. Dry laser peening is one of the ultrashort pulse laser processes, which requires high energy above the ablation threshold to produce sufficient peening effects². Laser peening is a surface modification method that uses laser-driven shock compression to improve the properties of metals, such as the residual stress hardness, and fatigue properties. It is unclear as to whether peening effects can be obtained when the pulse duration is extended. This is because the peening effect is sensitive to thermal effects.

We found an optimum pulse duration for dry laser peening in the femtosecond-to-picosecond regime, in which the laser intensity exceeds the air breakdown threshold³. As shown in Fig. 1(a), a pulse duration of 1 ps produced the most effective peening effects under conditions wherein the laser energy was constant; as shown in Fig. 1(b), this was caused by a decrease in the laser fluence due to a beam expansion of less than 1 ps, in addition to an increase in the thermal effect above 1ps. When the laser intensity exceeds the air breakdown threshold, it is necessary to select the pulse duration while considering laser-air and laser-metal interactions.

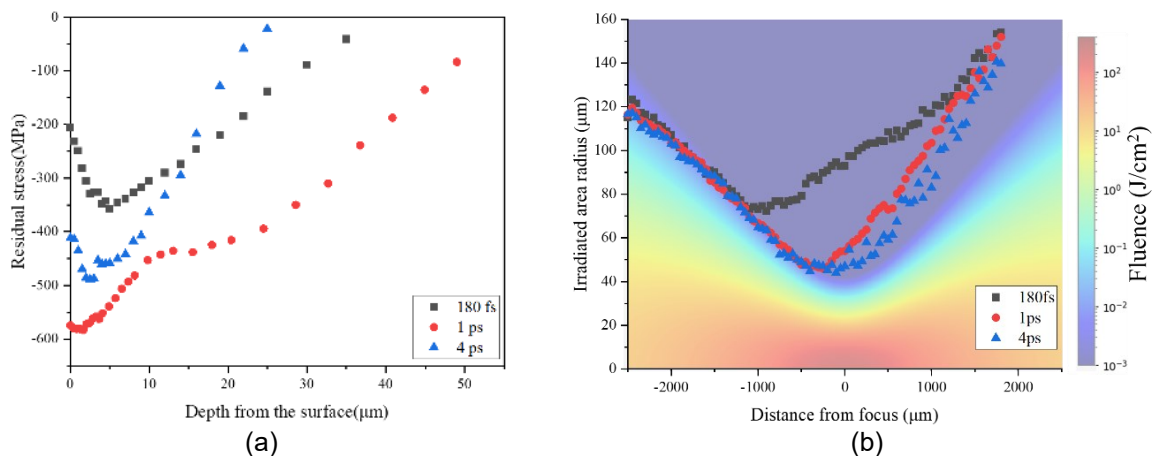


Figure 1: (a) Depth profile of the residual stress at each pulse duration. (b) Laser focusing distribution and irradiation area radius around the focal position at each pulse duration.

References:

- (1) S. L. Chin, S. A. Hosseini, W. Liu, Q. Luo, F. Théberge, N. Aközbek, A. Becker, V. P. Kandidov, O. G. Kosareva, H. Schroeder, *Can. J. Phys.*, 83, 863, (2005).
- (2) T. Sano, T. Eimura, R. Kashiwabara, T. Matsuda, Y. Isshiki, A. Hirose, *J. Laser Appl.*, 29, 012005, (2017).
- (3) I. Nishibata, M. Yoshida, Y. Ito, N. Sugita, A. Hirose, T. Sano, *Appl. Phys. Express*, 14, 062001, (2021).

Utilizing Triplet-Triplet Energy Transfer Kinetics to Explore the Dynamics of Nucleic Acids at the Single-Molecule Level

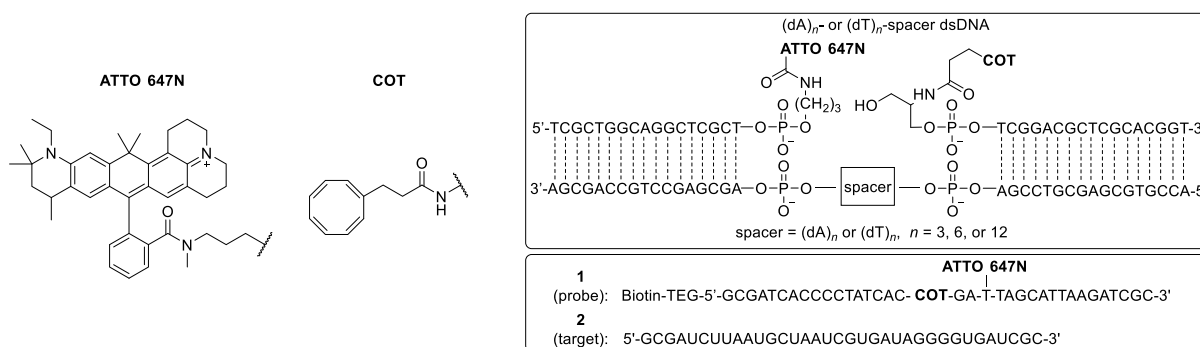
Jie XU,^a Shuya FAN,^a Lei XU,^a Atsushi MARUYAMA,^b Mamoru FUJITSUKA,^a Kiyohiko KAWAI^{a,*}

a: SANKEN (The Institute of Scientific and Industrial Research), Osaka University, Japan

b: Department of Life Science and Technology, Tokyo Institute of Technology, Japan

Email: kiyohiko@sanken.osaka-u.ac.jp

Biomolecules are dynamic and the achievement of functions is through the structural transitions of biomolecules upon being triggered by other effectors and the surrounding environment change. The timescales of the structural transitions vary in a wide time range and are crucial for biological functions. To explore the structural dynamics of biomolecules, we can introduce fluorescent molecules into biomolecules and measure the kinetics of the corresponding photo-induced chemical reactions such as electron transfer and energy transfer reactions occurring on fluorescent molecules.^{1,2} The most extensively used chemical reactions are those occurring in the singlet excited state (S_1) of fluorescent molecules. However, the S_1 normally has a lifetime within 10^{-8} s. For processes taking place on the timescales longer than 10^{-8} s, the S_1 -based kinetics is rarely valid and therefore leaves the processes hidden. Different from S_1 , the triplet excited state (T_1) usually has a lifetime of $\sim 10^{-2}$ s. Thus by tracing the kinetics of T_1 -involved reactions, the dynamics of biomolecules can be accessed on a timescale of up to six orders of magnitude wider than via the S_1 -based kinetics. In this work, by utilizing the kinetics of triplet-triplet energy reaction (TTET) reaction via measuring the triplet blinking using fluorescence correlation spectroscopy (FCS), we explored the structural dynamics of nucleic acids at the single-molecule level.³ The results demonstrated that the TTET kinetics is governed by the structural dynamics of nucleic acids and thereby reflects the length- and sequence-dependent dynamics of nucleic acids. Our work manifested the utilization of TTET kinetics for studying the structural dynamics of nucleic acids and detecting a cancer microRNA biomarker at the single-molecule level in the time range from μ s to ms.



Scheme 1. The chemical structures of ATTO 647N (triplet energy donor) and cyclooctatetraene (COT, triplet energy acceptor), the double-stranded DNA platform used for studying the structural dynamics of nucleic acids, the molecular beacon probe (**1**, probe), and the model microRNA biomarker (**2**, target).

References:

- (1) Kawai, K.; Fujitsuka, M.; Maruyama, A. *Acc. Chem. Res.* 2021, **54**, 1001–1010.
- (2) Kawai, K.; Maruyama, A. *Chem. Eur. J.* 2020, **26**, 7740–7746.
- (3) Xu, J.; Fan, S.; Xu, L.; Maruyama, A.; Fujitsuka, M.; Kawai, K. *Angew. Chemie Int. Ed.* 2021, **60**, 12941–12948.

Optical luminescence from protein-directed Au₋₂₀ clusters upon hard X-ray irradiation

Zuoyue LIU,^a Kyung Oh JUNG,^b Ryo TAKAHATA,^c Masanori SAKAMOTO,^c Toshiharu TERANISHI,^c Mamoru FUJITSUKA,^{a,*} Guillem PRATX,^{b,*} Yasuko OSAKADA,^{a,d,*}

a: SANKEN (The Institute of Scientific and Industrial Research), Osaka University, Japan

b: Department of Radiation Oncology and Medical Physics, Stanford University, USA

c: Institute for Chemical Research, Kyoto University, Japan

d: Institute for Advanced Co-creation Studies, Osaka University, Japan

Email: liuzuoyue45@sanken.osaka-u.ac.jp

Hard X-ray excited optical luminescence (hXEOL) is promising in bio-imaging field, but development of contrast agents is limited. Previously, we used protein-directed Au₂₅ clusters as a contrast agent for hXEOL.¹ Recently, protein-directed Au₋₂₀ clusters were found to have higher emission quantum yield (15%) than Au₂₅ clusters (4%).² In this study³, we employed protein-directed Au₋₂₀ clusters as contrast agents and investigated their luminescent properties.

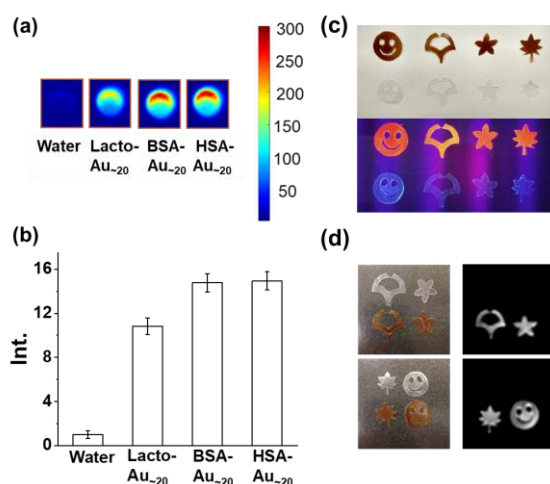


Figure 1: (a) hXEOL images and (b) signal of protein-directed Au₋₂₀ clusters with water as control. (c) Images of HSA-directed Au₋₂₀ clusters embedded films and control films under natural light (top) and UV light (365 nm, bottom) irradiation. (d) Images of HSA-directed Au₋₂₀ clusters embedded films and control films under natural light (left) and hard X-ray (right) irradiation.

Three kinds of proteins were used for the synthesis of the Au₋₂₀ clusters, namely, bovine serum albumin (BSA), human serum albumin (HSA) and lactoferrin. Upon hard X-ray irradiation, clear emission was observed from the solutions of three protein-directed Au₋₂₀ clusters (Fig. 1a and 1b). When embedded in films (PEG/PVA), we observed red emission from HSA-directed Au₋₂₀ clusters under UV light (Fig. 1c). Furthermore, the HSA-directed Au₋₂₀ clusters in the films displayed clear emission under hard X-ray irradiation, compared to the control films (Fig. 1d). These results demonstrated the potential applications of the protein-directed Au₋₂₀ clusters in biological imaging field.

References:

- (1) Osakada, Y.; Pratx, G.; Sun, C.; Sakamoto, M.; Ahmad, M.; Volotskova, O.; Ong, Q.; Teranishi, T.; Harada, Y.; Xing, L.; Cui, B. *Chem. Commun.* **50**, 3549 (2014).
- (2) Zhang, P.; Yang, X.; Wang, Y.; Zhao, N.; Xiong, Z.; Huang, C. *Nanoscale* **6**, 2261 (2014).
- (3) Liu, Z.; Jung, KO.; Takahata, R.; Sakamoto, M.; Teranishi, T.; Fujitsuka, M.; Pratx, G.; Osakada, Y. *RSC. Adv.* **10**, 13824 (2020).

Synthesis and photocatalytic improvement of metal-porphyrin containing nanodisks from covalent organic frameworks

Xinxi LI,^a Yasuko OSAKADA^a, Mamoru FUJITSUKA^{a*}

^a: The Institute of Scientific and Industrial Research, Osaka University, Japan

Email: xinxili45@sanken.osaka-u.ac.jp

We have previously shown that metal-free porphyrin covalent organic frameworks (COFs) can be exfoliated in common solvent, and the synthesized disk-shaped polymers can be used as photocatalysts, exhibiting photocatalytic activity of H₂ generation that is 2-5 times higher than the original COFs.¹ (Figure 1a) However, the generality of the enhanced photocatalytic activity by exfoliation has not yet been clarified, and oxidation reactions such as the generation of reactive oxygen species need to be investigated. In this study, we newly synthesized nanodisc polymers derived from metalloporphyrin COFs and investigated their photocatalytic H₂ evolution and oxidative photocatalysis.

Organic polymers with nanodisc-like shapes were synthesized by exfoliating metalloporphyrin-based COFs (DhaMTph) in 4-ethylpyridine (epy) (Figure 1). The DhaMTph used in this study were synthesized from dihydroxyterephthalaldehyde (Dha) and, copper or nickel tetra-aminophenyl-metalloporphyrin (CuTph or NiTph) were prepared using a modified method.²

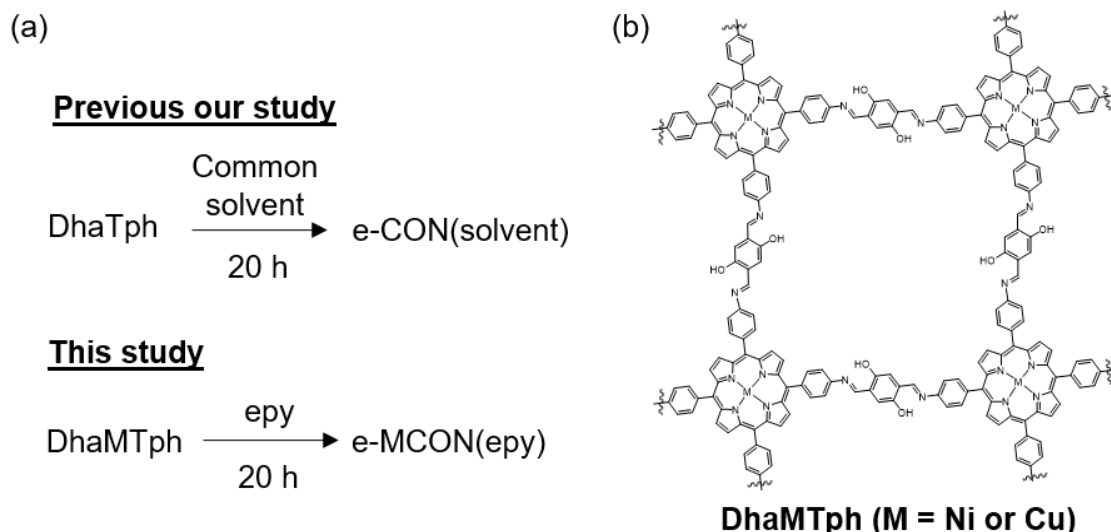


Figure 1: (a) Comparison of synthesis route between previous study and this study. (b) Chemical structure of DhaMTph (M = Ni or Cu).

The crystallinity of DhaCuTph and e-CuCON(epy) was evaluated by powder XRD. After the synthesis of e-CuCON(epy) by exfoliation from DhaCuTph, the strong peak at 3.6° assigned to (100) facet was reduced by approximately 60%. AFM images demonstrated that e-CuCON(epy) had diameters of 30-50 nm, consistent with HR-TEM results. The thickness of e-CuCON(epy) was 1-3 nm. After light irradiation for 3 hours, we observed that the photocatalytic activity of e-CuCON(epy) for H₂ evolution reaction was enhanced by a factor of seven compared to DhaTph. In the poster, we will also discuss on the characterization of e-CuCON(epy), and photocatalytic oxidation processes of e-MCON(epy).

References:

- (1) Li, X.; Goto, T.; Nomura, K.; Zhu, M.; Sekino, T.; Osakada, Y. *Appl. Surf. Sci.* **513**, 145720(2020)
- (2) Kandambeth, S.; Shinde, D. B.; Panda, M. K.; Lukose, B.; Heine, T.; Banerjee, R. *Angew. Chem., Int. Ed.* **52**, 13052(2013).

Machine-learning-assisted Multi-parameter Screening for Flow and Electrochemical Reactions

Shinobu Takizawa,^{a,b} H. D. P. Wathsala,^a Masaru Kondo,^c Akimasa Sugizaki,^a
Md. Imrul Khalid,^a Kazunori Ishikawa,^a Satoshi Hara,^a Takayuki Takaai,^a
Takashi Washio,^{a,b} and Hiroaki Sasai^{a,b}

a: SANKEN (The Institute of Scientific and Industrial Research), Osaka University, Japan

b: Artificial Intelligence Research Center, SANKEN, Osaka University, Japan

c: Department of Materials Science and Engineering, Graduate School of Science and Engineering, Ibaraki University, Japan

Email: taki@sanken.osaka-u.ac.jp; sasai@sanken.osaka-u.ac.jp

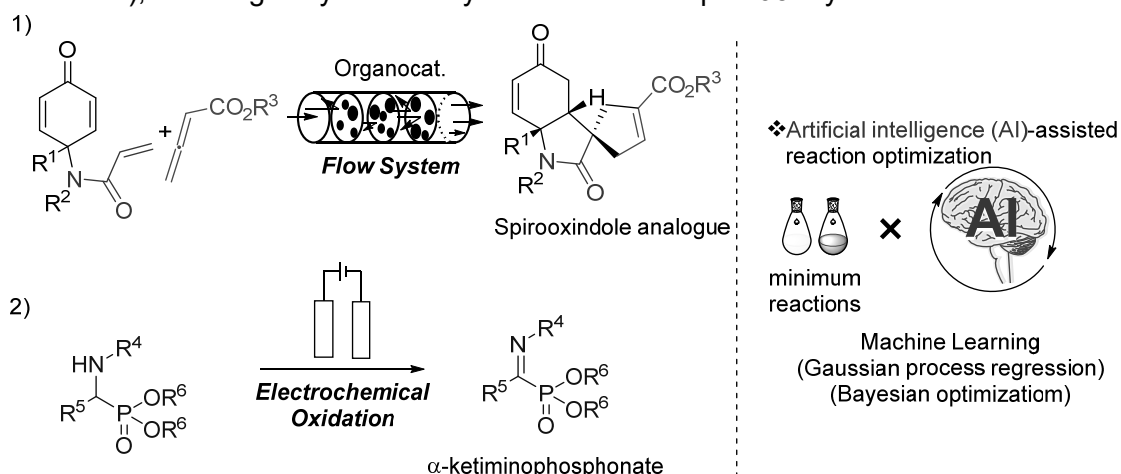
Optimization of conditions is a crucial and unavoidable process. In particular, developing a new synthetic reaction requires tedious screening and optimization of the relevant parameters, resulting in a wastage of a longer duration, a large amount of chemicals and energy. Thus a rapid, economical and effective protocol have been highly demanded in synthetic chemistry. Herein, Machine Learning (ML) optimization of multi-parameter screening for flow and electrochemical reactions is established by utilizing Gaussian Process Regression (GPR)^{1,2} and Bayesian Optimization (BO)³ with a minimum number of experimental studies.

1. Exploration of flow reaction conditions using GPR for organocatalyzed domino reaction²

The GPR was successfully applied to multi-parameter flow reaction screening for organocatalyzed Rauhut-Currier/[3+2] annulation sequence. After brief experimental screening, the GPR with the experimental data (up to 10 entries) could rapidly predict the optimal conditions (flow rate, temperature and reagent amount), leading to the formation of functionalized chiral spirooxindole analogues in high yields with up to 98% ee as a single diastereomer within one minute.

2. BO-assisted simultaneous multi-parameter screening for electrochemical oxidation for the synthesis of α -ketiminophosphonates³

The BO and experimental assessment using positive and negative results were successfully combined to accomplish the simultaneous multiparameter screening for electrochemical oxidation. The BO with the experimental data (up to 12 entries) could rapidly predict the five optimal parameters (current, substrate and electrolyte concentrations, temperature, and reaction time), resulting in cyclic sulfonyl ketimines with up to 98% yield.



References:

- (1) Sato, E.; Fujii, M.; Tanaka, H.; Mitsudo, K.; Kondo, M.; Takizawa, S.; Sasai, H.; Washio, T.; Ishikawa, K.; Suga, S. *J. Org. Chem.* **86**, 16035 (2021).
- (2) Kondo, M.; Wathsala, H. D. P.; Sako, M.; Hanatani, Y.; Ishikawa, K.; Hara, S.; Takaai, T.; Washio, T.; Takizawa, S.; Sasai, H. *Chem. Commun.* **56**, 1259 (2020).
- (3) Kondo, M.; Sugizaki, A.; Khalid, Md. I.; Wathsala, H. D. P.; Ishikawa, K.; Hara, S.; Takaai, T.; Washio, T.; Takizawa, S.; Sasai, H. *Green Chem.* **23**, 5825 (2021).

Sensing RNA Internal Loops and Their Binding Molecules by a Small-Molecule Fluorescence Probe ANP77

Bimolendu Das, Asako Murata, Kazuhiko Nakatani*

*Department of Regulatory Bioorganic Chemistry, SANKEN (The Institute of Scientific and Industrial Research), Osaka University, Japan
Email: nakatani@sanken.osaka-u.ac.jp*

Recent discoveries of RNAs functions in regulating gene expression and their involvement in the development of human diseases demonstrated RNAs as attractive drug targets. Small-molecules binding to the pathogenic RNAs and modulating their functions become an increasingly growing area of research towards drug discovery. However, identifying a small-molecule that detects a particular motif of RNAs and discriminates them from other cellular RNAs with high specificity and binding affinity remains a fundamental challenge in RNA-targeted drug discovery. Considering the substantial distribution of the internal loops involving two contiguous cytosines opposite to a single nucleotide base (Y/CC; Y = C, U, or A) within the biologically significant functional RNAs, developing small-molecule probes targeting the Y/CC sites is necessary to gain profound insight into their functions and roles in biochemical processes. Herein, we report **ANP77** as a small-molecule probe for sensing RNA internal loop of Y/CC motifs and molecules binding to the motifs.¹ The Y/CC motifs interact with **ANP77** via the formation of a 1:1 complex and quench the fluorescence of **ANP77**. The flanking sequence-dependent binding to C/CC and U/CC sites was assessed by fluorometric screening, provided the binding heat maps. The quenching phenomena of **ANP77** fluorescence was confirmed with intrinsic potential drug target pre-miR-1908. Finally, the binding-dependent fluorescence quenching of **ANP77** was utilized in the fluorescence indicator displacement assay to demonstrate the potential of **ANP77** as an indicator by using the RNA-binding drugs Risdiplam and Branaplam.

References:

- (1) Das, B.; Murata, A.; Nakatani, K. *Nucleic Acids Res.* **49**, 8462 (2021).

Design, Synthesis, and Biological Evaluation of HDAC8-targeting PROTACs

Jiranan CHOTITUMNAVEE,^{a,b} Yasunobu YAMASHITA,^a Yukari TAKAHASHI,^b Yuri TAKADA,^a Tetsuya IIDA,^{a,b} Makoto OBA,^b Yukihiko ITOH*^{a,b} and Takayoshi SUZUKI*^{a,b}

^a SANKEN, Osaka University, Mihogaoka, Ibaraki-shi, Osaka 567-0047, Japan.

^b Graduate School of Medical Science, Kyoto Prefectural University of Medicine, 1-5 Shimogamohangi-cho, Sakyo-ku, Kyoto 606-0823, Japan.

Email: itohy@sanken.osaka-u.ac.jp, tkyssuzuki@sanken.osaka-u.ac.jp

Proteolysis targeting chimeras (PROTACs), hybrid molecules consisting of a ligand of a protein of interest (POI) and a ubiquitin ligase (E3) ligand, can hijack the ubiquitin-proteasome system, which is a key protein degradation process in cells, and can selectively degrade the POI (Figure 1A).¹ Because the degradation of POI by PROTACs induces a decrease in POI levels in cells, PROTACs are useful tools for medicinal chemistry and chemical biology studies on POIs. In this study, we applied the PROTAC technology to histone deacetylase 8 (HDAC8).

HDAC8 is a member of HDAC family proteins and catalyzes deacetylation of cohesin.² HDAC8 also has a scaffolding function, and interacts with several transcription factors to control several gene expression.³ Furthermore, its overexpression causes pathological consequences in several diseases, such as the development of T-cell leukemia.⁴ However, it remains unknown how HDAC8 impacts human health and causes cancers, and there are no HDAC8 modulators in a clinical use/trial. Therefore, novel compounds that modulate HDAC8 functions are interest of not only chemical tools but also therapeutic agents targeting HDAC8. Thus, we attempted drug discovery study on HDAC8 PROTACs.

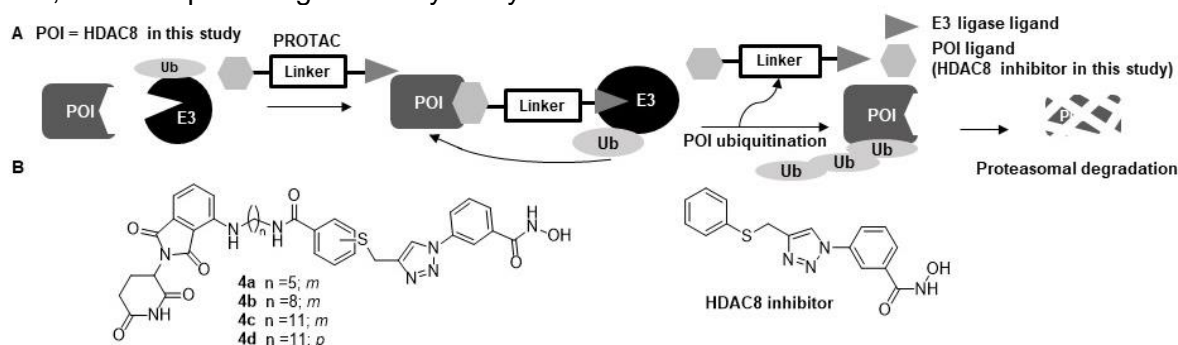


Figure 1: A) Mechanism of action of (HDAC8) PROTACs. B) Structures of designed PROTACs and a previously reported HDAC8 inhibitor

In this work, we designed and synthesized some HDAC8 PROTAC candidates in which our previously reported selective HDAC8 inhibitor⁵ is connected with a frequently used E3 ligase ligand, pomalidomide,⁶ via several linker lengths (Figure 1B). Among them, the PROTAC with an 11-carbon linker linked at the *meta*-position of phenyl ring in the HDAC8 inhibitor showed the most potent HDAC8 degradation activity without affecting levels of other HDACs such as HDAC1, 2, and 6. The mechanistic studies indicated that the HDAC8 degradation by the PROTAC is dependent on ubiquitin-proteasome system (Figure 1A). Remarkably, the PROTAC showed highly potent growth inhibitory activity against T-cell lymphoma Jurkat cells. These results suggested that HDAC8 PROTACs are useful as anticancer agents.

References:

- (1). Itoh Y. *Chem. Rec.* **18**, 1681 (2018)., (2). Deardorff MA. et. al. *Nature* **489**, 313 (2012)., (3). Kang Y. et. al. *Cell Death Dis.* **5**, e1476 (2014)., (4). Higuchi T. et al. *Blood* **121**, 18 (2013)., (5). Suzuki T. et. al. *ChemMedChem.* **9**, 657 (2014)., (6). Ito T, et. al. *Science* **327**, 1345 (2010)

The expression of MacAB is controlled by Rof through Rho dependent transcription termination system

Sohei Nakano,^{a,b} Seiji Yamasaki,^{a,b} Atsushi Taguchi,^{a,b} Kunihiro Nishino^{a,b,*}

a: Grad. Sch. Pharm. Sci, Osaka Univ., Japan

b: SANKEN., Osaka Univ., Japan

Email: nishino@sanken.osaka-u.ac.jp

The ATP-binding cassette-type drug efflux pump MacAB was originally reported as a macrolide specific pump. It is also known to be required for the virulence of *Salmonella enterica* when mice are inoculated via the oral route. MacAB exports not only antibiotics but also some kind of natural substrates such as heat-stable enterotoxin II and linearized siderophore products. Linearized siderophore products protect *S. enterica* from oxidative stress and this is required for this organism to survive in macrophages. The expression level of the *macAB* genes in *S. enterica* are low in a normal medium and those repression mechanism is not well understood. In this study, we attempted to identify the factor that affect the *macAB* expression. Firstly, genomic DNA was extracted from *S. enterica*, then digested with the restriction enzyme and inserted into the vector to make a genomic plasmid library. Then, the chromosomal *macAB-lacZY* fusion strain was transformed with the library for the screening of plasmids that affect the promoter activity of the *macAB* operon. Five candidate plasmids were isolated and three of them contained the *yaeR-rof* operon. It is suggested that Rof controls the expression of MacAB through Rho dependent transcription termination which locates at untranslated region upstream of *macAB*. This insight could lead to better understandings of the regulatory mechanism *macAB* in *S. enterica*.

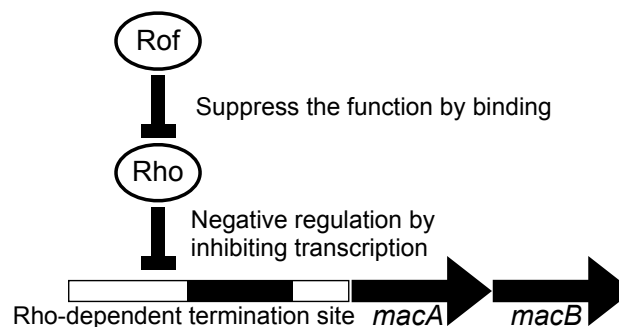


Figure : The mechanism how Rof control the expression of MacAB

References:

- (1) Nishino K.; Latifi T.; Groisman EA. *Mol. Microbiol* 59, 126-141(2006).
- (2) Yamagishi A.; Nakano S.; Yamasaki S.; Nishino K. *Microbiol. Immunol* 64(3) 182-188 (2020)

A photoswitchable fluorescent protein for hours-time-lapse and sub-second-resolved super-resolution imaging

Ryohei Noma,^a Tetsuichi Wazawa,^a Shusaku Uto,^a Kazunori Sugiura,^a Takashi Washio,^{a,b}
Takeharu Nagai,^{a,b,*}

a: SANKEN (The Institute of Scientific and Industrial Research), Osaka University, Japan

b: Transdimensional Life Imaging Division, Institute for Open and Transdisciplinary Research Initiatives, Osaka University, Japan

Email: ng1@sanken.osaka-u.ac.jp

Reversible photoswitchable fluorescent proteins (RSFPs) are a kind of fluorescent proteins whose fluorescence can be turned on and off by light irradiation, which are vital tools for super-resolution (SR) bioimaging (Fig. 1A). A RSFP, Kohinoor, enabled biocompatible SR imaging. However there was still room for improvement because of low fluorescence intensity, and slow maturation speed.¹ Here, we show a RSFP, Kohinoor2.0, which shows 2.6-fold higher fluorescence intensity, 2.5-fold faster chromophore maturation and 1.5-fold faster off-switching than those of Kohinoor. An analysis of pK_a of Kohinoor2.0 revealed that the chromophore phenolate of Kohinoor2.0 was under multiple equilibrium, and suggested the reason why Kohinoor2.0 was brighter than Kohinoor was molecular fraction of neutral states of Kohinoor2.0 was higher than that of Kohinoor. Furthermore, we successfully performed 4-h time lapse SR imaging of F-actin network or mitochondrial dynamics with a time resolution of 0.5 s in living mammalian cells by SPoD-OnSPAN (Super-resolution by Polarization Demodulation/On-State Polarization Angle Narrowing) (Fig. 1B).^{2,3}

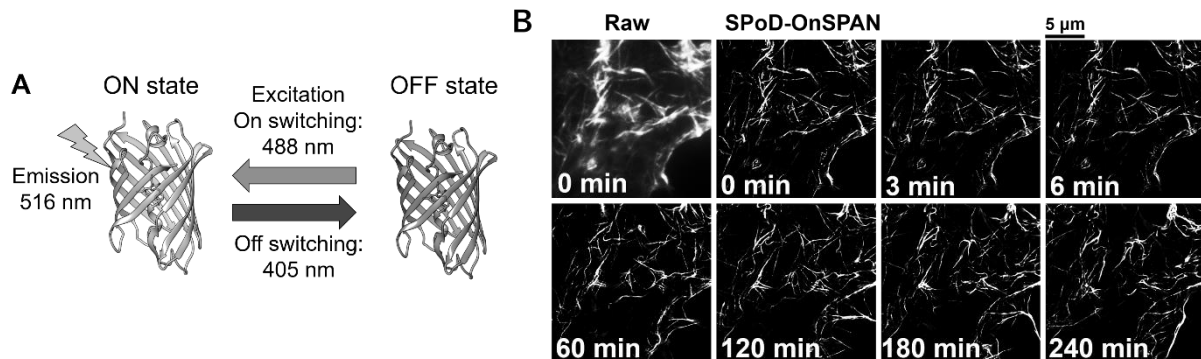


Figure 1: (A) Photoswitching scheme of Kohinoor and Kohinoor2.0. (B) SR imaging of dynamics of F-actin network in COS7 cell by Kohinoor2.0 and SPoD-OnSPAN with an interval of 3 min for 4 h.

References:

- (1) Tiwari, D. K; Arai, Y.; Yamanaka, M.; Matsuda T.; Agetsuma, M.; Nakano, M.; Fujita, K.; Nagai, T. *Nat. methods*. **12**, 515 (2015).
- (2) Wazawa, T.; Arai, Y.; Kawahara Y.; Takauchi, H.; Washio, T; Nagai, T. *Microscopy* **67**, 89 (2018).
- (3) Wazawa, T.; Noma, R.; Uto, S.; Sugiura, K.; Washio, T.; Nagai, T. *Microscopy* **70**, 340 (2021).

Manipulation of metal-insulator transition in VO₂ thin films by using step-terrace orientations of TiO₂(110) substrates

Kyungmin Kim^{a,*}, Shingo Genchi^b, Shiro Yamazaki^c, Hidekazu Tanaka^b, Masayuki Abe^a

a: Graduate School of Engineering Science, Osaka University, Japan

b: SANKEN(Institute of Scientific and Industrial Research), Osaka University, Japan

c: Department of Physics, School of Science, Tokyo Institute of Technology, Japan

Email: u764704g@ecs.osaka-u.ac.jp

Vanadium dioxide (VO₂) exhibits metal-insulator transition (MIT) near room temperature accompanied with a resistance change of 3 orders of magnitude. Thin film growth of VO₂ has been studied in an aim for device applications such as transistors. MIT property has been tuned by W-doping¹, fabrication of nanowires², etc. In addition to these methods, use of step-terrace (s-t) structures could be a promising candidate to control the MIT property since VO₂ is sensitive to the lattice strain at the interface between thin films and substrates. In this study, we grew VO₂ thin films on single crystal oxide TiO₂(110) substrates with s-t structures and investigated the step direction dependence of the MIT property. VO₂ thin films were prepared by pulsed laser deposition method on the substrate kept at 723 K in the oxygen of 0.95 Pa. The crystal orientation was investigated by x-ray diffraction and the surface morphology was measured by atomic force microscopy (AFM) before and after VO₂ deposition. Electrodes were prepared by photolithography and sputtering deposition. Microwires were fabricated by photolithography and reactive ion etching. The electric transport property of VO₂/TiO₂ microwires, which were perpendicular or parallel to the step direction, was measured to investigate the step direction dependence of the MIT property.

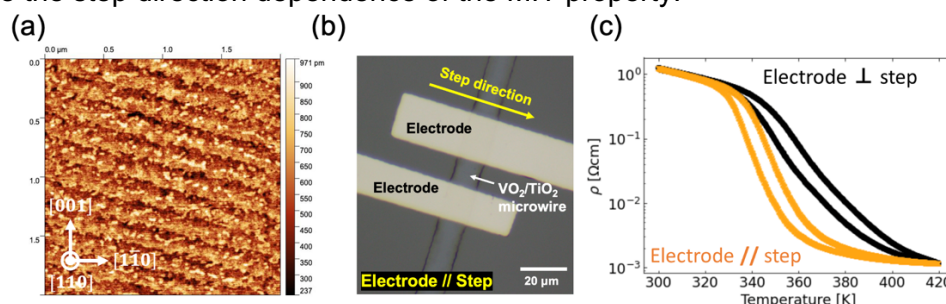


Fig. 1: (a) AFM image of 20 nm thick VO₂ thin film with step-terrace structure. (b) Optical microscope image of VO₂/TiO₂ sample. The electrodes were arranged parallel to the step direction. (c) Temperature dependence of the resistivity in VO₂/TiO₂ microwires with different step directions.

Figure 1(a) shows the AFM image of the VO₂(110) thin film grown on the TiO₂(110) step substrate. The homogeneous s-t structures of VO₂ reflecting the original s-t structures of TiO₂ were observed. Figure 1(b) shows the optical microscope image of the VO₂/TiO₂ sample, where electrodes were arranged parallel to the step direction. Figure 1(c) shows temperature dependence of the resistivity in VO₂/TiO₂ microwires, indicating the different electric properties depend on the step direction. Although both microwires exhibited 3 orders of magnitude resistance change, relatively sharp resistance change was observed when electrodes were arranged parallel to the step direction. These results suggest the different evolution of percolative path attributable to the local strain at the step edge. Our results show that use of VO₂ thin films with s-t structures is a promising method to control MIT property by changing the direction of the microwires.

References:

- (1) Takami, H.; Kawatani, K.; Kanki, T.; Tanaka, H. *Jpn. J. Appl. Phys.* **50**, 055804 (2011).
- (2) Takami, H.; Kanki, T.; Tanaka, H. *Appl. Phys. Lett.* **104**, 023104 (2014).

Relativistic femtosecond-pulsed electron microscopy

Jinfeng Yang,^{a,*} Koichi KAN,^a Masao GHODO,^a and Yoichi YOSHIDA^a

a: Sanken, Osaka University, Japan

Email: yang@sanken.osaka-u.ac.jp

Femtosecond atomic-scale imaging is a most challenging subject in advanced materials science and has long been a cherished dream tool for scientists wishing to study ultrafast structural dynamics in various materials. In this research, we aim to develop an innovative relativistic femtosecond-pulsed electron microscope by combining a radio-frequency electron acceleration technology into high-voltage electron microscope.

Figure 1 shows the relativistic femtosecond-pulsed electron microscope.¹⁻³ A radio-frequency (RF) photocathode electron gun, which was driven by a femtosecond Ti:Sapphire laser, was developed to generate 3-MeV-energy electron pulses with a duration of 100 fs containing 10^{6-7} electrons per pulse. The electron pulses were used successfully to detect high-quality diffraction patterns (DPs) with single-pulse observation (single-shot). The electron illumination system comprises two condenser lenses and an aperture to control and transfer the electron beam on the specimen. In imaging system, an objective lens, an intermediate lens and two projector lenses are used to magnify the transmission electron microscopy (TEM) image. The relativistic-energy TEM images or DPs are detected by a TI-doped CsI scintillator and a lens-coupled CCD camera. The prototypical microscope is 3.5 m in height and 0.8 m in diameter, which is a compact high-voltage electron microscope.

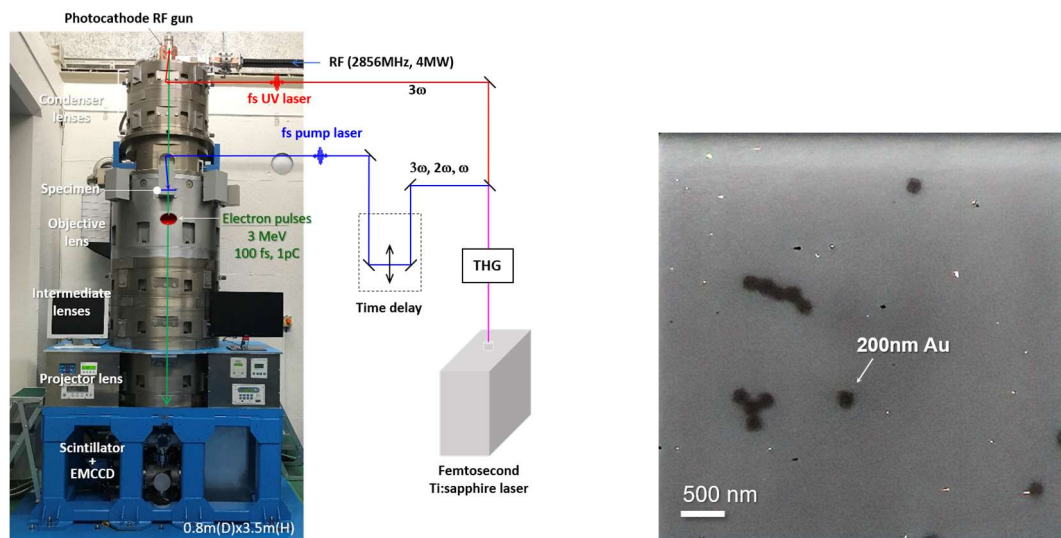


Figure 1: A relativistic femtosecond-pulsed electron microscope and TEM image of gold nanoparticles.

In the image mode, we succeeded to observed TEM images of gold nanoparticles with 10,000-pulse integration as shown in Fig. 1. In the low-magnification observation, the single-shot imaging with the femtosecond electron pulse is available. Finally, the ultrafast electron microscopy with relativistic femtosecond electron pulses is promising for studying ultrafast phenomena in materials, i.e. phase transformations and other structural dynamics.

This work was supported by a Basic Research (A) (21H04654, 22246127, 26246026, 17H01060, and 21H04654) of Grant-in-Aid for Scientific Research from MEXT, Japan.

References:

- (1) Yang J, Yoshida Y, Yasuda H, *Microscopy*, **67**, 291-295 (2018).
- (2) Yang J, "Electron microscopy: Novel microscopy trend", InTechOpen, 1-20 (2019).
- (3) Yang J, Gen K, Naruse N, Sakakihara S, Yoshida Y, *Quant. Beam Sci.* 2020, 4, 4 (2020).

Synthesis and Physical Properties of B-N Fused NIR-Absorbing Dyes with Naphthobisthiadiazole Unit toward Organic Semiconductor

Sakura UTSUNOMIYA,^a Soichi YOKOYAMA,^a Yutaka IE^{a,*}

a: SANKEN, Osaka University, Japan
Email: yutakaie@sanken.osaka-u.ac.jp

Near-infrared absorbing (NIR) dyes are attracting attention in the field of organic electronics such as organic semiconductors and organic solar cell materials. To extend absorption wavelength up to NIR region, the requirement of narrow highest occupied molecular orbital (HOMO)-lowest unoccupied molecular orbital (LUMO) gap of π -conjugated molecules is essential. The combination of donor-acceptor configuration with boron-bridged structure is an effective molecular design for narrow HOMO-LUMO gap, because the LUMO energy is effectively lowered by the introduction of boron-bridging.¹ We previously developed a fluorinated naphthobisthiadiazole (FNTz) unit, which showed good electron-accepting properties due to the low LUMO energy level. We revealed that an electron-accepting π -conjugated molecule incorporating FNTz as a core functioned as an acceptor material in organic solar cells. In this presentation, we report the synthesis and physical properties of novel B-N fused NIR-absorbing dyes, which are composed by electron-donating π -expanded pyrrole units and electron-accepting FNTz unit.

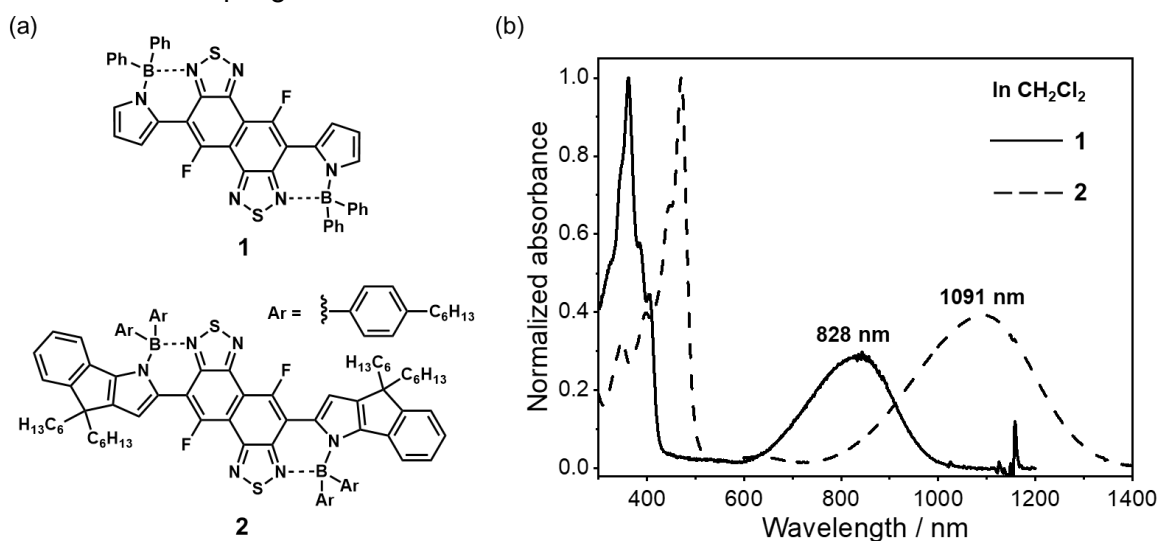


Figure 1. (a) Molecular structures of **1** and **2**. (b) UV-Vis-NIR absorption spectra of **1** and **2**.

Compounds **1** and **2** were synthesized by Stille coupling of brominated FNTz with stannylated pyrrole or indenopyrrole derivatives, respectively. Finally, the B-N fused reactions were performed by using dichloroarylborane (Figure 1a). UV-Vis-NIR measurements of compound **1** showed almost colorless solution with an absorption band at 822 nm (Figure 1b). Furthermore, the absorption band of compound **2** with π -extended pyrrole ring units reached to 1091 nm in NIR region.

References:

- (1) Nakamura, T.; Furukawa, S.; Nakamura, E. *Chem. Asian J.* **11**, 2016 (2016).
- (2) Chatterjee, S.; Ie, Y.; Seo, T.; Moriyama, T.; Wetzelaer, G. A. H.; Blom, P. W. M.; Aso, Y. *NPG Asia Mater.* **10**, 1016 (2018).

Single-Molecule Classification based on Intermolecular Hydrogen Bond by Modified Nano-Gap and Single-Molecule Time Series Analysis

Jiho RYU

Yuki KOMOTO, Takahito OHSHIRO, Masateru TANIGUCHI*

SANKEN, Osaka University, Japan
Email: taniguti@sanken.osaka-u.ac.jp

The development of detection/identification methods for amino acids is an important issue for understanding biological systems. Until now, there have been few analytical methods for amino-acid molecules because of limited selectivity and low detection limits. Single-molecule electrical measurement by nano-gap is one of the promising candidates for detection/identification of amino acid molecules. In this study, we focused on detecting L-aspartic acid (Asp), a target molecule for the diagnosis of several diseases. We utilized hydrogen-bond facilitated quantum tunneling enhancement for single-molecule electrical measurements by using mercaptoacetic acid (MAA) modified nano-gap. The measured current was investigated by machine learning based time series analysis method for accurate amino acid discrimination. Compared to measurements using bare nano-gap, it is found that MAA modification improves the difference in the conductance-time profiles between Asp and L-leucine (Leu) through the hydrogen bond facilitated tunneling phenomena for Asp, and not for Leu. We found that the accuracy of discrimination with MAA is 0.99 using over thirteen conductance signals. It is also found that this method enables determination of concentration even in the mixture of Asp and Leu. The method demonstrates the improvement of selective analysis for amino acids so that this will be potentially applicable for medical application, diagnosis and single-molecule peptide sequencer.

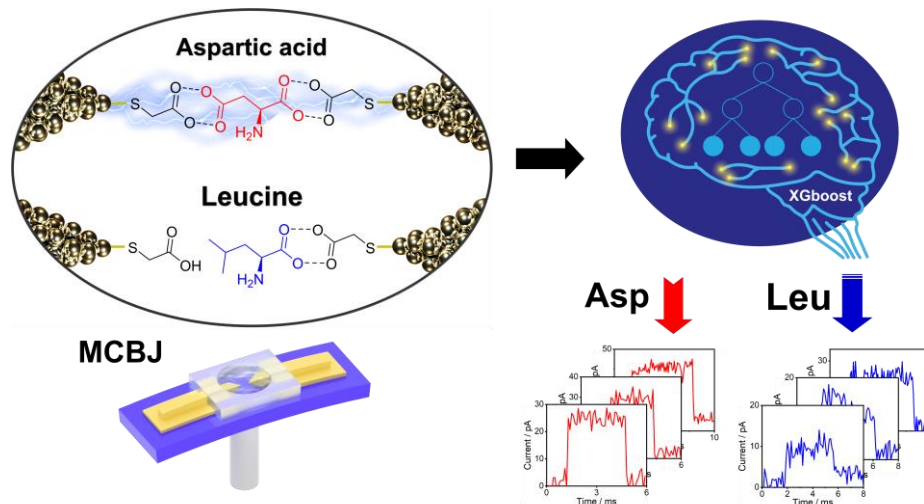


Figure 1. Schematic diagram for classifying Asp and Leu.

Single-Molecule Electrical RNA Detection Towards COVID-19 detection

Takahito OHSHIRO,^a Yuki KOMOTO,^b Masateru TAHIGUCHI^{a,*}
a: SANKEN Osaka University

Email: taniguti@sanken.osaka-u.ac.jp

In recent years, COVID-19 has spread throughout the world, and the pandemic is still continuing so that the development of the simple and easy diagnosis for the infection status is one of the most important public health issues. In the midst of this pandemic, mutant strains of COVID-19 have appeared in various regions of the world, and their susceptibility to infection, severity of symptoms, and impact on various age groups have changed with each new strain.

Single molecule electrical sequencing by nano devices is one of the potential candidates because it is portable, simple, and fast methodology. We have developed a single molecule sequencer using a nanopore device with integrated nanogap-electrodes. In this method, single-stranded nucleotide, such as DNA and RNA, exhibit electrical conductivities that reflect the electronic state of each nucleobase as they pass through the nanogap electrodes, and the obtained signals represents the characteristic conductivities of each nucleobase, resulting in the determination of the sequence. Based on the characteristic conductivities of each mononucleotide of DNA and RNA, we have succeeded in sequencing DNA and RNA (1-2). One of the features of this method is that it can identify not only natural nucleobases such as DNA and RNA, but also modified nucleobases, such as methylated nucleobases such as 5-methyl cytosine and 6-methyl adenine, which are post-translational modifications, and acquired modifications such as oxidized guanine, which are caused by aging and diseases. Some RNA acquired modifications are known to occur in viruses, and drugs targeting these modifications are being developed.

In this study, we performed single molecule sequencing of miRNAs extracted from refractory colorectal cancer cell. MicroRNA analysis (RNA-seq) has been the focus of attention for cancer diagnosis. However, the analysis of microRNAs is limited to type and quantity, and the accuracy of identification is not sufficient. On the other hand, it has been suggested that specific microRNAs can be identified with high accuracy using methylation as an indicator. Herein, we investigated the possibility of detecting and quantifying m6A (N6-methyladenosine) modification by using a nanogap electrode device to measure the single-molecule tunneling current of microRNAs, based on the electrical conductivity of each molecule. As a result, we succeeded in determining the methylation ratio. It was found that the methylation ratio was comparable to that of mass spectrometry (3). These results indicate that this method can be used to determine the sequence of RNA and to evaluate the methylation modification state, which may be useful for the detection of diseases and viruses and the diagnosis of mutant strains.

References:

- (1) Ohshiro T, Tsustui M, Matsubara K, Furuhashi M, Taniguchi M, Kawai T. Single-Molecule Electrical Random Resequencing of DNA and RNA. *Sci.Rep.*, 2, 501-507 (2012).
- (2) Ohshiro T., Tsutsui M., Yokota K, Taniguchi M., *Sci.Rep.* (2018), 8,8517
- (3) Ohshiro T, Konno M, Asai A, Komoto Y, Satoh T, Eguchi H, Doki Y, Taniguchi M, Ishii H, *Sci. Rep.* (2021), 11,19304

Summary about Nanotechnology Open Facilities, Osaka University

Akira KITAJIMA*, Kimihiro NORIZAWA

Nanotechnology Open Facilities, Osaka University, Japan

Email: kitajima@sanken.osaka-u.ac.jp

Nanotechnology Open Facilities (NOF) at Osaka University has been managed in close collaboration with Microstructural Characterization Platform, Nanofabrication Platform and Molecule & Material Synthesis Platform. NOF has a contribution to the development of nanofabrication technology using various quantum beams and the nanofabrication is the basic technology on the industrial research innovation. Additionally, NOF has contributed to the development and evaluation of the resist materials for EUV lithography and to the processing and evaluation of nanoscale devices and structures made of organic, inorganic and oxide materials.

NOF has collaborated with Osaka University Office for University-Industry Collaboration, the Chamber of Commerce and Industry and therefore has strengthened organic cooperation with local companies and off-campus research organization and strives to establish the basic technology and to create the foundation for new industry.

NOF tries to integrate our users with wisdom of our university and NOF as gateway of all-Japan framework for open use through our three Platforms does not only provide the equipment and facility, but also assist the research overall as the open facility for human resource development in nanotechnology and creation of knowledge and technology for innovation core.

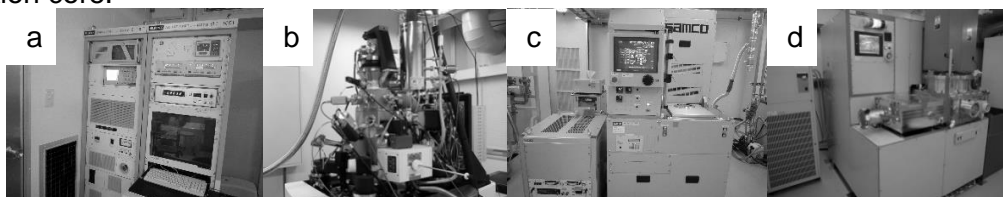


Figure 1. Share-Use Equipment (Nanofabrication Platform), (a)125keV EB Lithography, (b)NanoFab / Helium Ion Microscope, (c)Deep Reactive Ion Etching, (d)DC/RF Sputtering

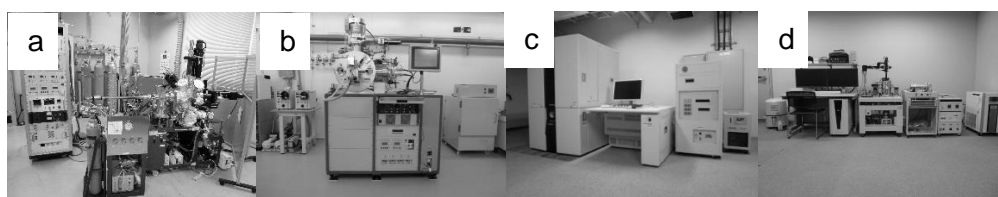


Figure 2. Share-Use Equipment (Molecular & Materials Synthesis Platform), (a)Pulsed Laser Deposition, (b)Ion Milling with SIMS as EPD, (c)Scanning Electron Microscope, (d)Scanning Probe Microscope

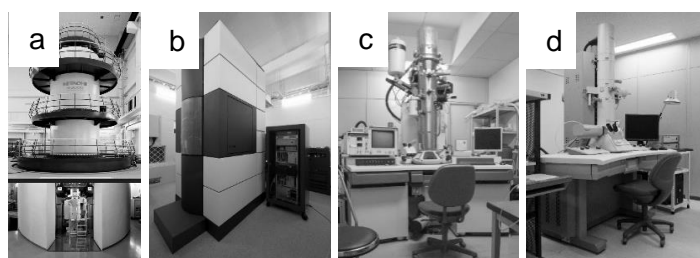


Figure 3. Share-Use Equipment (Microstructural Characterization Platform), (a)3000kV Ultra-High Voltage Transmission Electron Microscope, (b)Transmission Electron Microscope Titan Krios, (c)200kV Transmission Electron Microscope with FEG, (d)Transmission Electron Microscope H-7500

Modulated three-dimensional ferromagnetic anisotropy of pyramidal shape Fe nanofilms

Liliany N Pamasi^a, A. Irmikimov^a, Y. Sakai^a, T. Shimizua^a, H. Yang^a, N. Hosoito^a,

A. N. Hattori^b, A. I. Osaka^b, H. Tanaka^b, and K. Hattori^a

a: ¹Nara Institute of Science and Technology

b: Institute of Scientific and Industrial Research Osaka University

Email: liliany.noviyanty.lc4@ms.naist.jp

In nanostructured magnetic materials, such as ferromagnetic nanofilms, the magnetic behavior is widely determined by the interaction of the magnetization with its shape, by fabricating thin-film patterns with controlled boundaries between ferromagnetic regions, such as disks and squares, characteristic in-plane magnetic moment distributions such as magnetic vortices can be created^{1,2}. In this case, the magnetic interaction is restricted to the flat surface. On the other hand, in ferromagnetic nanofilms on three-dimensional structures such as pyramids, the creation of various magnetically stable structures such as symmetric and asymmetric magnetic vortices depending on the three-dimensional pyramid's size and thickness of the film is predicted from Landau-Lifshitz-Gilbert (LLG) simulations have been predicted². However, so far, there is no successful experimental demonstration have been obtained due to the difficulty in fabricating micro- and nano-sized 3D nanofilms with high accuracy².

Our group has successfully fabricated pyramidal structures with Si{111} clean faceted surfaces (edge width W 16 μm) on Si(001) substrate by combining Si substrate processing technology and ultra-high vacuum surface technology, and performed Fe deposition (film thickness Θ_{Fe} 30 nm). The magnetization field (M - H) curve of the pyramid-shaped Fe nanofilm controlled with atomic precision was measured by vibrating sample magnetometer, and the characteristic of the M - H curve (bending point due to stable magnetic vortex formation) predicted by LLG was observed³.

In the present study, in order to further understand the magnetic behavior of three-dimensional magnetic nanofilms, we have investigated 1) the thickness dependence of Fe film ($\Theta_{\text{Fe}} = 30$ -150 nm) in the pyramidal structure (W 16 μm), 2) the aspect ratio dependence of the pyramidal structure with different length (L) and fixed width (W), that is, the facet line structure (Figure 1, W 16 μm , $L / W = 1$ -10, Θ_{Fe} 150 nm) were measured. In this talk, we will report the details.

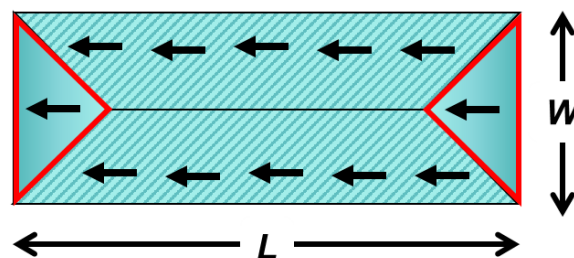


Figure 1: Facet line structure with different aspect ratio (L/W).

References:

- (1) A. Knittel et al., *New. J. Phys.* **12**, 113048 (2010).
- (2) R. P. Cowburn et al., *Phys. Rev. Lett.* **83**, 1042 (1999).
- (3) A. Irmikimov, L. N. Pamasi, K. Hattori, et al., *ACS Cryst. Growth Des.* **21**, 946 (2021).

Additive effects of Cu and K to perovskite solar cells

Ayu Enomoto,^a Atsushi Suzuki,^a Takeo Oku,^a Masanobu Okita,^b Sakiko Fukunishi,^b
Tomoharu Tachikawa,^b Tomoya Hasegawa^b

a: The University of Shiga Prefecture, Japan

b: Osaka Gas Chemicals Co., Ltd, Japan

Email: oe21aenomoto@ec.usp.ac.jp

Due to the COVID-19, distant workings are becoming to be necessary, and internet communication technology (ICT) is developing rapidly. For the ICT devices, electric energy is needed, and solar cells sensitive to the visible light are needed inside the buildings. To solve this problem, $\text{CH}_3\text{NH}_3\text{PbI}_3$ perovskite solar cells are expected to be alternative photovoltaic devices of silicon solar cells,¹⁻³ because of their high conversion efficiency, easy fabrication process, low cost and high sensitivity to the visible light.

The purpose of the present work is to investigate perovskite solar cells, which are expected to be the next generation solar cells. On the other hand, they have a serious problem of low durability. In order to improve the stability and conversion efficiencies of the devices, one of the effective methods is to introduce additives into the perovskite photoactive layer. The purpose of this study is to improve the stability and conversion efficiency of the perovskite solar cells by incorporating copper (Cu) at the lead site, and potassium (K) or guanidinium (GA) at the CH_3NH_3 site. Additive effects on the photovoltaic properties and crystalline structures were discussed by the experimental results and theoretical calculations of electronic structures and thermodynamic stabilities. As a result, the simultaneous addition of Cu and K to the $\text{CH}_3\text{NH}_3\text{PbI}_3$ perovskite crystals improved the stability and open-circuit voltage, which was due to the suppression of decomposition of the perovskite crystals.

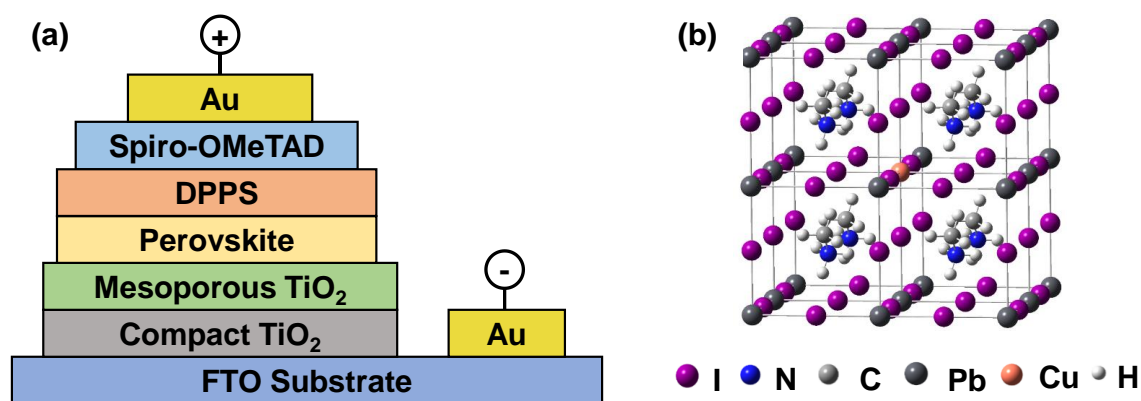


Figure 1: (a) Device structure of solar cells. (b) Electronic structures of $\text{MAPb}_{0.963}\text{Cu}_{0.037}\text{I}_3$.

References:

- (1) Ueoka, N.; Oku, T.; and Suzuki, A. *AIP Advances* **10**, 125023 (2020).
- (2) Karthick, S.; Hawashin, H.; Parou, N.; Vedraïne, S.; Velumani, S.; Boucle, J. *Solar Energy* **218**, 226 (2021).
- (3) Alanazi, T.I.; Game, O.S.; Smith, J.A.; Kilbride, R.C.; Greenl, C.; Jayaprakash, R.; Georgiou, K.; Terrill, N.J.; Lidzey, D.G. *RSC Adv*, **10**, 40341 (2020).

Effects of alkali metal and organic cation addition to Cu-based perovskite solar cells

Riku Okumura ^a, Takeo Oku ^{a,*}, Atsushi Suzuki ^a, Masanobu Okita ^b, Sakiko Fukunishi ^b, Tomoharu Tachikawa ^b, Tomoya Hasegawa ^b

a: Department of Materials Science, The University of Shiga Prefecture, Shiga 522-8533, Japan

*b: Osaka Gas Chemicals Co., Ltd., Osaka 554-0051, Japan
Email: oe21rokumura@ec.usp.ac.jp*

Perovskite solar cells are expected to be the next generation solar cells due to their low cost and easy fabrication process.^{1,2} In a previous study, it was reported that the conversion efficiency and durability of the devices were improved by adding copper and sodium to the perovskite precursor solution.³ In another previous study, it was shown using first-principle calculations that the substitution of methylammonium with ethylammonium (EA) improves the stability of the crystal structure.

The purpose of this study is to investigate the effects of co-addition of copper, sodium and EA to the $\text{CH}_3\text{NH}_3\text{PbI}_3$ perovskite compounds. The structural model used in the first-principle calculations is shown in Fig. 1. From the first-principles calculations of the band structures, the formation of a shallow band of copper d-orbitals, which functions as an acceptor level, would promote the carrier generation. The additional excitation process from copper d-orbitals to sodium s-orbitals would suppress the carrier recombination, thus improving the conversion efficiency. Furthermore, the stability of the crystals increased by the EA substitution at the CH_3NH_3 site from the results of the total energy calculations, which would lead to suppression of formation of lattice defects. The further addition of EA also improved the conversion efficiencies, which indicates the EA substitution would stabilize the crystal structure even in the presence of copper and sodium.

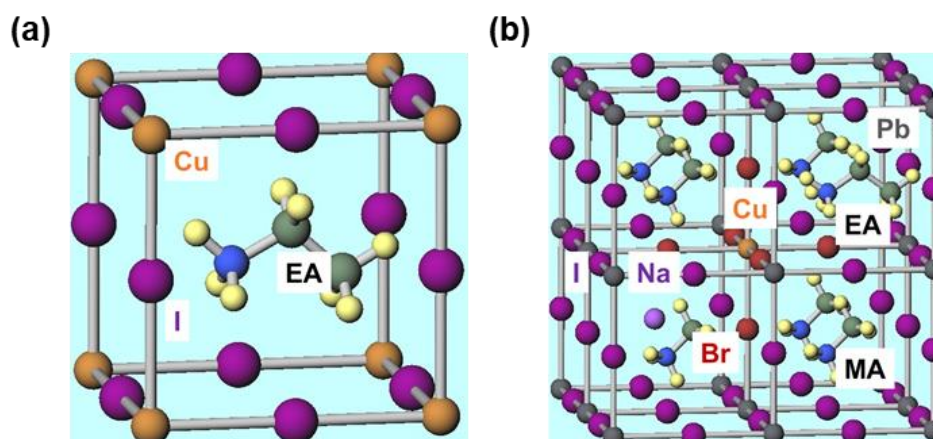


Figure 1: (a) Total substitution structure model of EACuI_3 and (b) partial substitution structure model of $\text{MA}_{0.750}\text{EA}_{0.125}\text{Na}_{0.125}\text{Pb}_{0.875}\text{Cu}_{0.125}\text{I}_{2.25}\text{Br}_{0.75}$.

References:

- (1) Ueoka, N.; Oku, T. *ACS Appl. Energy Mater.* **3**, 7272-7283 (2020).
- (2) Ueoka, N.; Oku, T.; Suzuki, A. *RSC Adv.* **9**, 24231 (2019).
- (3) Liu, D.; Li, Q.; Wu, K. *RSC Adv.* **9**, 7356 (2019).

Perovskite solar cell with guanidinium added to the photoactive layer

Iori Ono,^a Takeo Oku,^a Atsushi Suzuki,^a Masanobu Okita,^b Sakiko Fukunishi,^b
Tomoharu Tachikawa,^b Tomoya Hasegawa,^b

a: Department of Materials Science, The University of Shiga Prefecture, Japan

b: Osaka Gas Chemicals, Japan

Email: ov21ishimaji@ec.usp.ac.jp

From the expansion of COVID-19, various semiconductor devices are being required because of increase of indoor activities. Since small and light weight devices are suitable for the devices, development of photovoltaic devices capable of generating electricity with indoor visible light. Although silicon solar cells are currently the most common solar cells, they have a complicated fabrication process and are expensive. Recently developed $\text{CH}_3\text{NH}_3\text{PbI}_3$ (MAPbI_3) perovskite compounds have demonstrated numerous advantages, such as tunable band gaps, an easy fabrication process, high conversion efficiencies and sensitive to the visible light. However, MAPbI_3 compounds are unstable in air due to the migration of CH_3NH_3 (MA). MAPbI_3 crystals are known to be able to control their electronic states by the addition of other cations and anions, and this could be used to improve the stability of the perovskite photovoltaic devices. Doping with other molecules such as formamidinium ($\text{CH}(\text{NH}_2)_2$)^{1,2} and ethyl ammonium ($\text{CH}_3\text{CH}_2\text{NH}$)^{3,4} at the methylammonium (CH_3NH_3) sites improved the conversion efficiencies.

The purpose of this work is to investigate the effects of addition of guanidinium [$\text{C}(\text{NH}_2)_3$; GA] on MAPbI_3 perovskite solar cells fabricated at a high temperature of 190 °C in atmospheric air. Schematic illustration of the perovskite solar cells is shown in Fig. 1. The photovoltaic properties of the fabricated solar cells were investigated in terms of light-induced current density-voltage curves and external quantum efficiency. Microstructures of the perovskite thin films were investigated by X-ray diffraction, optical microscopy, scanning electron microscopy, and transmission electron microscopy. The addition of guanidinium iodide and the insertion of decaphenylpentasilane between the perovskite and hole transport layer improved the external quantum efficiency and short-circuit current density, and the conversion efficiencies were stable after 1 month. X-ray diffraction showed that the lattice constant of the perovskite crystals was increased by the addition of GA, and the GA addition also improved the surface morphology. First principles calculations on the density of states and band structures showed reduction of the total energy by the GA addition and the effectiveness of the nitrogen atoms in GA.

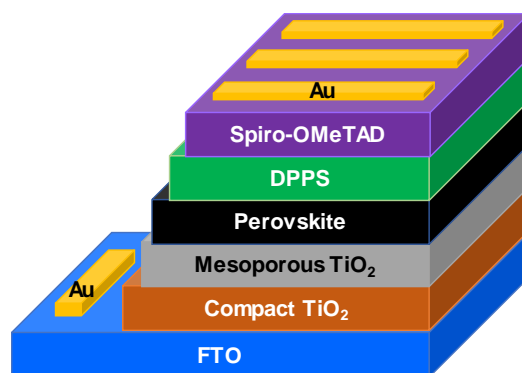


Figure 1. Schematic illustration of the perovskite solar cells.

References:

- (1) Zhao, W.; Yao, Z.; Yu, F.; Yang, D.; Liu, S. *Adv. Sci.* **5**, 1700131 (2018).
- (2) Li, N.; Luo, Y.; Chen, Z.; Niu, X.; Zhang, X.; Lu, J.; Kumar, R.; Jiang, J.; Liu, H.; Guo, X.; Lai, B.; Brocks, G.; Chen, Q.; Tao, S.; Fenning, P. D.; Zhou, H. *Joule* **4**, 8, (2020).
- (3) Lin, D.; Li, Q.; Wu, K. *RSC Adv.* **9**, 7356, (2019).
- (4) Nishi, K.; Oku, T.; Kishimoto, T.; Ueoka, N.; Suzuki, A. *Coatings* **10**, 410, (2020).

Material design based on first-principles calculation and characterization of lanthanide compound incorporated perovskite solar cells

Atsushi SUZUKI^{1*}, Kyo KISHIMOTO¹, Takeo OKU¹, Masanobu OKITA²,
Sakiko FUKUNISHI², Tomoharu TACHIKAWA², and Tomoya HASEGAWA²

1: The University of Shiga Prefecture, 2500 Hassaka, Hikone, Shiga 522-8533, Japan

2: Osaka Gas Chemicals Co. Ltd. 5-11-61 Torishima, Konohana-ku, Osaka 554-0051, Japan

Email: suzuki@mat.usp.ac.jp

The photovoltaic properties of the lanthanide incorporated perovskite solar cells were investigated by the experimental results and first-principles calculation.¹⁻³ The purpose of this work is focus on fabrication and characterization of the $\text{CH}_3\text{NH}_3\text{PbI}_3$ perovskite solar cells using lanthanide compounds with decaphenylcyclopentasilane (DPPS) for improving the stability of the photovoltaic performance. Incorporation of formamidinium iodine (FAI) and lanthanide (Eu, Sm, Tb, Ce) compound into the perovskite crystals improved external quantum efficiency and short circuit current density related to conversion efficiency. The addition of FAI and EuCl_2 improved the crystal growth and orientation, improving the stability of the photovoltaic performance. The carrier generation, charge transfer and carrier mobility related to short circuit current density were derived from the band structures and electron correlation of d, f-p orbital of lanthanide ion and halogen ion as ligand in the coordination structure. Incorporation of Eu (II) ion into the perovskite crystal caused the narrow band dispersion with decrease of effective mass, improving the carrier mobility related to short circuit current density and conversion efficiency. The total energies of the Eu-doped perovskite crystal expected the stabilities of the photovoltaic performance. In the case of the FAPbSmI_3 crystal, d orbital of Sm (II) ion was localized near valence band state, expecting for suppression of the carrier diffusion. In the case of the FAPbTbI_3 crystal, the 4f-orbital of Tb (III) ion was localized, and caused the flat band dispersion near valence band state, suppressing the charge transfer and carrier diffusion related to short circuit current density. In the case of the FAPbCeI_3 crystal, 5p orbital of iodine ion and d orbital of Ce ion was delocalized near valence and conduction band state. The lanthanide doped perovskite crystal have advantage to apply the photovoltaic devices with stability of the conversion efficiency as indoor power generation capable solar cell.

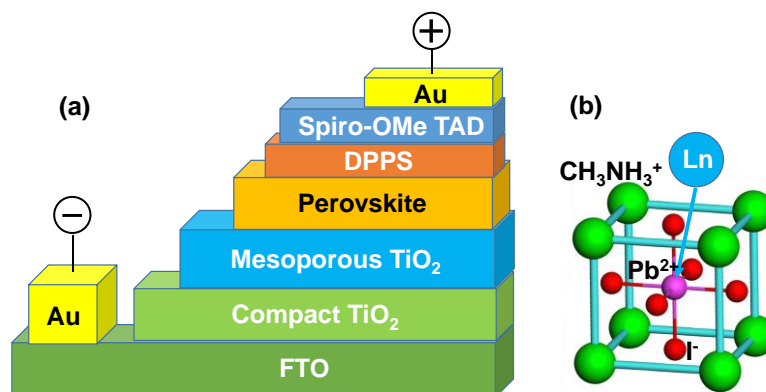


Figure 1: (a) Schematic diagram of perovskite solar cell (b) perovskite crystal doped with lanthanide (Ln: Eu^{2+} , Sm^{2+} , Tb^{3+} and Ce^{2+}).

References:

- (1) Song Z.; Xu W.; Wu Y.; Liu S.; Bi W.; Chen X.; Song H. *Small*, **16**, 2001770 (2020).
- (2) Wang L.; Zhou H.; Hu J.; Huang B.; Sun M.; Dong B.; Zheng G.; Huang Y.; Chen Y.; Li L.; Xu Z.; Li N.; Liu Z.; Chen Q.; Sun LD.; Yan CH. *Science*, **363**, 265-270 (2019).
- (3) Suzuki A.; Oku T. *Mater. Adv.* **2**, 2609-2616 (2021).